USGS
science for a changing world

Prepared in cooperation with the Lac du Flambeau Band of Lake Superior Chippewa Indians

Hydrology of Haskell Lake and Investigation of a Groundwater Contamination Plume, Lac du Flambeau Reservation, Wisconsin

Scientific Investigations Report 2020–5024

U.S. Department of the Interior
U.S. Geological Survey

Cover. Photograph showing Haskell Lake looking northeast from near mini-piezometer PZ4, May 3, 2017. Photograph by Andrew Leaf, U.S. Geological Survey.

Hydrology of Haskell Lake and Investigation of a Groundwater Contamination Plume, Lac du Flambeau Reservation, Wisconsin

By Andrew T. Leaf and Megan J. Haserodt

Prepared in cooperation with the Lac du Flambeau Band of Lake Superior Chippewa Indians

Scientific Investigations Report 2020–5024

U.S. Department of the Interior
U.S. Geological Survey

U.S. Department of the Interior
DAVID BERNHARDT, Secretary

U.S. Geological Survey
James F. Reilly II, Director

U.S. Geological Survey, Reston, Virginia: 2020

For more information on the USGS—the Federal source for science about the Earth, its natural and living resources, natural hazards, and the environment—visit https://www.usgs.gov or call 1–888–ASK–USGS.

For an overview of USGS information products, including maps, imagery, and publications, visit https://store.usgs.gov.

Suggested citation:
Leaf, A.T., and Haserodt, M.J., 2020, Hydrology of Haskell Lake and investigation of a groundwater contamination plume, Lac du Flambeau Reservation, Wisconsin: U.S. Geological Survey Scientific Investigations Report 2020–5024, 79 p., https://doi.org/10.3133/sir20205024.

Associated data release for this publication:
Leaf, A.T., and Haserodt, M.J., 2020, MODFLOW–NWT and MODPATH models, data from aquifer tests and temperature profilers, and groundwater flux estimates used to assess groundwater/surface-water interactions in Haskell Lake, Wisconsin: U.S. Geological Survey data release, https://doi.org/10.5066/P9ZQGGHY.

ISSN 2328-0328 (online)

Acknowledgments

Local Project Coordinator

Kristen Hanson, Environmental Response Program Coordinator, Lac du Flambeau Band of Lake Superior Chippewa Indians, Lac du Flambeau, Wisconsin

Field Support

Brent Olson, U.S. Geological Survey, Rhinelander, Wis.
Dan Baumann, U.S. Geological Survey, Rhinelander, Wis.

Technical Support

Randy Hunt, U.S. Geological Survey, Middleton, Wis.
Marty Briggs, U.S. Geological Survey, Storrs Mansfield, Connecticut

Geophysical Surveys

Dave Hart, Wisconsin Geological and Natural History Survey, Madison, Wis.
Carolyn Streiff, Wisconsin Geological and Natural History Survey, Madison, Wis.
Pete Chase, Wisconsin Geological and Natural History Survey, Madison, Wis.

Technical Reviewers

Paul Juckem, U.S. Geological Survey, Middleton, Wis.
Perry Jones, U.S. Geological Survey, Mounds View, Minnesota

Editor

Valerie Dressler, Madison Publishing Service Center, Bismarck, North Dakota

Groundwater Specialist Reviewer

Paul Juckem, U.S. Geological Survey, Middleton, Wis.

Bureau Approving Official

Janet M. Carter, Bureau Approving Official, U.S. Geological Survey Office of Science Quality and Integrity, Rapid City, South Dakota

Contents

Figures

Tables

Conversion Factors

U.S. customary units to International System of Units

Multiply	By	To obtain
	Length	
inch (in.)	2.54	centimeter (cm)
foot (ft)	0.3048	meter (m)
mile (mi)	1.609	kilometer (km)
	Area	
square mile (mi^2)	259.0	hectare (ha)
square mile (mi^2)	2.590	square kilometer (km^2)
	Volume	
cubic foot (ft^3)	0.02832	cubic meter (m^3)
fluid ounce (oz)	0.033814	milliliter (mL)
	Flow rate	
foot per day (ft/d)	0.3048	meter per day (m/d)
foot per year (ft/yr)	0.3048	meter per year (m/yr)
cubic foot per second (ft^3/s)	0.02832	cubic meter per second (m^3/s)
inch per year (in/yr)	25.4	millimeter per year (mm/yr)
	Hydraulic conductivity	
foot per day (ft/d)	0.3048	meter per day (m/d)
	Transmissivity*	
foot squared per day (ft^2/d)	0.09290	meter squared per day (m^2/d)

Temperature in degrees Fahrenheit (°F) may be converted to degrees Celsius (°C) as:

$$°C = (°F - 32) / 1.8.$$

International System of Units to U.S. customary units

Multiply	By	To obtain
	Length	
centimeter (cm)	0.3937	inch (in.)
meter (m)	3.281	foot (ft)
kilometer (km)	0.6215	mile (mi)
	Area	
hectare (ha)	0.003861	square mile (mi^2)
square kilometer (km^2)	0.3861	square mile (mi^2)
	Volume	
cubic meter (m^3)	35.31	cubic foot (ft^3)
milliliter (mL)	29.5735	fluid ounce (oz)
	Flow rate	
meter per day (m/d)	3.281	foot per day (ft/d)
meter per year (m/yr)	3.281	foot per year (ft/yr)
cubic meter per second (m^3/s)	35.31	cubic foot per second (ft^3/s)
millimeter per year (mm/yr)	0.03937	inch per year (in/yr)
	Hydraulic conductivity	
meter per day (m/d)	3.281	foot per day (ft/d)
	Transmissivity*	
meter squared per day (m^2/d)	10.76	foot squared per day (ft^2/d)

Temperature in degrees Celsius (°C) may be converted to degrees Fahrenheit (°F) as:

$$°F = °C \times 1.8 + 32.$$

Datum

Vertical coordinate information is referenced to the North American Vertical Datum of 1988 (NAVD 88).

Horizontal coordinate information is referenced to the North American Datum of 1983 (NAD 83).

Elevation, as used in this report, refers to distance above the vertical datum.

Supplemental Information

Specific conductance is given in microsiemens per centimeter at 25 degrees Celsius (μS/cm at 25 °C).

Concentrations of chemical constituents in water are given in either milligrams per liter (mg/L) or micrograms per liter (μg/L).

Abbreviations

ADCP	acoustic Doppler current profiler
EPA	U.S. Environmental Protection Agency
ERI	electrical resistivity imaging
GHB	General-Head Boundary (Package)
GIS	geographic information system
GPS	Global Positioning System
GUI	graphical user interface
HDPE	high-density polyethylene
HVSR	horizontal-to-vertical spectral ratio
^{1}H	hydrogen-1
^{2}H	hydrogen-2 (deuterium)
LAK	Lake (Package)
LDF Tribe	Lac du Flambeau Band of Lake Superior Chippewa Indians
LNAPL	light nonaqueous phase liquid
NOAA	National Oceanic and Atmospheric Administration
NWIS	National Water Information System
^{16}O	oxygen-16

^{18}O	oxygen-18
SFR2	Streamflow Routing (Package)
SWB	Soil-Water-Balance (model)
USGS	U.S. Geological Survey
UZF	Unsaturated-Zone Flow (Package)
VOC	volatile organic compound
WDNR	Wisconsin Department of Natural Resources
WGNHS	Wisconsin Geological and Natural History Survey

Hydrology of Haskell Lake and Investigation of a Groundwater Contamination Plume, Lac du Flambeau Reservation, Wisconsin

By Andrew T. Leaf and Megan J. Haserodt

Abstract

Haskell Lake is a shallow, 89-acre drainage lake in the headwaters of the Squirrel River, on the Lac du Flambeau Reservation in northern Wisconsin. The lake has long been valued by the Lac du Flambeau Band of Lake Superior Chippewa Indians (LDF Tribe) for abundant wild rice and game fish. In recent decades, however, wild rice has mostly disappeared from the lake and the fishery has declined. A petroleum contamination plume discovered in the 1990s in the shallow aquifer upgradient from the northern end of the lake poses a threat to the ecological health of the lake and the aquifer, which is the sole drinking water source for nearby residents and businesses. Understanding of the lake's hydrology is important to the LDF Tribe as they seek to restore wild rice and maintain the ecological health of the Haskell Lake/Tower Creek watershed. An improved understanding of lithology in the area of the contamination plume, documentation of a contamination pathway from groundwater in the plume source area to Haskell Lake, and an understanding of the plume extent beneath the lake are needed to advance remediation efforts. Evaluation of the fraction of groundwater discharge that is contaminated relative to the overall lake water budget is desired as a first step towards determining the extent of ecological effects from the plume.

A cooperative study between the U.S. Geological Survey and the LDF Tribe was initiated to quantify the lake water budget and the sources of water to the lake, to provide a rough estimate of the maximum quantity of groundwater discharge to the lake that may be contaminated, and to improve the conceptual understanding of the plume extent and subsurface materials in the area of contamination. The results of this study can help inform natural resource management of the Haskell Lake/Tower Creek watershed, including planned wild rice restoration and cleanup of the contaminant plume.

During 2016–17, field data on lake and groundwater levels, gradients, fluxes, and subsurface lithology were collected using a variety of techniques that ranged from basic measurement of water levels and streamflows to distributed temperature sensing, vertical temperature profiling, and several shallow geophysical methods. The data were used to inform a MODFLOW–NWT model that simulated the contributing groundwatershed, including the water budget for Haskell Lake and Tower Creek using the Lake, Streamflow-Routing, and Unsaturated Zone-Flow Packages. Particle tracking with the MODFLOW solution (using MODPATH 6) was used to improve understanding of the downgradient extent of the contamination plume, estimate groundwater flux through the plume area, and delineate the groundwater contributing area (groundwatershed) for the lake/creek system. Linear uncertainty estimates for model results were computed during model parameter estimation using the software package PEST++.

Results indicate groundwater discharge along the perimeter of Haskell Lake, with groundwater accounting for about 22 (± 11.5) percent of the lake water budget. Field data and particle tracking results indicate discharge of the entire contamination plume to Haskell Lake. Although the exact locations where contaminated groundwater enters the lake are unknown, the downgradient extent of the plume beneath Haskell Lake is likely limited to within about 700 feet from the shore. Groundwater flux through the plume accounts for at most about 1.4 percent of total groundwater discharge to Haskell Lake, or about 0.3 percent of the lake water budget. Most groundwater discharging to Haskell Lake and Tower Creek originates as terrestrial recharge. A lesser amount originates in or passes through neighboring lakes, including Buckskin, Crawling Stone, Broken Bow, Tippecanoe, and Jerms Lakes, as well as several unnamed kettles. The average age of simulated groundwater discharge to the lake is about 20 years.

Introduction

Haskell Lake History

Haskell Lake is a shallow, 89-acre drainage lake in the headwaters of the Squirrel River, on the Lac du Flambeau Reservation in northern Wisconsin (Vilas County, Wis.; fig. 1; Wisconsin Department of Natural Resources [WDNR], 2017a). This area has long been valued by the Lac du Flambeau Band of Lake Superior Chippewa Indians (LDF Tribe) for its natural resources. Historic documents and oral history record settlements on nearby Squirrel and Squaw Lakes (fig. 1) and campsites on Haskell Lake that date to at least the 19th century. Burial mounds in these locations indicate earlier occupation by prehistoric people. These settlements were located for access to fish and game, wild rice, sugar maples, and other natural resources. Tribal members continue to use the area today (2020) for a variety of subsistence activities (Leon Valliere, LDF Ojibwe Language Department Director, written commun., 2015; Cynthia Stiles, Tribal Archeologist, LDF Tribal Historic Preservation Office, written commun., 2018).

Haskell Lake was known for having extensive wild rice beds as early as 1837 and is currently (2020) recognized as a wild rice waterbody within the LDF Tribe's federally approved water-quality standards (National Archives and Records Administration, 1911; K. Hansen, LDF Tribe, oral commun., 2018; Gerry Mann, Lac du Flambeau Fish and Game Department Clerk, written commun., 2018; Cynthia Stiles, Tribal Archeologist, LDF Tribal Historic Preservation Office, written commun., 2018). Wild rice holds special cultural, spiritual, and social significance for the LDF Tribe and other Anishinaabe peoples and is also thought to be ecologically important (W. Graveen and A. Virden, LDF Tribe, oral commun., 2018). By the late 1990s, wild rice in Haskell Lake had declined, prompting reseeding efforts by the LDF Tribe. In 2015, a point intercept vegetation survey indicated no identifiable presence of wild rice on Haskell Lake (K. Hansen, LDF Tribe, oral commun., 2018). The cause of wild rice decline is unknown. Myriad anthropogenic and natural factors can affect wild rice viability, including water levels, nutrient inputs, sediment geochemistry, and biological factors such as disease or competition from other species (for example, Meeker, 1996, 1999; Weaver and others, 2005; WDNR, 2015a; Pastor and others, 2017).

Haskell Lake has also been valued for subsistence and recreational fishing. Previously, a hotel and bait shop operated at the northern end of the lake; however, in March of 2012, the first fish kill was recorded and the hotel and bait shop closed in 2016 (K. Hansen, LDF Tribe, oral commun., 2018).

A better understanding of the hydrology of Haskell Lake, including the water budget, contributing groundwater, and groundwater/surface-water interactions, is desired by the LDF Tribe as they seek to restore and manage wild rice and game fish and maintain the overall ecological health in the Haskell Lake/Tower Creek watershed (fig. 1).

Tower Standard Service Contamination Site

From the mid-1940s until 1997, the Tower Standard Service gas station and auto repair facility was operated near the north end of Haskell Lake (fig. 2). Petroleum contamination was documented in groundwater in 1992, when a nearby well was found to be contaminated (L. Wawronowicz, Natural Resources Director for LDF Tribe, written commun., 2018). The Tower Standard Service site was registered in 1997 in the WDNR Bureau for Remediation and Redevelopment Tracking System as site # 03–64–127899 (WDNR, 2017b). After the site was registered, groundwater-quality monitoring began and five underground storage tanks associated with the service station were removed. A pump and treat system was installed in 2001 and operated through October of 2004. In 2006, the Tower Standard Service site was considered remediated and was closed by the WDNR (2017b). In 2010, groundwater sampling for an unrelated investigation of perchlorate contamination from a separate source on an adjacent property detected petroleum odors (Weston Solutions, Inc., 2011). Subsequent field observations, groundwater and soil sampling, and a laser-induced fluorescence (for example, Bujewski and Rutherford, 1997) survey indicated the presence of residual light nonaqueous phase hydrocarbons (LNAPL) near the former Tower Standard Service station underground storage tanks and the migration of dissolved-phase volatile organic compound (VOC) contamination to Haskell Lake (Weston Solutions, Inc., 2014; Bristol Environmental Remediation Services, LLC, 2016b; Dakota Technologies Company, Inc., 2016). Contaminants of concern at the site include petroleum-range hydrocarbons, lead and lead scavengers, and several solvents and their degradants that may have come from the auto repair facility (Weston Solutions, Inc., 2014; Bristol Environmental Remediation Services, LLC, 2016a, b; REI Engineering, Inc., 2016; Northern Lake Service, Inc., 2017; K. Hansen, LDF Tribe, oral commun., 2018). Prior to the study documented in this report, concentrations of benzene exceeding 1,000 parts per billion, or 200 times the U.S. Environmental Protection Agency (EPA) drinking water standard, had been detected in groundwater within a few feet of the Haskell Lake shoreline (at MW16D, fig. 2), but the downgradient extent of the plume had not been defined.

Dissolved petroleum and solvent-derived contamination in the shallow aquifer and the presence of an on-going source in the residual LNAPL presents an immediate environmental concern for the LDF Tribe. The shallow aquifer provides the sole drinking water source to residents and businesses in this area. In addition to the public health and economic implications, the LDF Tribe is concerned about the potential effects of contaminated groundwater discharge on the ecological health of Haskell Lake. As of this report (2020), assessments of the contamination extent and remediation options are being coordinated by the LDF Tribe, the EPA, and the WDNR. A depiction of the groundwater petroleum contamination plume, as estimated by Weston Solutions, Inc. (2016), is shown in figure 2. For the purposes of this report, the general area shown in figure 2 is defined as the Haskell Lake contamination site or contamination site.

An improved understanding of subsurface lithology in the area of the plume is important for the selection and design of an appropriate remediation technology. From a legal and regulatory standpoint, documentation of a contamination pathway

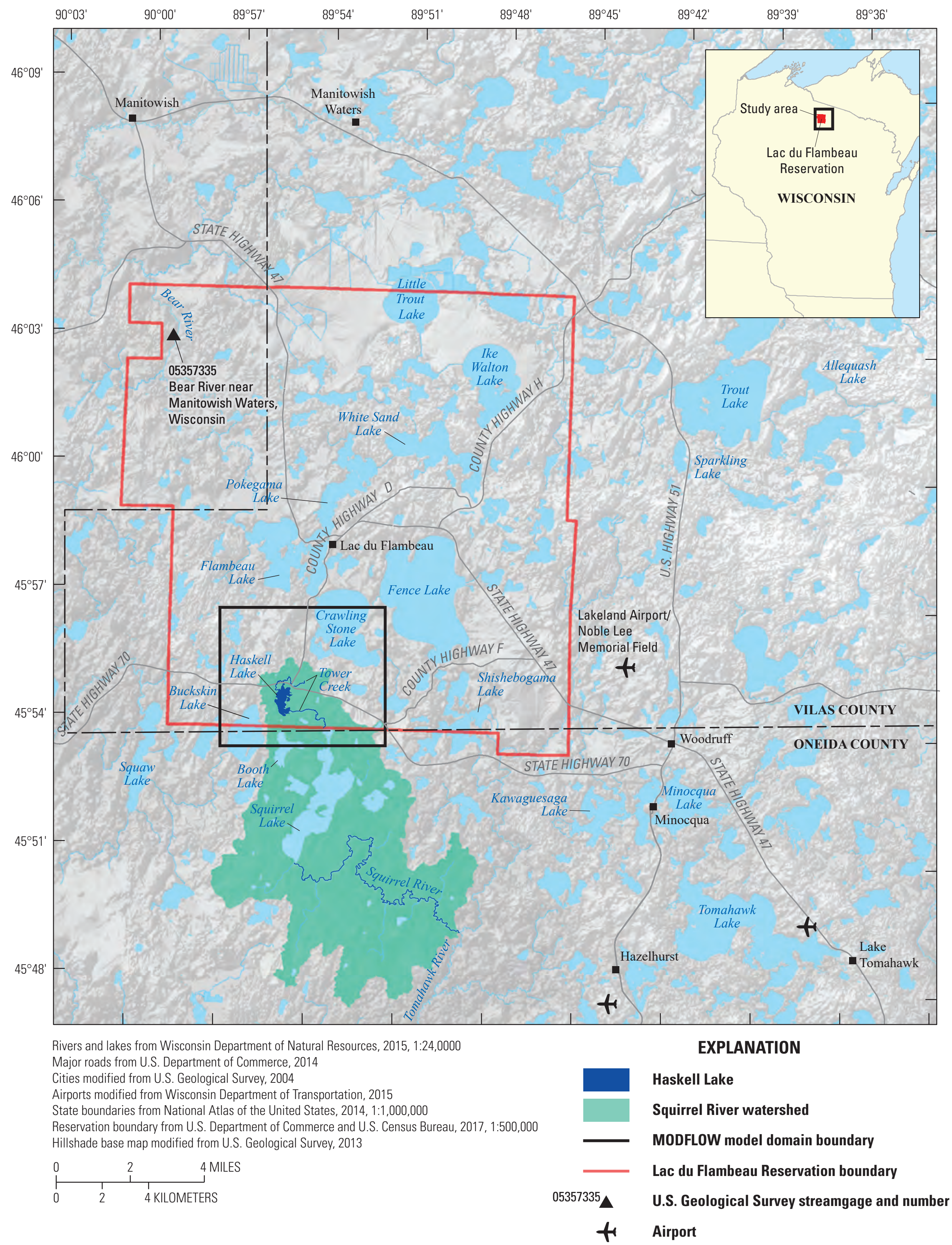

Figure 1. Location of the study area, Lac du Flambeau Reservation, Wisconsin.

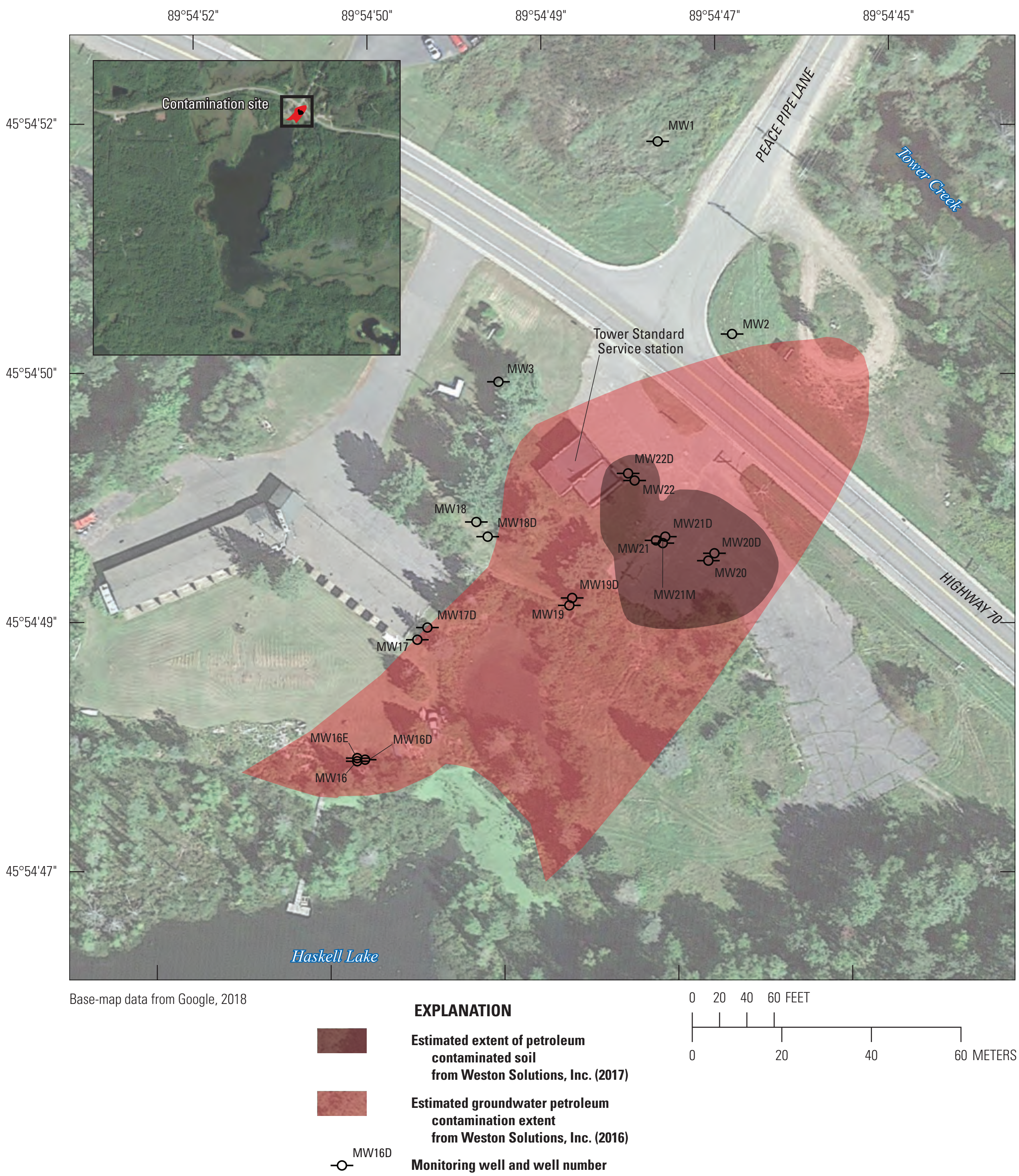

Figure 2. Monitoring well network and petroleum plume extent at the Haskell Lake contamination site.

from the groundwater system to Haskell Lake (that Haskell Lake is a receptor of the contamination) and an understanding of the downgradient plume extent are needed to advance the site remediation process (K. Hansen, LDF Tribe, oral commun., 2018). Finally, evaluating the quantity of groundwater discharge to the lake that may be contaminated, relative to the overall lake water budget, can provide a preliminary basis for evaluating the extent of ecological effects.

Previous Investigations

Previous groundwater investigations in this area include an analytic element groundwater flow model (Juckem and others, 2014) constructed to assess contributing areas to drinking-water supply wells and the fate of infiltration from waste-water treatment lagoons. This model was developed using the program GFLOW (Haitjema, 1995) to represent the groundwater flow system at the scale of the Lac du Flambeau Reservation, but the model is two dimensional and lacks detail in the areas surrounding Haskell Lake. Other previous work is discussed in the “Site Description” section.

Study Overview and Objectives

The LDF Tribe initiated this cooperative study with the U.S. Geological Survey (USGS) to better understand the hydrology of Haskell Lake and the transport of petroleum contamination to the lake. Specifically, the goals of the study were to (1) quantify the lake water budget and the sources of water to the lake; (2) provide an estimate of the maximum quantity of groundwater discharge to the lake that may be contaminated; (3) improve understanding to the plume extent beneath the lake by assisting the LDF Tribe with lakebed pore water sampling and simulation of advective transport; and (4) improve knowledge of the subsurface hydraulic properties and, to the extent feasible, the conceptual model of the subsurface at the contamination site.

The study was completed in two phases. The first phase, beginning in spring of 2016, involved a distributed temperature sensing survey of the lakebed in the likely area(s) of groundwater discharge downgradient from the plume (Leaf, 2020). Results of the distributed temperature sensing study were used to guide sampling of lakebed pore water for VOCs at three locations (appendix 9). The second phase, beginning in fall of 2016, expanded the focus to include the lake water budget and surrounding groundwater flow system, as well as the subsurface lithology at the contamination site. Field data, including lake and groundwater levels, slug tests, shallow geophysics, daily precipitation, and streamflow were collected. Lakebed pore water also was sampled at four additional locations to improve understanding of the plume extent beneath the lake. The data were used to inform a three-dimensional finite difference groundwater flow (MODFLOW-NWT) model that simulated the water budget of Haskell Lake and Tower Creek, the contributing groundwater flow system, and the flow paths of groundwater passing through the area of the contamination plume.

Purpose and Scope

This report presents the results of an investigation of the hydrology of Haskell Lake and its contributing groundwater flow system, including the collection and interpretation of field data and development of a finite difference groundwater flow model. The report includes (1) a description of the hydrologic setting and Quaternary geology for the MODFLOW model domain (study area) and at the Haskell Lake contamination site; (2) a summary of the field data collection methods; (3) presentation and discussion of field data results; (4) a description of the groundwater modeling approach, including model construction and parameter estimation; (5) a summary of the model results; and (6) a discussion of model limitations and assumptions made during this study.

The main body of the text is intended to summarize the study and highlight the key findings. Additional details are provided in the appendixes.

Site Description and Hydrologic Setting

Haskell Lake is in the Northern Highlands Lake District of Wisconsin, where irregular topography and a nascent drainage network reflect the recent retreat of the Laurentide Ice Sheet only 10,000 years ago (Attig, 1985). Annual precipitation in the area averages about 32 inches (National Oceanic and Atmospheric Administration [NOAA], 2018a). Annual evaporation from lakes averages 21–29 inches, leaving a net annual precipitation surplus of 3–11 inches (Juckem and others, 2014; Hunt and others, 2013; Krabbenhoft and others, 1990). Previous work has indicated that average annual groundwater recharge varies spatially from about 6 to 20 inches per year, depending on vegetation, soils, and other characteristics (Dripps and others, 2006), and spatial average recharge varies annually from about 14 to 21 inches per year (Hunt and others, 2013). Previous studies and base-flow separation of daily flow records at the Bear River streamgage (USGS site 05357335; fig. 1; U.S. Geological Survey, 2018) indicate that more than 80 percent of streamflow is groundwater derived (Hunt and others, 2013; Gebert and others, 2011).

A surplus of precipitation over evapotranspiration and myriad surface depressions have resulted in prevalent lakes and wetlands throughout the study area, with lakes alone constituting about 20 percent of the land area of the Lac du Flambeau Reservation (Batten and Lidwin, 1996; Patterson, 1989). Lakes generally can be classified as seepage lakes, which occupy closed depressions and, therefore, do not have an outlet stream, or as drainage lakes, which have outlets (for example, Born and others, 1979). Lakes on the Lac du Flambeau Reservation are generally thought to be well-connected to the groundwater system and, therefore, reflective of the water table position, with the exception of some seepage lakes that are perched. Drainage lakes generally have less fluctuations in water level compared to seepage lakes because of the stabilizing effect of their outlets (Juckem and others, 2014).

Conceptual Model of the Haskell Lake Water Budget

Haskell Lake receives flow from Tower Creek (SW_{in}), which originates in a wetland to the northeast. Tower Creek continues out of Haskell Lake to the southeast (SW_{out}) through a wetland complex to Squirrel Lake, which is the headwaters of the Squirrel River. Haskell Lake and Tower Creek receive flow from groundwater (GW_{in}), which originates as precipitation and snowmelt infiltrating past the root zone (terrestrial recharge), and from seepage from nearby lakes that are higher in elevation. Haskell Lake also receives some water directly from precipitation (P) and loses water through evapotranspiration (ET). Overland (Hortonian) runoff directly to Haskell Lake is assumed to be negligible because of the hummocky topography and high infiltration rates of the surrounding sandy soils. The Haskell Lake water budget is assumed to be steady. In other words, while components such as precipitation and groundwater inflow might vary from year to year, no long-term trends in lake level are assumed. This study aims to quantify the contributions of these water budget components, summarized in figure 3 and equation 1, to the overall water budget of Haskell Lake.

$$SW_{in} + GW_{in} + P = SW_{out} + GW_{out} + ET \qquad (1)$$

where

SW_{in} is surface-water inflow,
GW_{in} is groundwater inflow,
P is precipitation,
SW_{out} is surface-water outflow,
GW_{out} is groundwater outflow, and
ET is evapotranspiration.

Quaternary Geology

The geology of Vilas County consists of as much as 280 feet of Pleistocene glacial till, debris flow deposits, and stream sediments overlying Proterozoic igneous and metamorphic bedrock (fig. 4). Most of the overlying unconsolidated material was deposited during the end of the Wisconsin

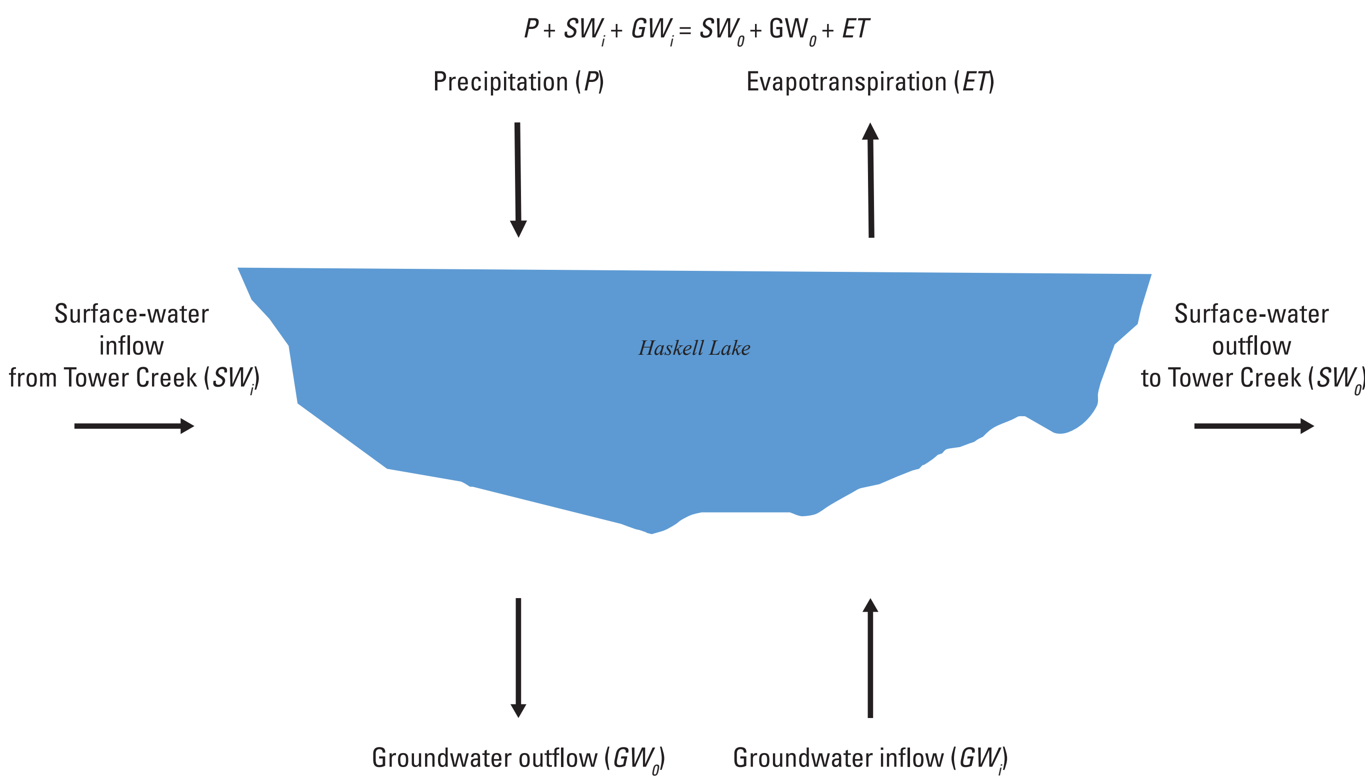

Figure 3. Haskell Lake water budget schematic.

glaciation (25,000–10,000 years ago) as ice was melting during the transition from the glacial to interglacial period. The underlying bedrock has been mapped as Paleoproterozoic mafic metavolcanic rock; bedrock outcrops are rare. Within the study area, most of the Quaternary sediment is from the Wildcat Lake Member of the Cooper Falls Formation, which was deposited by the Wisconsin Valley lobe of the Laurentide Ice Sheet (Attig, 1985). Materials in the Wildcat Lake Member include:

- till deposited at the base of the ice,
- debris flows created by the accumulation of debris melting out at the upper surface of the ice, and
- sands and gravels deposited by meltwater streams running beneath the ice in tunnels or meandering over outwash plains beyond the ice margin.

The till deposits of the Wildcat Lake Member locally overlie older sands and gravels and are overlain by the debris flow and meltwater deposits of the Wildcat Lake Member.

The Wildcat Lake Member till is typically less than 7 feet thick, generally uniform in texture, and compacted from the weight of the overlying ice. The debris flow sediments are as much as 26 feet thick, more variable in texture, and typically less compacted than the till. The till and debris flow sediments contain appreciable silt and clay. Attig (1985) reported an average sand:silt:clay ratio of 71:21:8 for the Wildcat Lake Member till and 75:20:5 for the debris flow deposits. Although the till and debris flow deposits contain larger clasts including pebbles and cobbles, boulders greater than 8 inches are exclusive to the debris flows (Attig, 1985).

The meltwater stream deposits include short narrow ridges (eskers) left by streams flowing beneath the ice, ice-marginal fans (Wgf), and braided outwash plains. Braided stream deposits on solid ground retained their depositional shape (Wgp), whereas deposits on remnant ice blocks subsequently collapsed when the ice melted, forming an uneven, hummocky land surface (Wgc) dotted with kettle depressions. Figure 4 shows deposits mapped by Attig (1985) overlain on shaded relief developed from a recent lidar survey (Vilas County Land Information & Mapping Department, 2016), which mapped land-surface elevations at high resolution (about 1 meter in the horizontal direction and a few centimeters in the vertical direction). The Wgp and Wgc deposits are visible in the lidar as relatively flat and hummocky areas, respectively (fig. 4). Mismatch between the boundaries of the units in Attig (1985) and the lidar texture can be attributed to the difficulty of inferring unit boundaries in a heavily forested area, using mostly the aerial imagery and topographic maps available at the time (1985).

Although not mapped explicitly by Attig (1985), debris flow sediments and till of the Wildcat Lake Member (Wt) are likely present within the study area. Attig (1985) made several cross sections of Pleistocene geology across Vilas County, including one east of the study area (fig. 5), which includes undifferentiated till and debris flows of the Wildcat Lake Member identified in geologic logs. No published county cross sections have been constructed through the study area or to the west of the study area, but nearby well construction reports indicate that the debris flow and till deposits may also be present at the contamination site, as illustrated in figure 6. Poorly sorted debris flow sediments are common near the margins of collapsed areas such as Haskell Lake (Attig, 1985). Lidar (Vilas County Land Information & Mapping Department, 2016) and Attig (1985) indicate a transition from collapsed to planar meltwater deposits near the western and northern ends of Haskell Lake (fig. 4). Finally, numerous boulders present along the western shoreline of Haskell Lake, low permeabilities encountered in slug testing and pore water sampling, and boulders encountered in previous drilling (for example, Bristol Environmental Remediation Services, LLC, 2016a) indicate the presence of debris flow and possibly till sediments at the contamination site (fig. 2).

Since glaciation, organic-rich sediments have accumulated in depressions where saturated conditions allow organic material to accumulate. Organic sediments vary in thickness across Vilas County from absent to more than 16 feet (Attig, 1985). Results of a study at Allequash wetland, approximately 16 miles northeast of Haskell Lake in the Trout Lake watershed (fig. 1), indicated peat thicknesses exceeding 52 feet (Anderson and Lowry, 2007). Haskell Lake, Tower Creek, and the surrounding wetlands contain extensive organic deposits, described in the "Haskell Lake Substrate" section (fig. 4).

Hydrogeologic Units

The sand and gravel deposits in Vilas County are considered aquifers and produce yields suitable for domestic consumption (Batten and Lidwin, 1996). Till and debris flow deposits typically yield minimal amounts of water (Patterson, 1989). Across Vilas County, the glacial sand and gravel aquifer typically ranges from 100 to 200 feet thick. Hydraulic conductivity estimates from aquifer testing across Vilas County average about 20 feet per day in the sand and gravel deposits and less than 1 foot per day in the till and debris flow deposits (Patterson, 1989). Estimated horizontal hydraulic conductivity from slug tests in wells at the Trout Lake research site (15 miles northeast of Haskell Lake) ranged from 10 to 60 feet per day for sandy units and from about 0.002 to 2 feet per day in silty units, with a 5:1 ratio of horizontal to vertical hydraulic conductivity (Kenoyer, 1986). Few wells in Vilas County are screened in the Proterozoic bedrock because of the relatively thick and prevalent sand and gravel aquifer deposits (Attig, 1985); although the bedrock may produce sustainable yields from connected fracture networks.

Haskell Lake Substrate

The substrate beneath Haskell Lake is primarily a dark brown, diatomaceous sapropel mixed with silt (approximately 40–60 percent organic, 10 percent carbonate, and

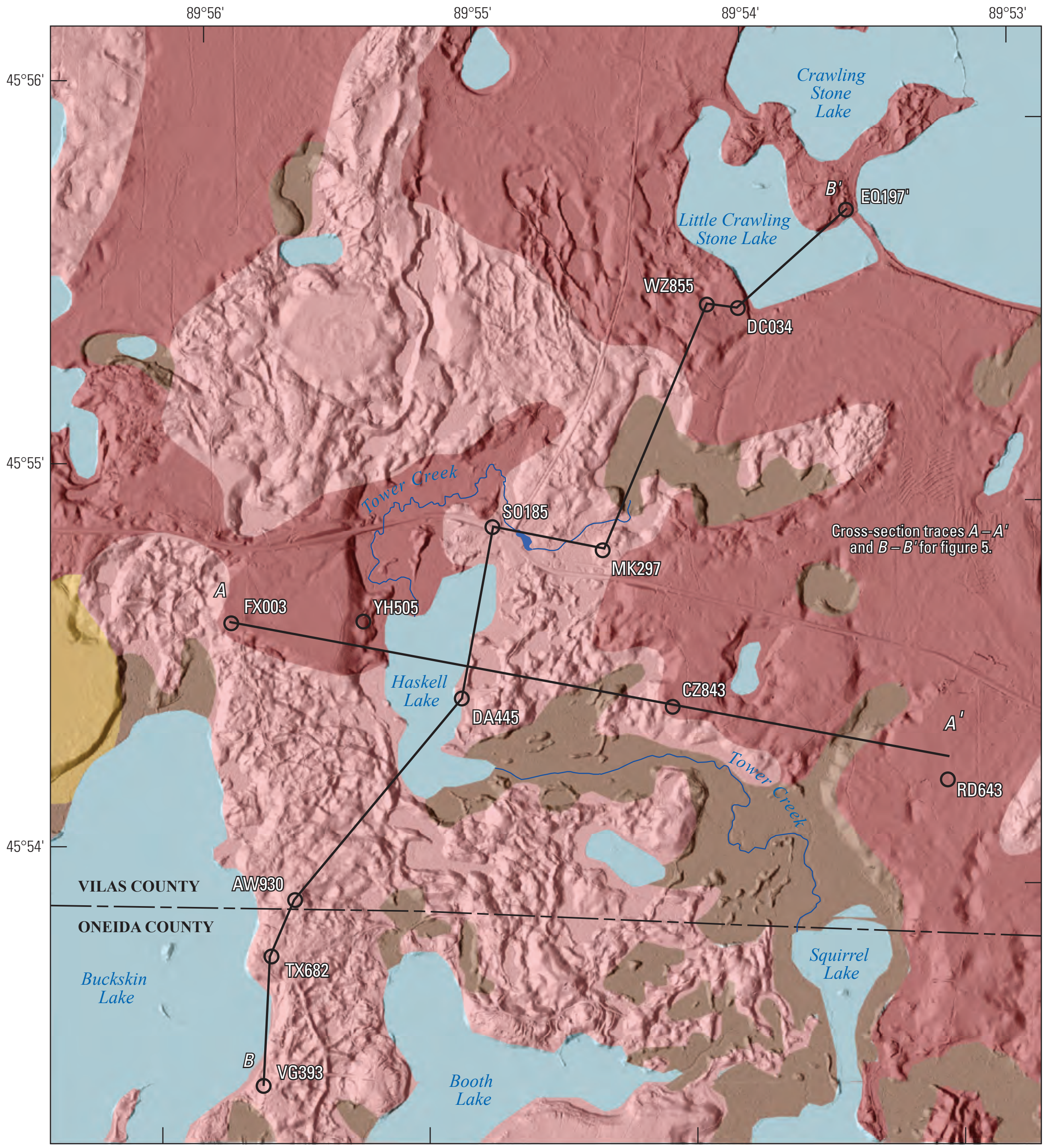

Hillshade base map modified from Vilas County Land Information and Mapping Department (2016)
Vilas County Geologic Units from Attig, 1985, 1:100,000
Oneida County Geologic Units modified from Attig and Rawling (2016), 1:100,000

EXPLANATION

Surficial geologic units

- Wgc — Wildcat Lake Member collapsed stream sediment
- Wgp — Wildcat Lake Member braided system sediment in plains
- Wgf — Wildcat Lake Member stream sediment in ice-marginal fans
- o — Organic sediment
- Open water

VG393 **Well location with construction report and label**

Figure 4. Quaternary units mapped by Attig (1985) overlain on lidar (Vilas County Land Information & Mapping Department, 2016), including locations of the well construction reports shown in the cross sections in figure 6.

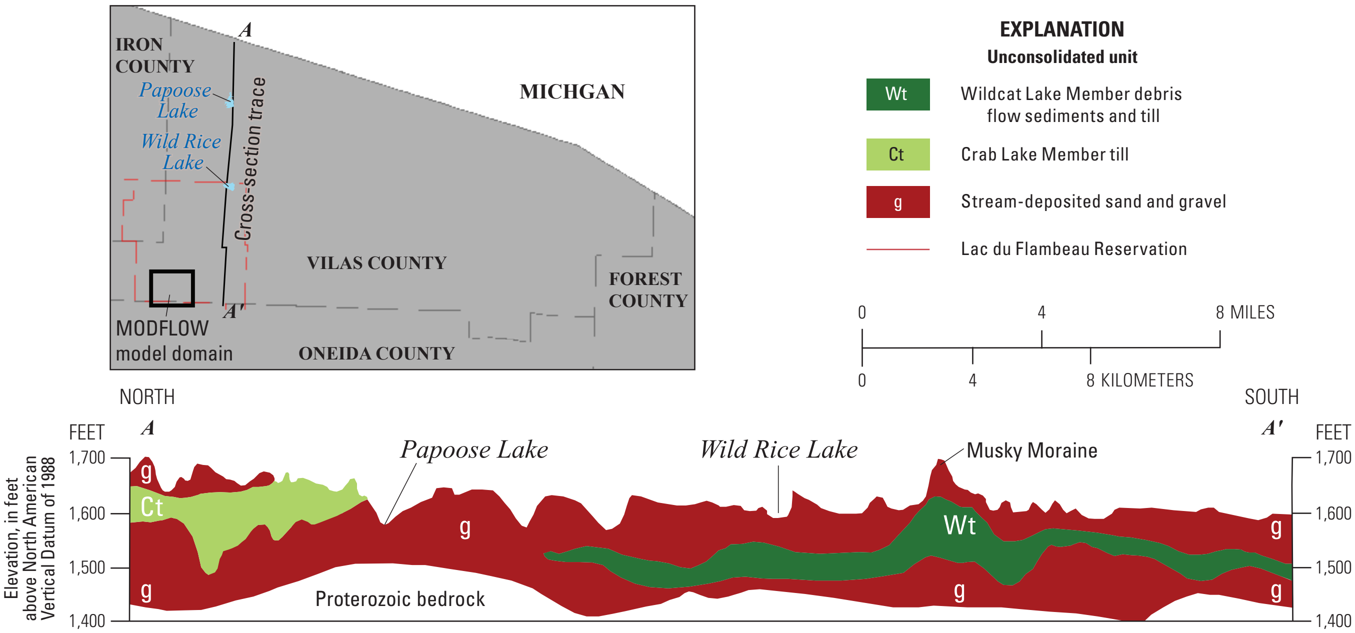

Figure 5. Cross section east of the study area (modified from Attig, 1985).

30–50 percent inorganic material), with a high water content in the upper 6 feet (Heck and others, 2013). Sapropel is a generic term often used to describe dark-colored, carbon-rich sediments, especially in postglacial settings where an increase in biological productivity following ice-retreat results in a transition from mineral to organic sediments deposition (Emeis, 2009). The sapropel in Haskell Lake overlies the sand and gravel stream deposits, ranging in thickness from absent near the shoreline to more than 30 feet thick away from shore. Although the upper layers of the sapropel are loose and highly flocculant, field experience indicates this material to be of low permeability, as evidenced by frequent difficulty in extracting pore water with a peristaltic pump, and by slow water level recovery in piezometers installed in the lakebed. The extent to which preferential flow paths (through discrete areas of higher permeability) exist in the sapropel is unknown. Unknown preferential flow paths could modify the flow paths of the contamination plume in ways that are difficult to predict with a groundwater flow model. The existence of extensive preferential flow paths (sufficient to raise the bulk permeability of the lakebed) would tend to concentrate groundwater discharge near the shore.

Subsurface Conditions at the Contamination Site

The contamination site is at the north end of Haskell Lake, between the lake and State Highway 70 (fig. 2). Depth to bedrock in this area is thought to range from about 50 to 80 feet below land surface. Subsurface materials include extensive sand and gravel but also finer-grained deposits, including possible interbeds of fine-grained materials in the upper 15 feet of the source area (Cascade Technical Services, 2016; Dakota Technologies Company, Inc., 2016; K. Hansen, LDF Tribe, oral commun., 2017). Most or all of the petroleum contamination extends from the source area southwest towards Haskell Lake (fig. 2). However, the location of the source area near a groundwater divide between Haskell Lake and Tower Creek raises the possibility of occasional flow towards Tower Creek with seasonal changes in recharge conditions. An existing network of monitoring wells at the contamination site was used in this study for collection of groundwater levels and slug testing, as described in the "Field Data Collection Methods" section.

Study Approach

Haskell Lake Water Budget and Contributing Source Area

The Haskell Lake water budget and groundwater contributing area of the Haskell Lake/Tower Creek system were estimated using a steady-state, finite difference groundwater flow model (Leaf and Haserodt, 2020) constructed with the USGS programs MODFLOW–NWT (Niswonger and others, 2011) and Soil Water Balance (SWB) code (Westenbroek and others, 2010). The model includes groundwater recharge estimated from daily climate records, simulation of groundwater levels and flow in the glacial aquifer, groundwater/surface-water interactions, and the stage and water budget for Haskell Lake. The model was informed using existing data and field data that were collected for this study between July 2016 and November 2017, as discussed in the "Field Data

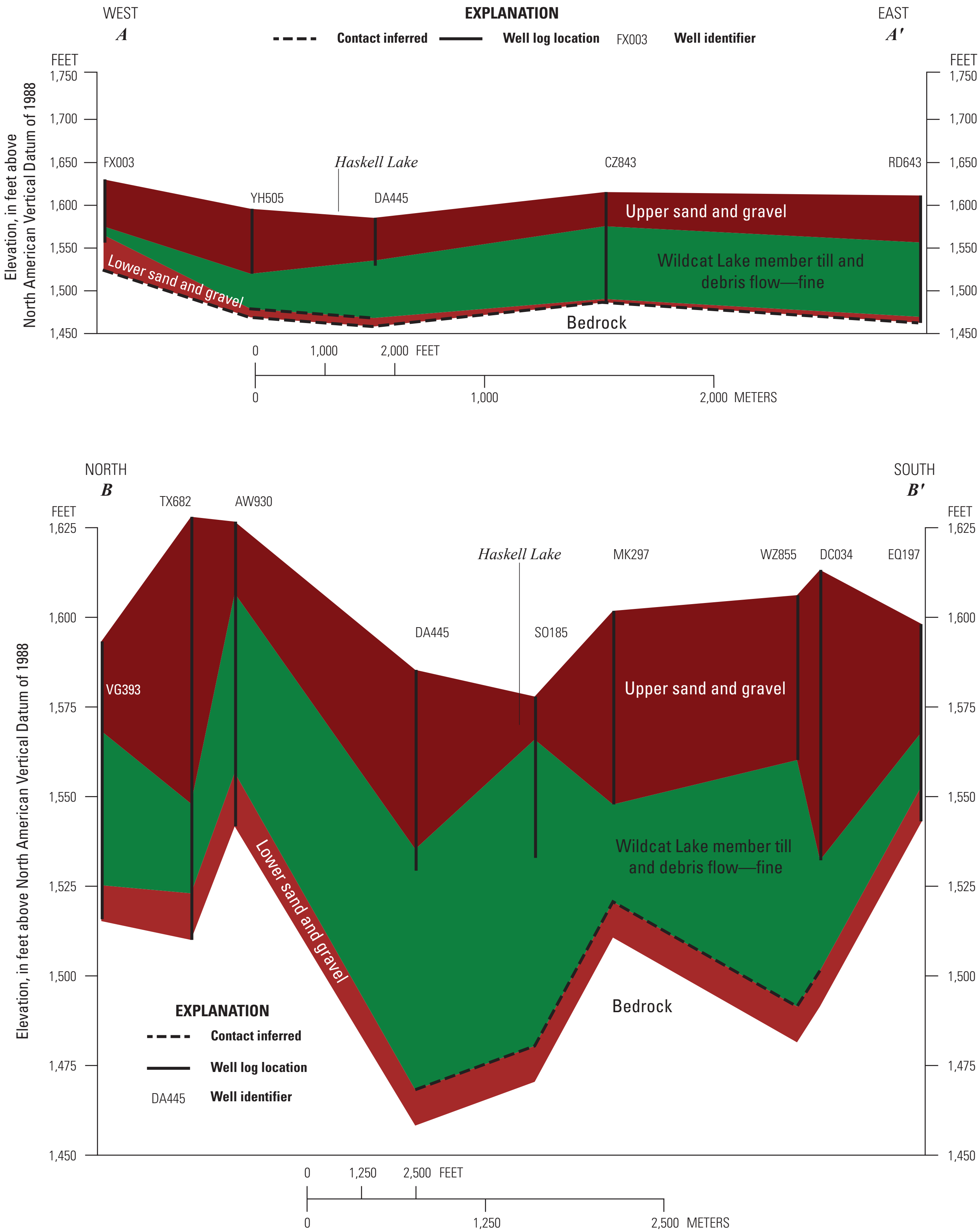

Figure 6. South-north and east-west cross section constructed from well construction report lithologic data; cross-section traces are on figure 4.

Collection" section. The areal footprint of the model is shown in figure 1.

A mass balance of measured and estimated concentrations of the stable isotope oxygen-18 (^{18}O) was used to independently estimate the groundwater inflow component of the lake water budget, following the methods of Krabbenhoft and others (1990).

Subsurface Characterization

Characterization of the glacial aquifer and subsurface conditions at the contamination site included shallow geophysical surveys led by the Wisconsin Geological and Natural History Survey (Carolyn Streiff and Dave Hart, written commun., 2017), which provided information on depth to bedrock and qualitative indication of the potential distribution of the contaminant plume. A brief description of the geophysical surveys is given in the "Field Data Collection" section and expanded on in appendix 7. Slug tests also were completed in existing monitoring wells at the contamination site to inform hydraulic conductivities used in the model and to aid future remediation plans. Finally, pore water sampling of the sediments beneath Haskell Lake was completed to help delineate the downgradient extent of the petroleum contamination plume.

Field Data Collection

This section summarizes field data collected for this study, between July 2016 and November 2017, with a brief description of methods, followed by a summary of the results. Field data collected for this study are available in the report appendixes, the National Water Information System (NWIS; U.S. Geological Survey, 2018), and the companion data release (Leaf and Haserodt, 2020). Additional details are provided in the referenced appendixes.

Methods

Estimation of the Haskell Lake water budget and delineation of the contributing groundwater flow system were informed by field measurements of groundwater and lake levels, daily precipitation, and Tower Creek streamflow. The locations and relative magnitude of groundwater discharge to Haskell Lake were evaluated indirectly using a network of mini-piezometers and temperature measurements of the lakebed and pore water sediments. Net groundwater discharge to Haskell Lake was indirectly estimated using a stable isotope (^{18}O) mass balance. Understanding of the plume extent beneath Haskell Lake was directly informed by pore water sampling and indirectly informed by other data through the groundwater flow model. Understanding of depth to bedrock and hydraulic conductivity at the contamination site was improved through various geophysical methods and slug testing. Each type of field data collection is described in more detail below and in the referenced appendixes.

Groundwater Levels

Depth to water was measured quarterly in existing monitoring wells at the contamination site (fig. 7), following standard USGS procedures (Cunningham and Schalk, 2011). In addition, the MW16 well nest (MW16, MW16D and MW16E) was instrumented with pressure transducers for continuous recording of water levels (Cunningham and Schalk, 2011) from July 2016 to February 2018 (USGS sites 455448089545001, 455448089545002, and 455448089545003; fig. 8; appendix 1). Some of the wells measured on March 1, 2017, could not be measured in subsequent quarters because of access restrictions.

Lake Levels

Lake water level elevations were measured seasonally at Squirrel, Crawling Stone, Booth and Buckskin Lakes and at two unnamed lakes along Old Prairie Road northwest of Haskell Lake, using a survey-grade Global Positioning System (GPS) unit (locations shown on fig. 9 and measured elevations shown on fig. 10; appendix 2). One-time water level measurements were also measured for Tippecanoe, Broken Bow, and Jerms Lakes (fig. 9) in October 2016. Water levels for Haskell Lake were recorded continuously for the study period (USGS site 455430089550001; fig. 11).

Precipitation and Tower Creek Discharge

A continuous streamgage (USGS site 05392187) and collocated precipitation monitoring site (USGS site 455452089551701) were installed on Tower Creek at State Highway 70 (fig. 9) and were operated for the duration of the project (U.S. Geological Survey, 2018). Streamflow (fig. 12) was estimated from measured stream stage and periodic discharge measurements using a rating curve (Turnipseed and Sauer, 2010). Base flow was determined from hydrograph separation using the modified base-flow-index (BFI) method (Wahl and Wahl, 1988; Institute of Hydrology, 1980). Streamflow at three other sites along Tower Creek (USGS sites 05392186, 05392188, and 05392189; locations shown on fig. 9) was measured using methods by Turnipseed and Sauer (2010) during a synoptic flow survey on November 2, 2017. The results of the synoptic flow survey are summarized in appendix 4.

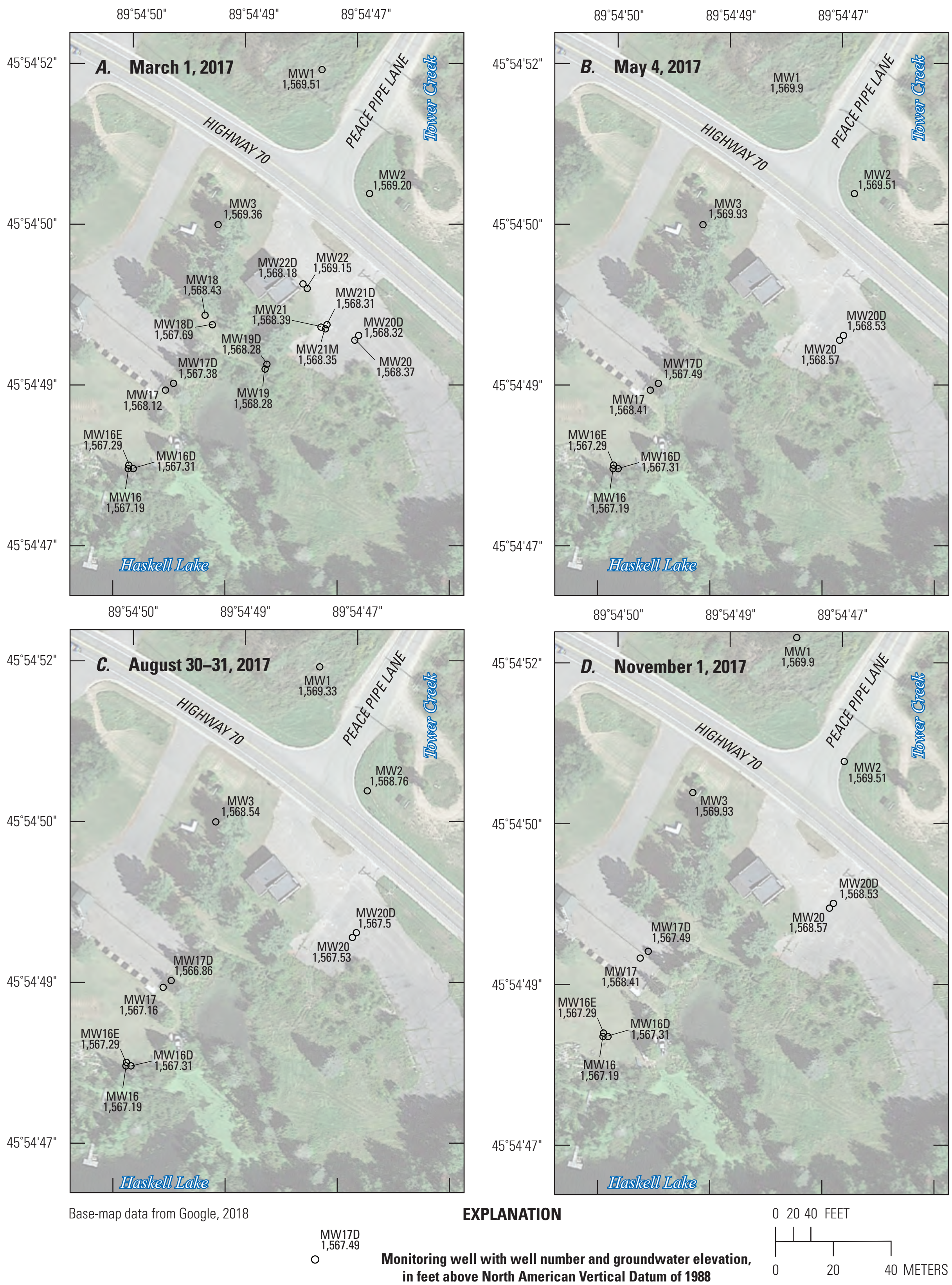

Figure 7. Measured groundwater levels at the Haskell Lake contamination site. *A*, March 1, 2017; *B*, May 4, 2017; *C*, August 30–31, 2017; and *D*, November 1, 2017. Deep intervals at nested wells are indicated by the "D" suffix (with shallow wells having no suffix). At location MW16, "D" indicates an intermediate depth, with "E" indicating the deepest interval, near the bedrock surface.

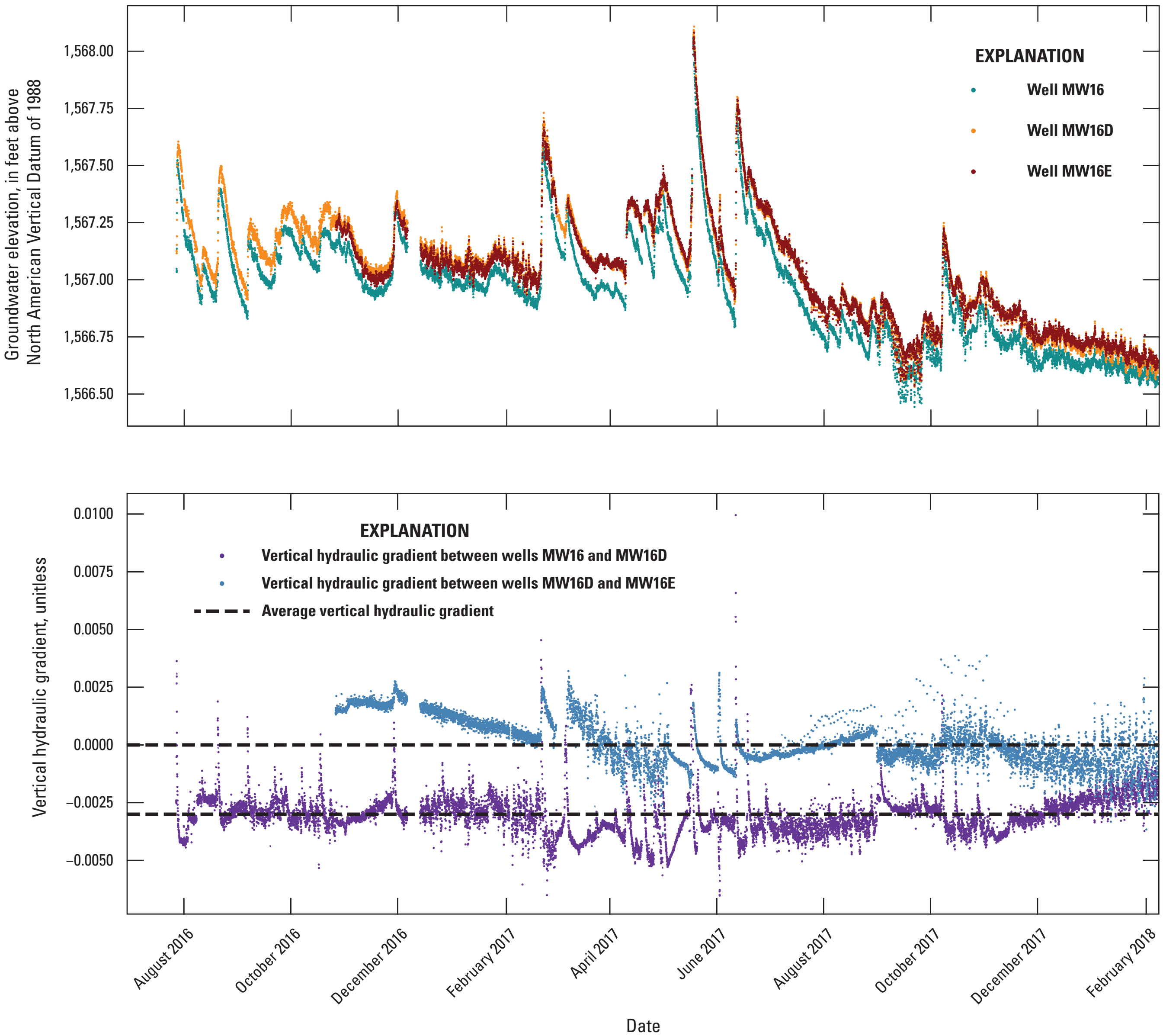

Figure 8. Continuous groundwater elevation record and calculated vertical hydraulic gradients in MW16 well nest (U.S. Geological Survey sites 455448089545001 [MW16], 455448089545002 [MW16D], and 455448089545003 [MW16E]).

Groundwater Discharge to Haskell Lake

Groundwater discharge to Haskell Lake was evaluated at several scales using the following field methods:

- A network of mini-piezometers was established around Haskell Lake (fig. 9) and measured in May, August, and November 2017. The mini-piezometers provided information on groundwater levels a few feet beneath the lake, which were compared to lake levels to establish hydraulic gradients (appendix 3).
- Groundwater discharge fluxes to the lake were also estimated by monitoring lakebed temperature at various depths of up to 1 foot beneath the lakebed using vertical temperature profilers (fig. 9). Phase lags and differences in the amplitude of the diurnal temperature signals can provide information on the rate of groundwater flux through the lakebed; with more rapid attenuation of thermal diurnal signals with depth expected in areas of high groundwater discharge (appendix 6).
- A distributed temperature sensing survey was performed with the goal of identifying areas of groundwater discharge to Haskell Lake downgradient from the petroleum contamination plume. A fiber-optic cable was installed on the lakebed, and

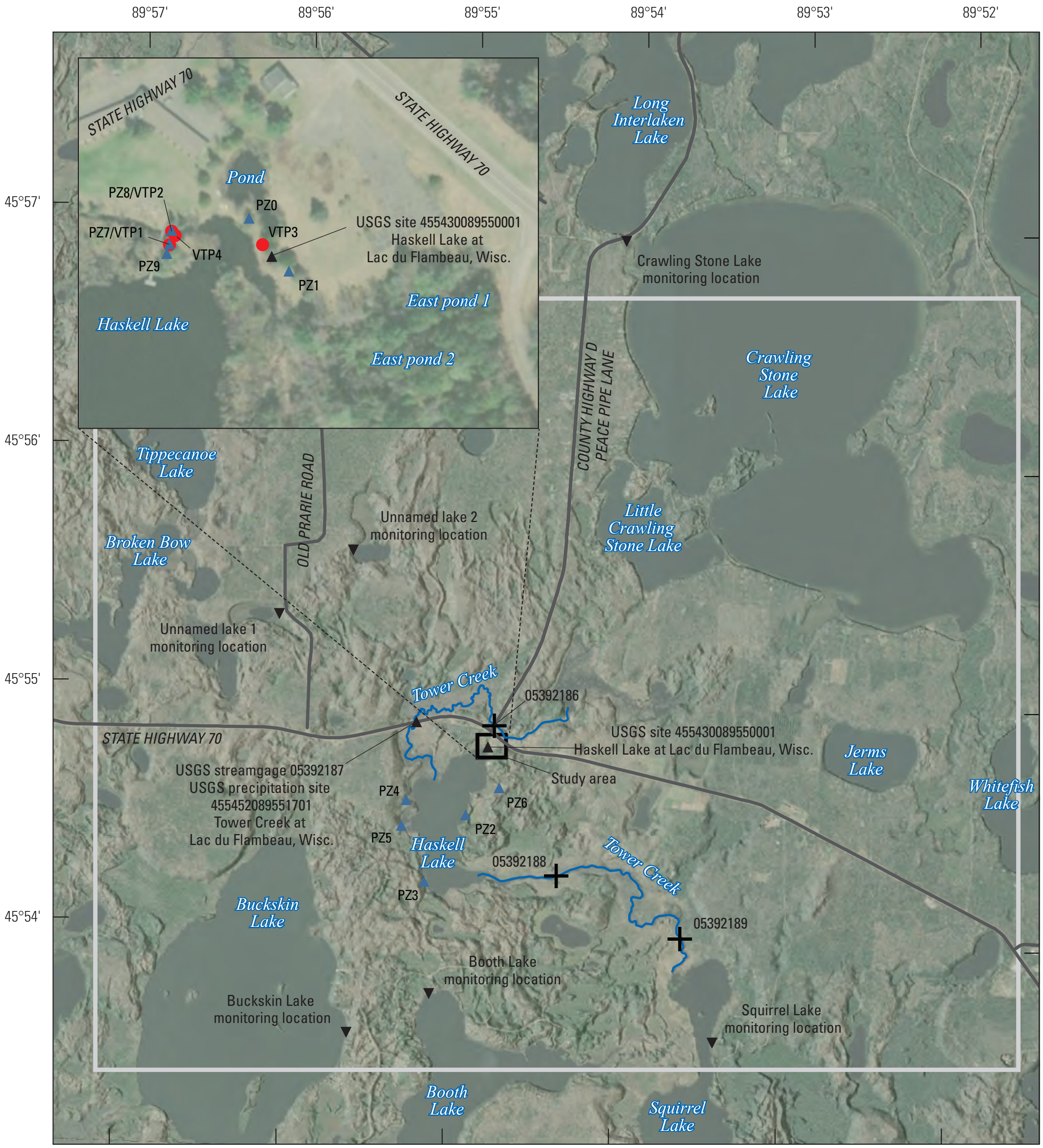

Rivers and lakes from Wisconsin Department of Natural Resources, 2015, 1:24,0000
Major roads from U.S. Department of Commerce, 2014
Hillshade base map modified from Vilas County Land Information and Mapping Department (2016)
Map image is the intellectual property of Esri and is used herein under license.

0 0.5 1 MILE
0 0.5 1 KILOMETER

EXPLANATION

- **MODFLOW model domain**
- **Lake level monitoring location and label**
- **Major roads**
- **Mini-piezometer**
- **Vertical temperature profiler**
- **Synoptic flow survey locations**
- **U.S. Geological Survey (USGS) site and label**

Figure 9. Location map showing lake level monitoring sites, U.S. Geological Survey sites, synoptic flow survey locations, vertical temperature profilers, and mini-piezometers around Haskell Lake, Wisconsin.

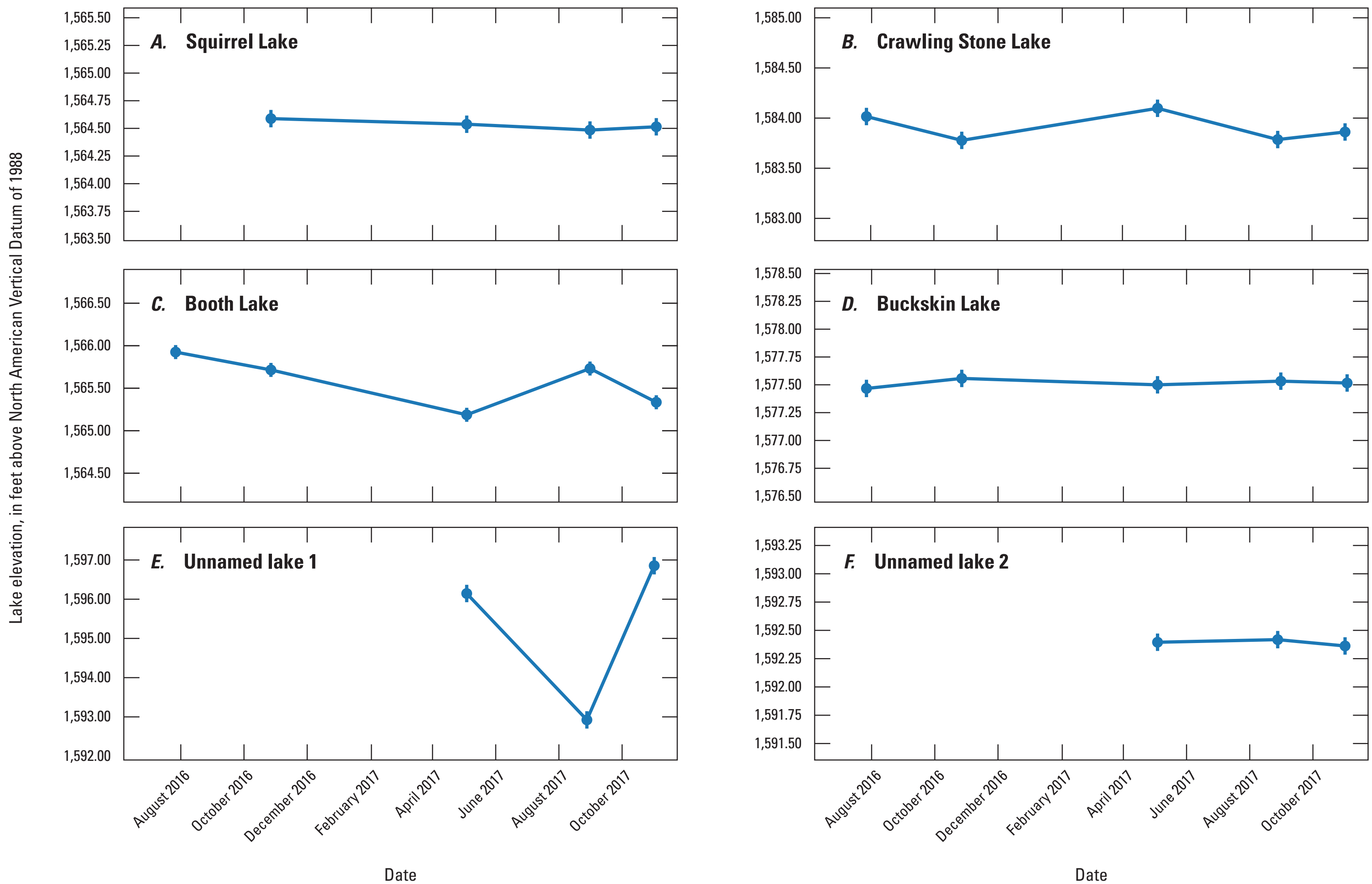

Figure 10. Seasonal water levels measured for lakes near Haskell Lake, July 2016 to November 2017.

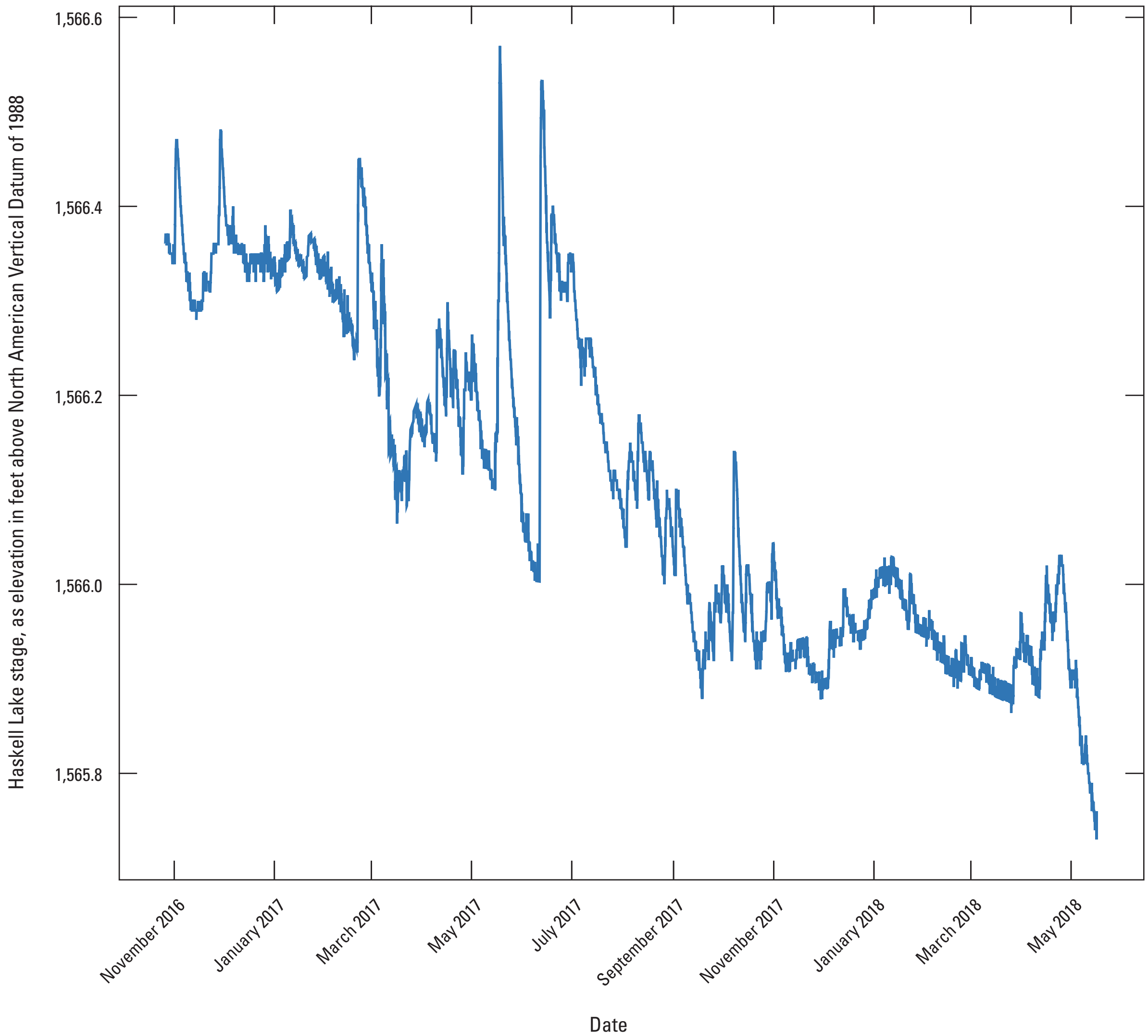

Figure 11. Continuous water levels measured at Haskell Lake, October 2016 to May 2018.

temperatures along the cable were measured continuously from July 27, 2016, to August 1, 2016. Average temperatures for the early morning prior to sunrise, when the confounding effects of solar radiation are absent, were interpreted to indicate relative quantities of groundwater discharge, with cooler average temperatures signifying greater amounts of groundwater discharge (Leaf, 2020).

- The stable isotopes ^{18}O and deuterium (hydrogen-2 [^{2}H]) are naturally occurring in water molecules and conservative at typical groundwater temperatures, meaning they do not degrade or interact with aquifer solids. At the water surface, however, evaporation causes fractionation by preferentially removing lighter isotopes (oxygen-16 [^{16}O] and hydrogen-1 [^{1}H]), leaving behind higher concentrations of the heavier isotopes (^{18}O and ^{2}H). Fractionation makes stable isotopes a useful tool for discriminating among sources of water that have different exposure to evaporation (for example, Leaf and others, 2015; Krabbenhoft and others, 1990; Özaydin and others, 2001).

Stable isotopes were used in this study to provide an estimate of the groundwater influx to Haskell Lake independent of the groundwater model. Water samples were collected periodically at the Tower Creek streamgage (USGS site 05392187) between October 2016 and February 2018 and on three occasions from Haskell Lake during the fall and spring turnover events. Analysis of water isotopes was completed at the USGS Reston Stable Isotope Laboratory (https://isotopes.usgs.gov/). The methods of Krabbenhoft and others (1990), including the local meteoric water line established in that study, were then used to estimate a lake water budget from the stable isotope data (appendix 8).

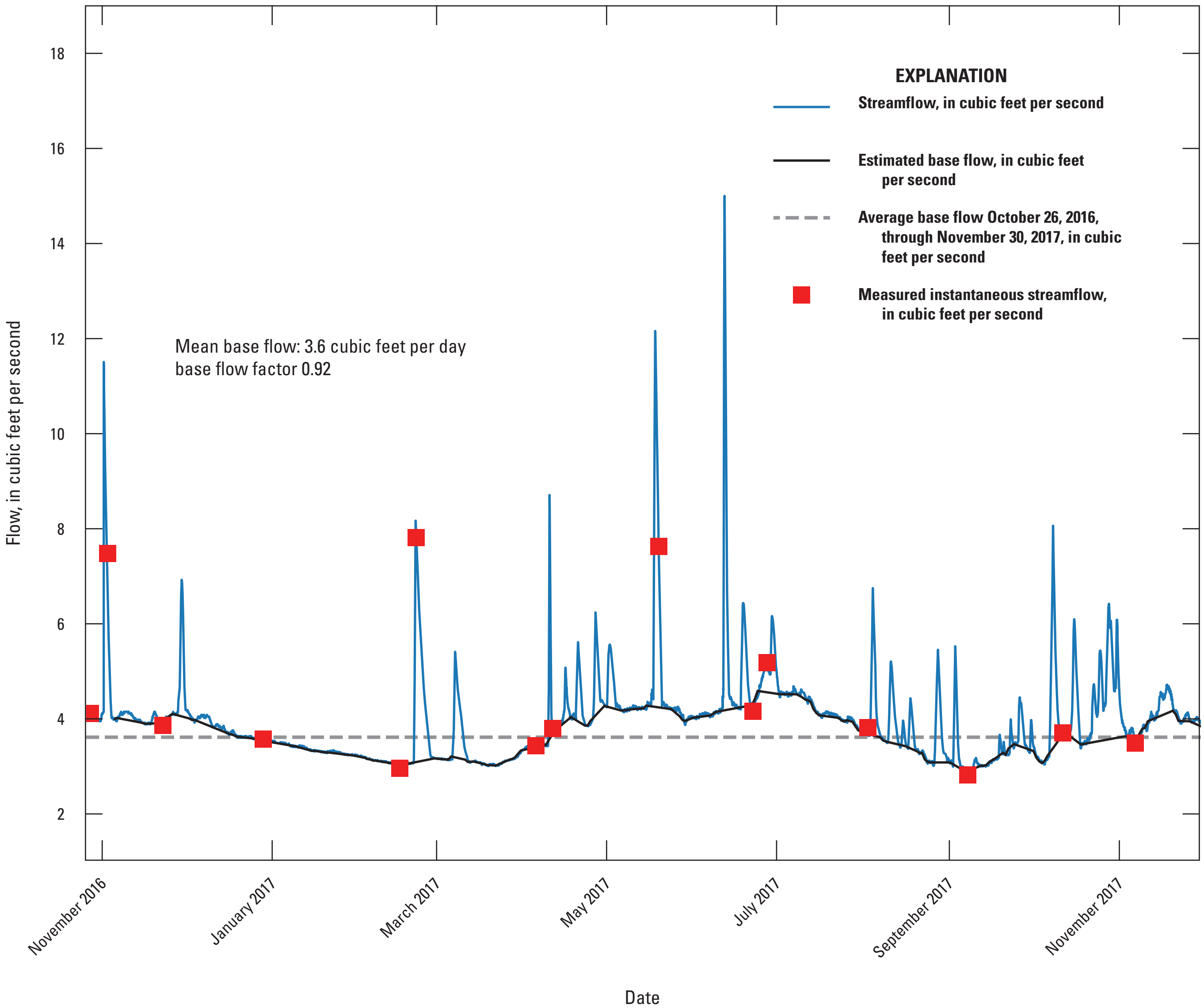

Figure 12. Continuous streamflow record for Tower Creek at U.S. Geological Survey site 05392187, with manual instantaneous streamflow measurements and separated base flow, October 26, 2016, to November 30, 2017.

Depth to Bedrock

A horizontal-to-vertical spectral ratio passive seismic survey was led by Wisconsin Geological and Natural History Survey staff on May 15–16, 2017, and June 27–28, 2017, to improve knowledge of depth to bedrock around the study area (appendix 7). Unlike traditional seismic methods that use an active sound source, passive seismic uses naturally occurring vibrations in the Earth to estimate the depths to subsurface contacts between materials, such as the bedrock surface. Although the method allows for rapid data collection, the results are generally less accurate and errors in estimated depths can be 25 percent or greater (Chandler and Lively, 2016). Therefore, a refraction seismic survey was also completed at the Haskell Lake contamination site.

Aquifer Hydraulic Conductivity

Slug tests were performed in monitoring wells MW1, MW2, MW3, MW16, MW16D, MW16E, MW17, MW17D, MW20, and MW20D, following standard USGS procedures (Cunningham and Schalk, 2011; appendix 5). Results from the tests provide estimates of aquifer hydraulic conductivity in the areas of the aquifer immediately adjacent to the screened intervals of these wells.

Electrical resistivity imaging and electromagnetic ground conductivity (EM31) surveys were led by Wisconsin Geological and Natural History Survey staff (appendix 7) to investigate lithologic heterogeneity (for example, sand and gravel compared to debris flow deposits) and bedrock surface elevations, if feasible.

Pore Water Sampling

Lakebed pore water samples were collected on August 3, 2016, and August 29–30, 2017, following the methods described in appendix 9, to improve understanding of the downgradient extent of the petroleum contamination plume and where the plume discharges to Haskell Lake. PushPoint (Henry) sampling devices (M.H.E. Products, 2003) and stainless steel drive-point piezometers (Solinst, 2013) were installed temporarily into the lakebed, with samples collected using a peristaltic pump and a low-flow sampling approach (appendix 9). Samples were submitted to the LDF Tribe following collection and then analyzed by Northern Lake Service (2016, 2017) for VOCs (EPA method 8260), 1,2–dibromoethane (ethylene dibromide; EPA method 504.1), arsenic, cadmium, lead, and several redox parameters (appendix 9).

Results and Discussion

Groundwater Flow and Discharge to Haskell Lake

Measured water levels in the surrounding lakes generally varied within plus or minus (±) 0.5 foot during the study period, with the exception of Unnamed Lake 1, a small seepage lake, where a range of 4 feet was observed (fig. 10). Continuous water levels recorded for Haskell Lake provide a sense of the natural variability that is missed by synoptic seasonal measurements (fig. 11). Such short-term variability might locally reverse hydraulic gradients but does not appreciably affect larger regional flow patterns (for example, the direction of groundwater flow between two lakes that are several feet or more different in elevation). Viewed spatially, the average water levels of the surrounding lakes and lack of other discharge features indicate a general direction of groundwater flow towards Haskell Lake and Tower Creek (fig. 13).

The 2017 quarterly groundwater measurements in the contamination site monitoring wells are shown on figure 7. Deep intervals at nested wells are indicated by the “D” suffix (with shallow wells having no suffix). At location MW16, “D” indicates an intermediate depth, with “E” indicating the deepest interval, near the bedrock surface. Groundwater elevations were highest in May following spring recharge and declined through August and November. Vertical hydraulic gradients at most paired wells were generally downward during all four quarters, except at the MW16 well nest near Haskell Lake where consistent upward gradients were measured. The magnitude of the downward gradients generally decreased from spring to fall, following the overall seasonal trend in groundwater levels. Overall, the groundwater elevation data show downward and lateral movement of groundwater across most of the contamination site, except in the areas near Haskell Lake where the MW16 well nest shows consistently upward groundwater movement towards the lake (fig. 7).

Continuous water level records at the MW16 well nest (fig. 8) show seasonal fluctuations within 1 foot of the mean. Rapid responses to precipitation and snowmelt are consistent with the position of the water table within 2 feet of land surface at this location. In contrast to the variable gradients measured in the other well nests, the upward gradient between MW16 (the shallowest well) and MW16D (the middle well) was relatively steady at about −0.003, with the exception of the spring months of 2017 when the upward gradient increased to about −0.005, likely in response to snowmelt. The gradient between MW16D (the middle well) and MW16E (the deepest well) averaged slightly positive, which would indicate downward flow. This result could be explained by higher hydraulic conductivity values in the lower interval providing an enhanced connection to the lake, or as an artifact of survey error in the wellhead elevations.

Average hydraulic gradients measured by the mini-piezometers around Haskell Lake are shown in figure 14, and plots of all measurements are shown in figure 15. Although knowledge of lakebed permeability is needed in addition to gradients to estimate discharge fluxes, gradients measured by the mini-piezometers provide a qualitative indication of the variability in groundwater discharge around Haskell Lake, assuming hydraulic conductivities are similar. The measured gradients indicate groundwater discharge (negative values) to Haskell Lake around most of its perimeter, with the possible exception of the area near the outlet, which was not measured, and the positive November 2017 gradient at location PZ8 (fig. 14), which was thought to be erroneous based on the consistent negative gradients measured elsewhere. Larger gradients on the western side of the lake are consistent with a steeper gradient in the water table between Buckskin Lake and Haskell Lake (fig. 13). Measured gradients near the petroleum contamination plume indicate groundwater discharge to Haskell Lake downgradient from the plume source area. Average, early morning lakebed temperatures recorded during the distributed temperature survey indicate stronger groundwater discharge near shore, with some possible areas of preferential discharge either beneath or along the outside edge of the floating bog near the dock for Haskell Lake Lodge (fig. 16).

Groundwater flux into the lake was successfully estimated at one vertical temperature profile site, VTP4 (location shown in figure 9), using the VFLUX program (Irvine and others, 2015, 2017). An average upward flux of 1.9 ± 0.3 feet per day was estimated at VTP4. This result agrees with the upward vertical hydraulic gradients observed in the nearby mini-piezometers and in the MW16 well nest.

Precipitation and Tower Creek Base Flow

Flows in Tower Creek estimated from continuous recording of stage and periodic manual instantaneous measurements of streamflow are shown in figure 12. Base flow averaged 3.6 cubic feet per second during October 26, 2016, and November 30, 2017, and accounted for about 92 percent of the

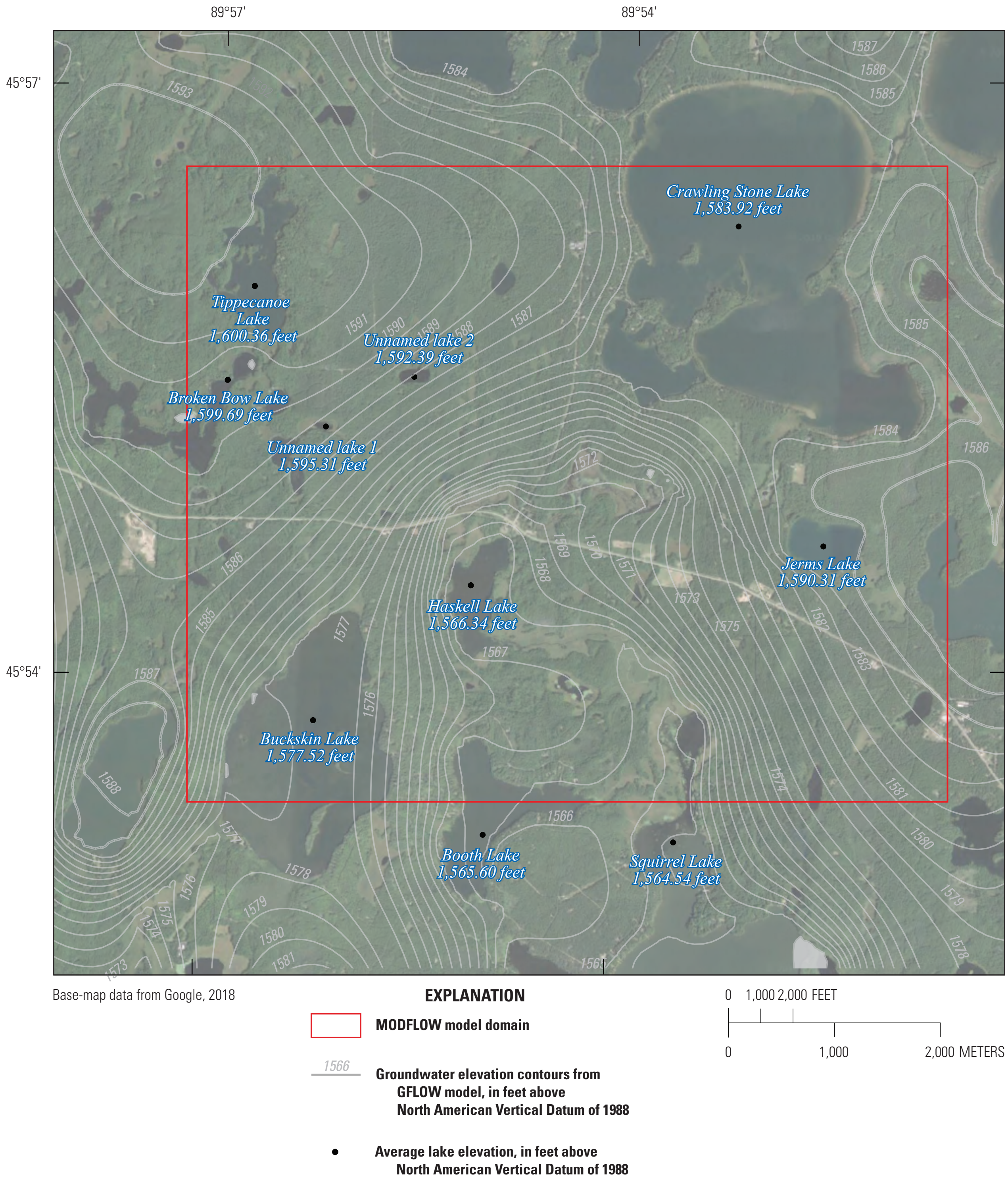

Figure 13. Average lake elevations measured between July 2016 and November 2017, with contours of equal water-table elevation from the GFLOW groundwater flow model described in appendix 10.

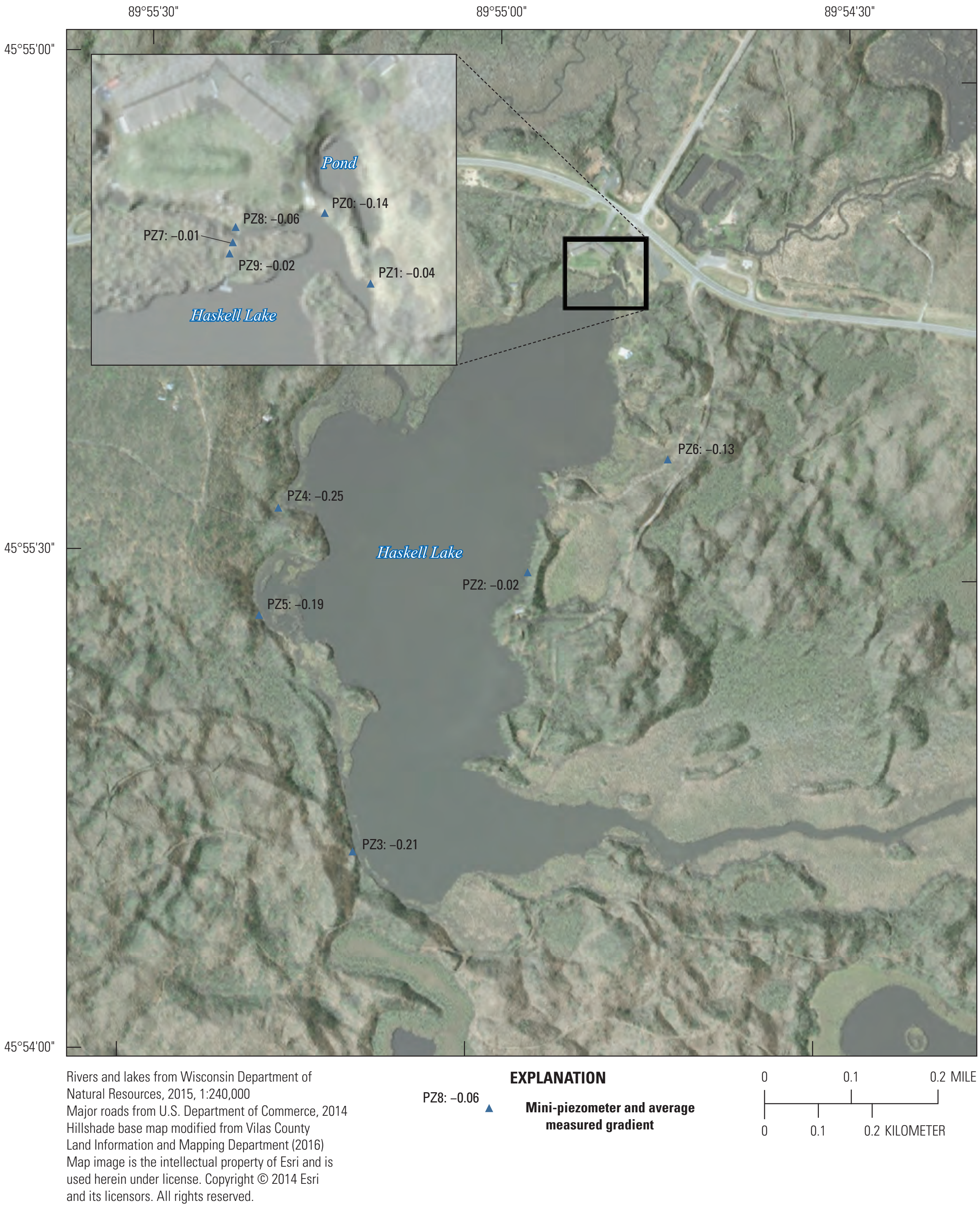

Figure 14. Average hydraulic gradients measured in mini-piezometers, 2017.

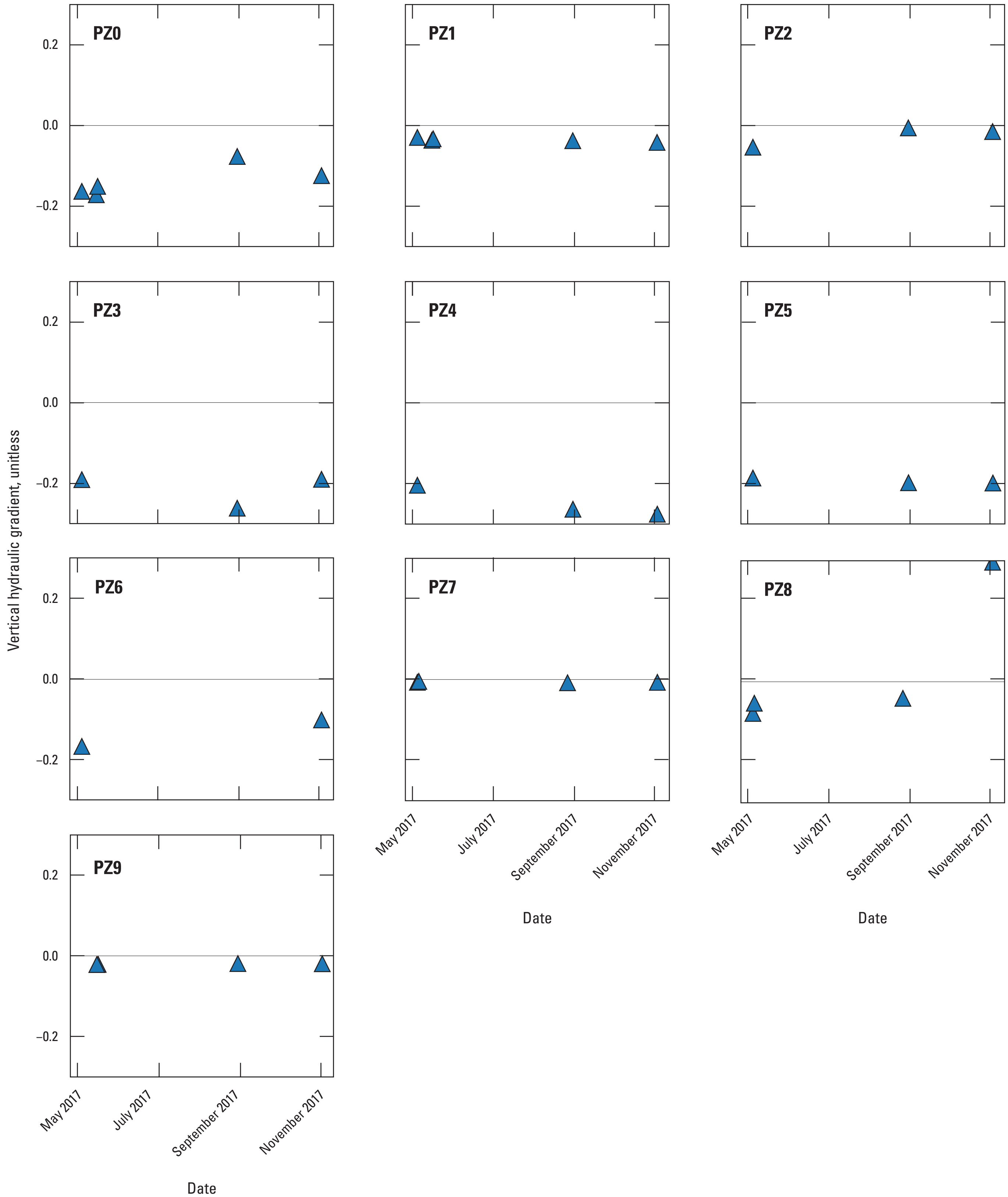

Figure 15. Vertical hydraulic gradients measured in mini-piezometers, 2017.

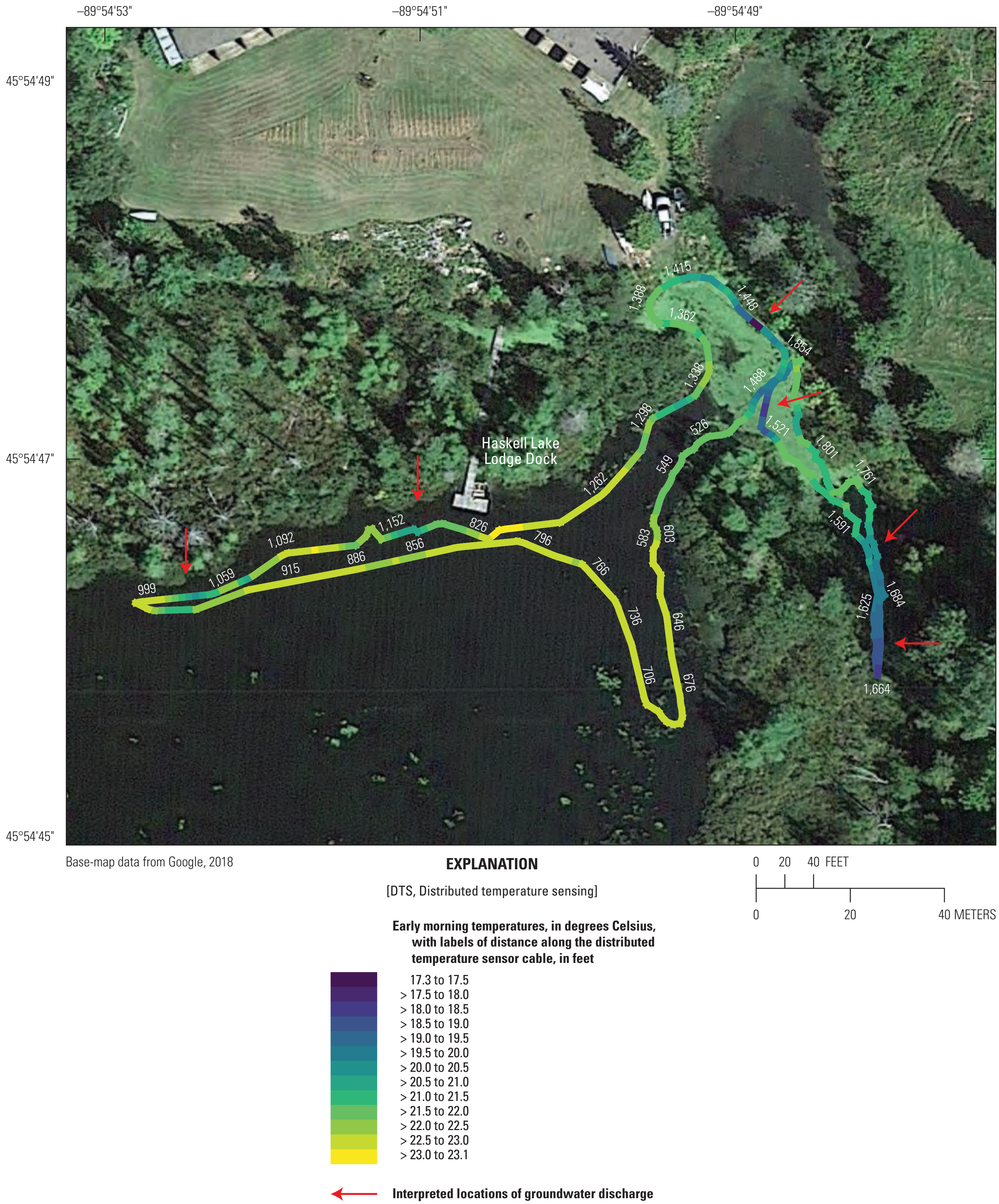

Figure 16. Average early morning lakebed temperatures measured with a distributed temperature sensor on July 28, 2016, through August 1, 2016.

total flow in the creek. This period was wetter than normal, with 44.8 inches recorded at Lakeland Airport (NOAA, 2018b; fig. 1), compared to a long-term average of 32 inches per year (for 1981–2010; NOAA, 2018a). Therefore, the long-term average base flow in Tower Creek is likely lower than the average for 2017. Figure 17 compares daily total precipitation for Lakeland Airport (NOAA, 2018b), the Minocqua weather station (NOAA, 2018a; fig. 1), and the Tower Creek precipitation site (USGS site 455452089551701; U.S. Geological Survey, 2018); values are only summed for the nonwinter seasons because the Tower Creek precipitation site did not record liquid equivalents of snow.

The November 2, 2017, synoptic flow survey of Tower Creek (fig. 9) was completed during base-flow conditions that were near the average base flow for the study period; estimated average streamflow for November 2, 2017, at the Tower Creek streamgage (USGS site 05392187) was 3.8 cubic feet per second (compared to the 3.6 cubic feet per second base flow average for the study period). Therefore, the measured streamflow values are assumed to reflect average groundwater recharge in the upstream watershed and the distribution of groundwater discharge along Tower Creek.

Depth to Bedrock and Aquifer Hydraulic Conductivity

Results of the passive seismic survey, combined with the earlier interpretation of Batten and Lidwin (1996) indicate that Haskell Lake and Tower Creek occupy a historical valley in the bedrock surface (fig. 18) that predates the most recent glaciation. Depths to bedrock ranged from 46 to 178 feet below land surface across the study area, with bedrock depths at the contamination site ranging from approximately 50 to 80 feet (fig. 18; appendix 7).

Slug test results yielded horizontal hydraulic conductivity estimates that ranged from approximately 1 to 60 feet per day, with the highest values occurring at the MW20 well nest (40 to 60 feet per day) and MW16E (19 feet per day), which is thought to be screened near the bedrock surface. The remaining wells tested had values less than 10 feet per day, with values of 1 foot per day at the MW17 well nest (appendix 5). Hydraulic conductivities of less than 10 feet per day are indicative of a moderate to high silt content (for example, Fetter, 1994; Schwartz and Zhang, 2003) and may indicate the predominance of debris flow and possibly till deposits in the upper 30 feet of sediments west of the plume center (fig. 2). Higher values at the MW20 well nest and MW16E are consistent with poorly sorted sand and gravel (for example, Fetter, 1994; Schwartz and Zhang, 2003) and, therefore, may indicate outwash of the Wildcat Lake Member and sands and gravels predating the Wildcat Lake Member at depth.

Pore Water Sampling

Pore water samples were successfully collected in seven locations, including four locations along the shoreline, and three locations away from shore along the dock for Haskell Lake Lodge (fig. 19). Collecting pore water samples from the lakebed sapropel was difficult. Only one-half of the sites attempted were successfully sampled (appendix 9). The sapropel was only successfully sampled at locations PW7 and PW11 (at respective depths of 31 and 36 feet; fig. 19). The remaining five samples were collected from mineral sediments near the shore, or beneath the sapropel. The difficulties encountered with sampling the lakebed sapropel sediments present a fundamental challenge to defining the downgradient extent of the plume in the field. A customized coring method that preserves pore water in situ within the sapropel would probably be required.

Detections of the contaminants of concern included benzene, lead, 1,1,2-trichloroethane, and naphthalene (table 9.1; Northern Lake Service, Inc., 2017). Benzene was detected in the three deepest samples collected along the dock, at depths of 11–36 feet, with the highest concentrations below 30 feet, at distances of 30–70 feet from shore (locations PW11 and PW7). Also detected in PW7 was 1,1,2-trichloroethane, a degradant of the solvent 1,1,2,2-tetrachloroethane (Agency for Toxic Substances and Disease Registry, 1989). Samples collected along the shore at a depth of about 1 foot had no benzene above the detection limit but had minor amounts of other VOCs (PW3 and PW6b). Samples collected at locations PW0 and PW1 had no benzene or other VOC detections. Sampling of other locations was precluded by access issues or an inability to pump pore water from the lakebed sediments. These results indicate that the fine lakebed sediments may be limiting vertical discharge of the plume.

Stable Isotope Mass Balance

The ratio between the stable isotopes of oxygen ($^{18}O/^{16}O$) was used with the mass balance method (Krabbenhoft and others, 1990; Özaydin and others, 2001) to estimate a total groundwater inflow to Haskell Lake of 104 inches per year (8.7 feet per year [ft/yr]) across the same lake area used in the MODFLOW model. A first-order sensitivity analysis estimated a 95 percent confidence interval of ± 67 inches per year, following the methods of Krabbenhoft and others (1990) and Krabbenhoft (1988). The large error stems from Haskell Lake and Tower Creek being isotopically similar to the groundwater (with respect to $^{18}O/^{16}O$), making it difficult to distinguish the groundwater contribution. Additionally, the stable isotope mass balance method requires numerous assumptions about the various input terms, particularly those used to estimate the

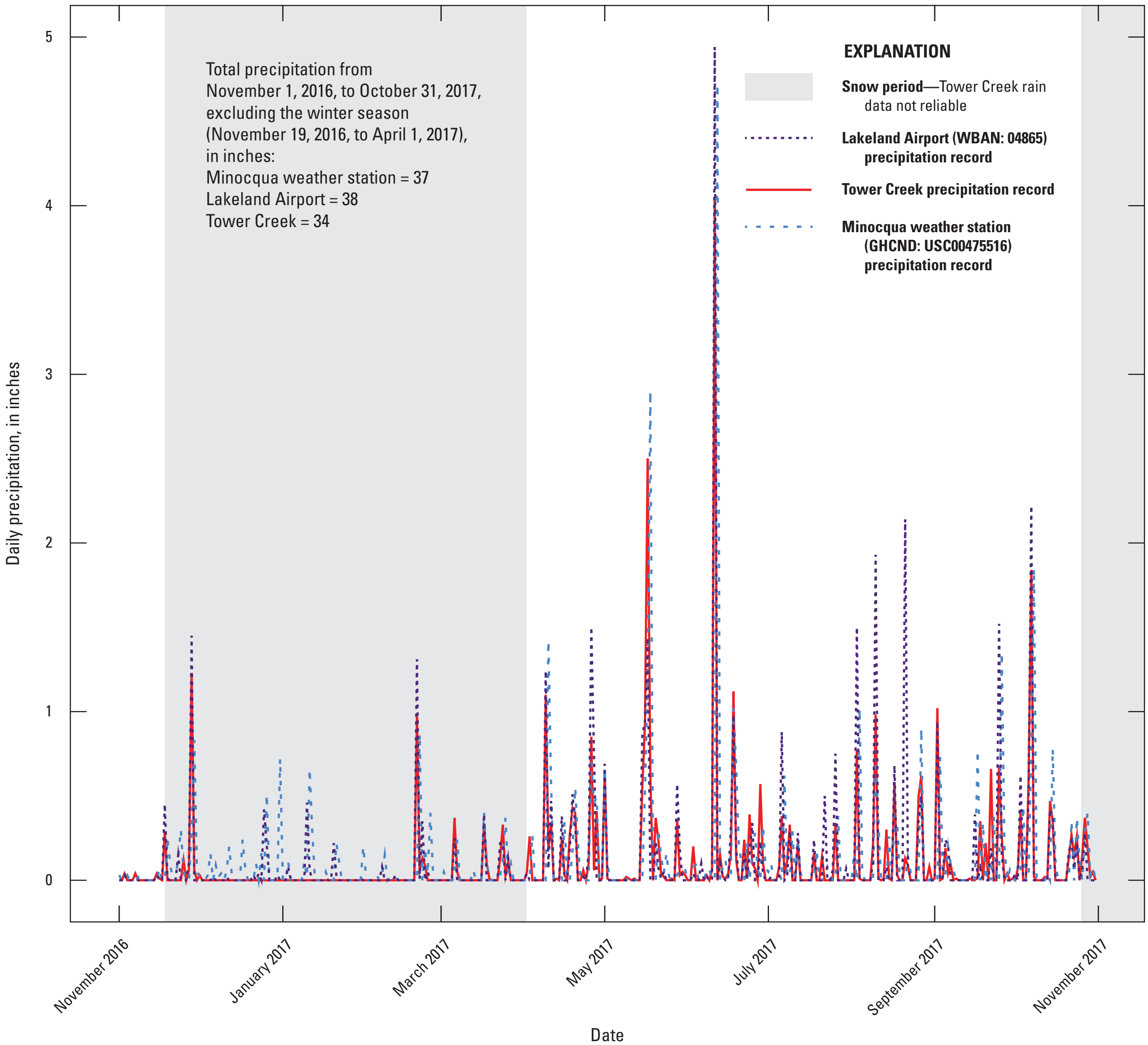

Figure 17. Precipitation recorded at Lakeland Airport, the Minocqua weather station, and the Tower Creek precipitation site (USGS site 455452089551701), November 2016 through October 2017.

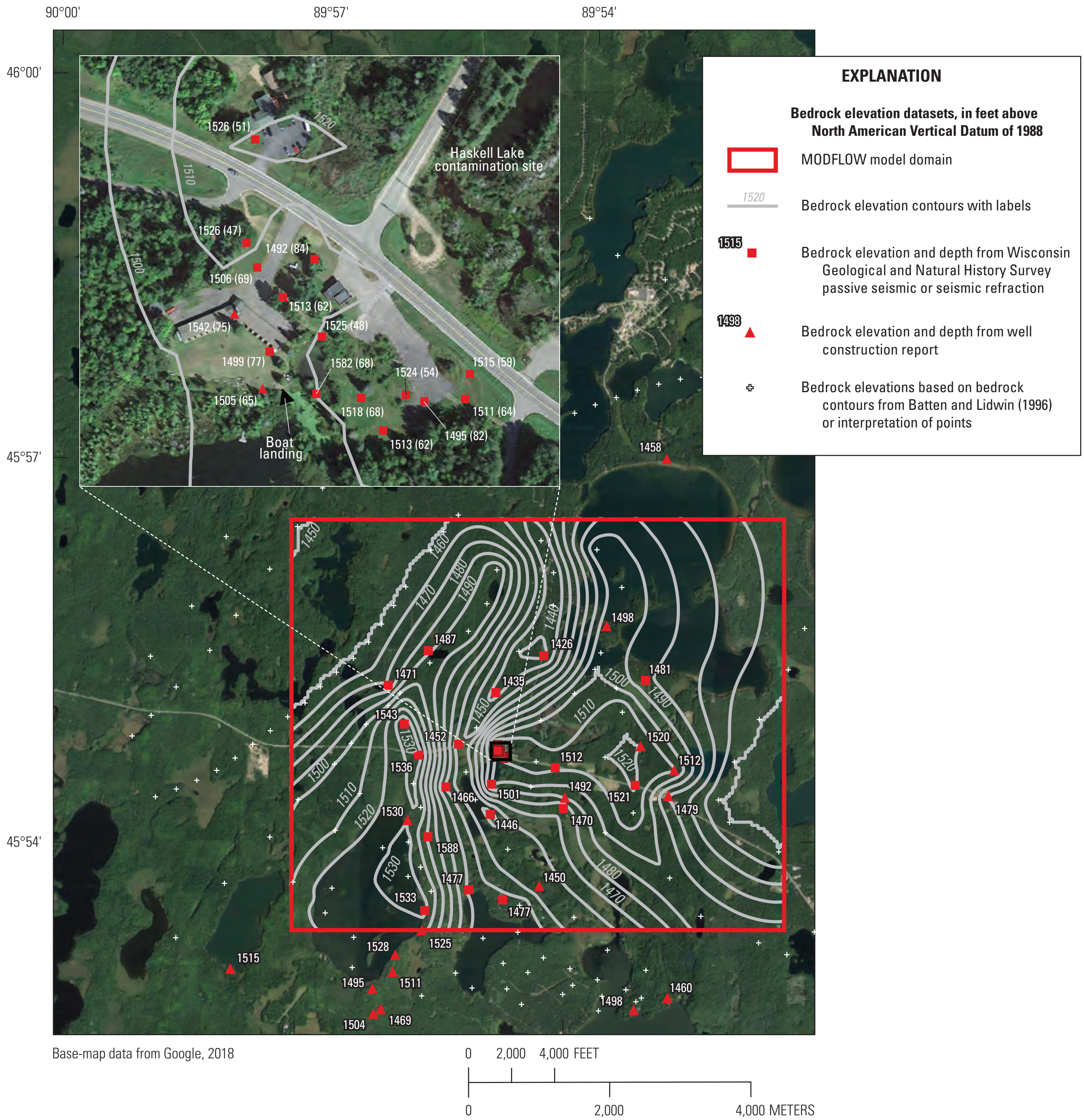

Figure 18. Bedrock surface elevations derived from the passive seismic and seismic refraction surveys completed May 15–16, 2017, and June 27–28, 2017, combined with the earlier interpretation of Batten and Lidwin (1996). Values in parentheses indicate depths to bedrock, in feet below land surface.

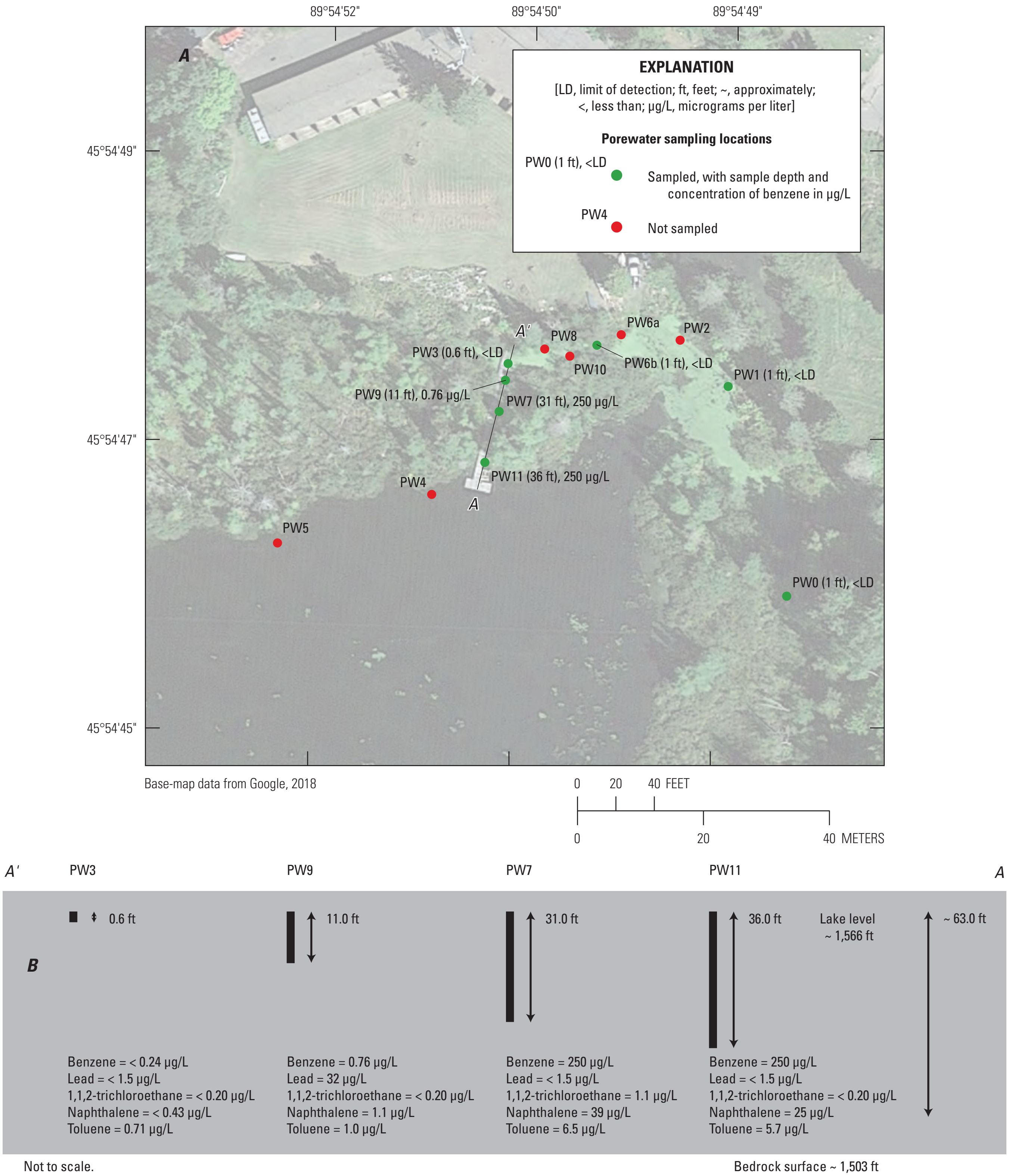

Figure 19. Results of pore water sampling completed August 3, 2016, and August 29–30, 2017. *A*, map; *B*, cross section showing samples collected along the Haskell Lake Lodge dock. Lengths in parentheses following the sample locations indicate the sample depth, in feet below the sediment-water interface. Samples were collected between 0.6–36 feet below the sediment-water interface. Lake sediment and underlying glacial till are assumed to be 63 feet thick near the dock based on an estimated bedrock surface elevation of 1,503 feet and lake level of 1,566 feet because the top of the sediment-water interface was at or near the lake level in these locations.

stable isotope ratio for the lake evaporate, and is sensitive to the measured lake stable isotope ratio. Additional background on process and limitations for this estimated groundwater inflow flux is provided in appendix 8.

MODFLOW Model

The Haskell Lake water budget and groundwater contributing area of the Haskell Lake/Tower Creek system were estimated using a finite difference groundwater flow model constructed with the USGS program MODFLOW–NWT (Niswonger and others, 2011). The MODFLOW–NWT model focuses on the glacial aquifer, with the Proterozoic bedrock surface represented as a lower no-flow boundary. The areal footprint of the model is shown in figure 1. The model represents the groundwater system in a steady-state configuration, meaning all input stresses to the model, including recharge rates and groundwater flow across the model boundary, are representative of average conditions for the study period of November 1, 2016, to October 31, 2017, when most of the field data were collected. Similarly, the model simulates groundwater levels and stream base flows representative of that same period.

Haskell Lake was simulated within the MODFLOW–NWT model using the Lake (LAK) Package (Merritt and Konikow, 2000), which couples simulation of the lake stage and water budget with the groundwater flow solution. Similarly, Tower Creek was simulated using the Streamflow-Routing (SFR2) Package (Niswonger and Prudic, 2005). Groundwater discharge to wetlands and springs was simulated using the Unsaturated-Zone Flow (UZF) Package (Niswonger and others, 2006). Potential infiltration below the root zone was applied to the UZF Package using results from a separate Soil-Water-Balance (SWB) code simulation (Westenbroek and others, 2010) that estimated deep infiltration from daily climate records, as well as landcover, soil, and topographic data (table 10.1). The UZF Package simulates infiltration or recharge to the water table in places where the simulated water table is below land surface (top of the model); groundwater discharge is simulated in places where the water table is above land surface.

The overall MODFLOW–NWT solution couples these various packages together by routing groundwater discharge from springs and wetlands into Tower Creek and Tower Creek discharge to and from Haskell Lake, while also simulating groundwater exchange with these various features. The resulting model output contains an estimate of the lake water budget, as well as information on groundwater levels and flow directions, which can be used to delineate a contributing area to the lake. The model was informed using existing data and field data collected for this study between July 2016 and November 2017, as discussed in the “Field Data Collection” section. A brief summary of the modeling approach is provided here; additional details are provided in appendix 10.

Model Grid and Layering

The model domain consists of a uniform grid of 393 rows and 471 columns of 50-foot-square cells. The model has five layers that represent the unconsolidated Quaternary deposits, with layers 1 and 2 representing the upper sand and gravel deposits of the Wildcat Lake Member, layer 3 representing the finer Wildcat Lake Member till and debris flows, and layers 4 and 5 representing any older sand and gravel deposits overlying the bedrock. Because of its low average permeability relative to the glacial aquifer (Batten and Lidwin, 1996), the Proterozoic bedrock was assumed to be a no-flow boundary and constitutes the bottom of the model. Model top elevations were sampled from the lidar data (Vilas County Land Information & Mapping Department, 2016) by taking the average within each cell. Layer bottom elevations were developed from well construction reports, the passive seismic survey results, and the interpretations of Attig (1985) and Batten and Lidwin (1996); more details are provided in appendix 10. A cross section of the model layering is presented in figure 10.1.

Boundary Conditions

Boundary conditions that control groundwater flow around Haskell Lake include terrestrial recharge originating from precipitation and snowmelt, regional groundwater flow into and out of the model perimeter, and groundwater discharge to and from surface-water features such as lakes, streams, and wetlands within the model domain.

Terrestrial recharge was estimated using the SWB computer code (Westenbroek and others, 2010), which partitions daily precipitation into evapotranspiration, surface runoff, and deep infiltration, accounting for daily temperature ranges, soil and landcover characteristics, topography, and snow processes. The SWB simulation was run for 1997–2018, using the data sources described in appendix 10 (table 10.1). The resulting time series of deep infiltration estimates at each model cell were then averaged for July 26, 2016, through November 30, 2017 (spanning the complete set of collected field data) and applied to the model as infiltration to the UZF Package (Niswonger and others, 2006).

Regional groundwater flow across the model perimeter was obtained from an updated version of the GFLOW model of Juckem and others (2014), with areal recharge adjusted from 9.2 inches per year to 13.7 inches per year, so that the model matched average base flow at the Bear River streamgage (USGS site 05357355) during the study period (appendix 10).

Surface-water boundary conditions for the MODFLOW model were developed as follows, using information from the Wisconsin Hydrography Dataset (WDNR, 2015b), lidar (Vilas County Land Information & Mapping Department, 2016), and field data collected for this study:

- Groundwater exchange with Haskell Lake was simulated using the LAK Package (Merritt and Konikow, 2000), which simulates lake stage by computing a lake water balance. The lake bathymetry, which is used to compute changes in lake area and volume with changes in stage, was defined using aquatic survey data from the LDF Tribe (K. Hanson, LDF Tribe, oral commun., 2016).
- Tippecanoe, Jerms, and Unnamed Lakes 1 and 2 were simulated using the LAK Package, allowing simulated lake levels and groundwater seepage to vary as a function of groundwater levels. Crawling Stone, Buckskin, Squirrel, Booth, Broken Bow, and Whitefish Lakes are only partially within the model and, therefore, cannot be represented with the LAK Package. Levels for these lakes were specified in the simulation using the General-Head Boundary (GHB) Package. Average water level elevations (fig. 13) measured by a survey-grade GPS (fig. 10) were used as GHB input.
- Tower Creek was represented using the SFR2 Package (Niswonger and Prudic, 2005), which simulates accumulated base flow and stream stage by computing a water balance for the portion of the stream within each model cell.
- Groundwater discharge to small ponds and wetlands and rejected recharge were simulated using the UZF Package, with discharge elevations determined from the model top (average lidar elevation in each model cell). To account for high water levels during the study (other lakes that were measured in this study had levels that were 1.5–4.3 feet higher than the lidar elevations (Vilas County Land Information & Mapping Department, 2016), the surface elevations of the kettles in the model top were uniformly increased by 2 feet. Simulated groundwater discharge in riparian areas was routed to the nearest stream reach or Haskell Lake.

Pumping is assumed to have a negligible effect on the groundwater flow system within the study area because most pumped water is returned to the system via septic mounds. Therefore, pumping was not included in the model. A map showing the boundary conditions is presented in appendix 10 (fig. 10.2).

Aquifer Properties and Boundary Condition Resistance

Aquifer hydraulic conductivity was specified using a network of pilot points (Doherty, 2003) spaced uniformly every 23 cells (1,150 feet). Hydraulic conductivity values for individual model cells were interpolated from the pilot points via kriging. In layers 1 and 2, zones were created for the collapsed and braided stream units (fig. 4), and interpolation of hydraulic conductivity was only performed between pilot points within the same zone. Additional pilot points were included near the Haskell Lake contamination site to represent apparent heterogeneity in hydraulic conductivity encountered in the slug tests (fig. 10.2).

The LAK, GHB, and SFR2 Packages require a leakance term representing lake or streambed sediment permeability and thickness, which control the rate of exchange between groundwater and surface water. Pilot points were used to estimate the lakebed leakance of Haskell Lake, within separate zones representing the near-shore (littoral) area where the low-permeability sapropel is thin to absent, and deeper (profundal) areas where sapropel is thick. Uniform leakance was applied to all other lakes and Tower Creek.

Estimation of Groundwater Discharge Through the Plume Area

Particle tracking was used to delineate groundwater flow paths from the plume source area to Haskell Lake and Tower Creek and to estimate the maximum amount of groundwater discharge to these surface-water bodies that could potentially be contaminated. All particle tracking was performed with the program MODPATH6 (Pollock, 2012). A grid of imaginary particles spaced approximately every 6 feet was created within the dissolved contamination plume delineated by Weston Solutions, Inc. (2016) (fig. 2). The particles were initialized at the vertical midpoint of each model layer and tracked forward until they discharged to a surface-water boundary cell. Groundwater discharge through the boundary cells with terminating particles was then summed individually for Haskell Lake and Tower Creek and compared to the overall water budget for these waterbodies. Although the summed discharges do not represent an actual load of contaminant mass, they provide a maximum estimate of the quantity of discharge to the lake that may be contaminated, because the summed discharges incorporate the entire volume of aquifer beneath the areal extent of the plume delineated by Weston Solutions, Inc. (2016). In reality, the level of contamination varies vertically beneath the plume footprint. For example, at the MW16 well nest, the concentration of total VOCs is three orders of magnitude higher in the middle well compared to the shallow well (Weston Solutions, Inc., 2016). Near the source area, contamination is concentrated in the vadose zone and upper one-half of the surficial aquifer (Weston Solutions, Inc., 2014).

Delineation of the Groundwatershed and Sources of Groundwater Discharge to Haskell Lake and Tower Creek

A second particle tracking simulation evaluated the sources of groundwater discharge to Haskell Lake and the upper portion of Tower Creek (above Haskell Lake).

Knowledge of the sources and approximate age of groundwater discharge to Haskell Lake can provide a basis for understanding how land-use changes in the groundwatershed (the groundwater contributing area for Haskell Lake and the upstream portion of Tower Creek) might affect Haskell Lake. Particles were placed at the top of the aquifer in each model cell and traced forward until they discharged at a surface-water feature. Particles discharging to Haskell Lake, the upper portion of Tower Creek, and adjacent riparian wetlands were identified and grouped by source area (for example, individual lakes or terrestrial recharge). The total discharge contributed by each source was then computed by summing the recharge or surface-water leakage fluxes in the cells where the particles originated. Flux-weighted average traveltimes for particles from each source area also were computed using the source fluxes associated with each particle.

Model Parameter Estimation

Parameter estimation is the process of adjusting model parameters so that model inputs and model outputs acceptably match “hard” knowledge (observations of water levels and flows) and “soft” knowledge regarding the conceptual understanding of the hydrogeologic system. Parameter estimation for the MODFLOW model was performed via history matching. Uncertain input parameters such as hydraulic conductivity and recharge were systematically adjusted until simulated values “best” matched equivalent field observations (targets), including groundwater levels and stream base flows. The overall approach was similar to that of Leaf and others (2015), which followed the general guidelines of Doherty and Hunt (2010); more details are provided in appendix 10.

A total of 137 weighted observations were developed from available data, including:

- Historical water level measurements obtained from WDNR well construction reports;
- Average groundwater levels measured for this study between July 27, 2016, and November 1, 2017, in monitoring wells at the contamination site (fig. 7; appendix 1).
- Average water level of Haskell Lake (fig. 13) recorded at USGS site 455430089550001 (fig. 9) between October 28, 2016, and November 1, 2017.
- Average water levels and gradients from continuous data for the MW16 well nest for July 27, 2016, through November 1, 2017 (fig. 8).
- Average lake levels for Unnamed Lakes 1 and 2, from seasonal GPS measurements collected in October of 2016 and May, August, and November of 2017 (figs. 10, 13); one-time lake level measurements of Jerms and Tippecanoe Lakes, made in October of 2016 (fig. 13); and one-time measurements of two ponds (East pond 1 and 2) adjacent to the contamination site on the southeast side, made in November of 2017 (fig. 9).
- Average gradients between the mini-piezometers and Haskell Lake (fig. 14), from seasonal measurements collected in the spring, summer, and fall of 2017 (fig. 15).
- Average base flow computed for the Tower Creek streamgage (USGS site 05392187) for November 1, 2016, to October 31, 2017.
- One-time base-flow measurements collected along Tower Creek on November 2, 2017, under near-average conditions for the study period (USGS sites 05392186, 05392188, and 05392189).

The observations were assigned weights to reflect their uncertainty and relative importance (table 10.2).

Estimated parameters included 2,118 pilot points representing horizontal and vertical hydraulic conductivity, 12 lakebed leakance pilot points for Haskell Lake, uniform lakebed leakance values for the remaining 9 lakes simulated with the LAK and GHB Packages, a single parameter representing Tower Creek leakance, a multiplier value applied to the recharge array, average precipitation and evaporation over Haskell Lake, and the height of the Haskell Lake outlet sill (table 10.3). Initial hydraulic conductivity values for pilot points were based on estimates of hydraulic conductivity from slug test results (appendix 5), literature values from Patterson (1989), and values reported by Hunt and others (2013) for the nearby Trout Lake area (fig. 1). Initial values of lakebed leakance were based on results from Hunt and others (2013). Prior to formal parameter estimation, the initial values were adjusted by trial and error to provide an approximate fit to the observation data.

Parameter estimation was performed via nonlinear regression using the PEST++ and BeoPEST software packages (Welter and others, 2015; Schreüder, 2009). Singular value decomposition and Tikhonov regularization (Doherty and Hunt, 2010) were used to allow identifiable parameters (those informed by the observation data) to be estimated, while maintaining all other parameters at their preferred values or a preferred state. A preferred condition of homogeneity was applied for pilot points away from the contamination site based on the findings of Hunt and others (2013). Additional pilot points in the area of the contamination site were only regularized with singular value decomposition (the preferred homogeneity condition was not applied). This allowed neighboring pilot points at the contamination site to more easily assume different values, consistent with the conceptual model of heterogeneity. More detail on the parameter estimation methods are given by Leaf and others (2015) and Hunt and others (2013). Initial and estimated parameter values and the uncertainty bounds used in parameter estimation are presented in table 10.3.

Inspection of the singular value decomposition results using the pyEMU software (White and others, 2016) indicates that only a few of the 2,000 plus parameters can be estimated on the basis of the observation dataset. The small number of identifiable parameters stems from the sparsity of groundwater levels or groundwater discharge measurements away from Haskell Lake and Tower Creek. As a result, the conceptual understanding of this system from the data collected for this study and the previous work of others (for example, Juckem and others, 2014; Hunt and others, 2013) is more influential to model outcomes in areas of sparse data.

An added benefit of PEST++ is the automatic inclusion of linear (first-order, second-moment) uncertainty calculations as part of the parameter estimation process (Welter and others, 2015). Although subject to important limitations, linear methods provide an easy and efficient way to assess the effects that uncertainties in model input parameters and observation data have on the model forecasts (White and others, 2016; White, 2017), including the effects of uncertainty in the myriad unidentifiable parameters in the Haskell Lake groundwater model. Linear uncertainty estimates were computed on the basis of parameter sensitivities at the “best” parameter estimates, for the water budget components of Haskell Lake and Tower Creek, estimated average traveltimes from the sources of discharging groundwater, and estimates of groundwater discharge through the petroleum contamination plume.

MODFLOW Model Results and Discussion

The model generally matches the observed data, with recharge rates and hydraulic conductivities that are consistent with previous work (for example, Hunt and others, 2013; Dripps and others, 2006). Additional detail on model fit to field observations and estimated hydraulic conductivity values is given in appendix 10 (figs. 10.3 through 10.6). Simulated recharge rates, groundwater/surface-water interactions, and water budget results are presented in this section of the report. Model output quantities are presented with posterior uncertainty ranges that represent a 95-percent confidence interval or two standard deviations on either side of the mean for an assumed normal distribution. All uncertainty ranges were computed using the linear uncertainty analysis feature in PEST++ (Welter and others, 2015). Posterior uncertainties reflect uncertainty in the model inputs (prior uncertainty) and the effects of the history matching to observed data, which can reduce uncertainty by constraining the model input parameters.

Recharge

Annual recharge rates simulated in the groundwater model are shown in figure 20. Parameter estimation resulted in a multiplier of 1.0 (no multiplier) being applied to the SWB model output. The resulting average areal recharge rate of 13.32 inches per year over the model domain (including open water, where recharge was assumed to be zero) is similar to the uniform value of 13.7 inches per year used in the GFLOW model modified from Juckem and others (2014) to match average base flow in the Bear River for the study period. The spatial variability and overall average of 18.43 inches per year for terrestrial recharge (not including areas of open water) are consistent with values reported by Hunt and others (2013) and Dripps and others (2006) for wetter than average years. Recharge is generally lowest in wetland areas and where the soils are less sandy. Simulated recharge is zero in areas where the water table is near the land surface, including many areas along Tower Creek (figs. 1, 4) where groundwater discharge to riparian wetlands is simulated (fig. 21). Recharge is anomalously high in a few discrete low-lying areas, where accumulating runoff provides additional source water for infiltration in the SWB simulation (fig. 20).

Groundwater Flow and Groundwater/Surface-Water Interactions

Simulated water table elevations, groundwater/surface-water interactions, and the simulated groundwatershed for Haskell Lake are shown in figure 21. The light grey lines are contours of equal water table elevation at 2-foot intervals. The contours indicate the general direction(s) of groundwater flow, which are perpendicular, in the direction of steepest decent. The groundwatershed for Haskell Lake and Tower Creek is the area where groundwater ultimately discharges to the lake, creek, or adjacent riparian wetlands. Sources of discharging groundwater include terrestrial recharge or leakage from surrounding lakes that are higher in elevation.

The red and blue shaded areas in figure 21 indicate groundwater discharge to surface water (blue) or surface-water leakage to groundwater (red). Buckskin, Tippecanoe, and Crawling Stone Lakes and the two unnamed lakes along Old Prairie Road contribute discharge to Tower Creek and Haskell Lake. With the possible exception of some hyporheic flow, Tower Creek receives groundwater discharge along its entire length and, therefore, does not contribute leakage. Similarly, Haskell Lake is simulated as receiving groundwater discharge around its entire perimeter, consistent with the field data. Simulated groundwater discharge to Haskell Lake is concentrated along the shoreline, where resistance to groundwater

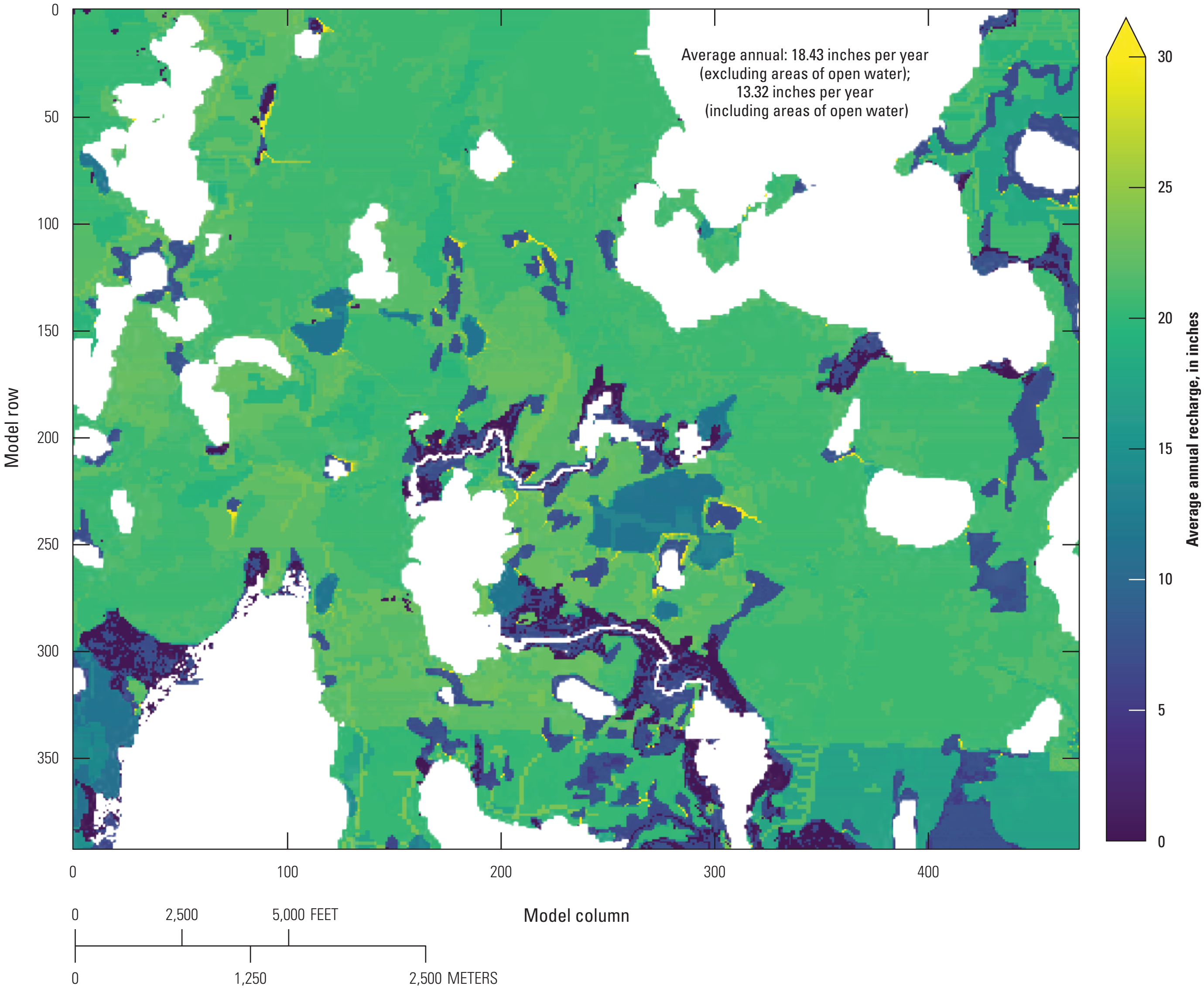

Figure 20. Average annual recharge rates simulated in the groundwater flow model (representing July 26, 2016, through November 30, 2017). No recharge was applied to surface-water features (shown in white); interaction between these features and the groundwater system is simulated with the Lake, General-Head Boundary, and Streamflow-Routing Packages.

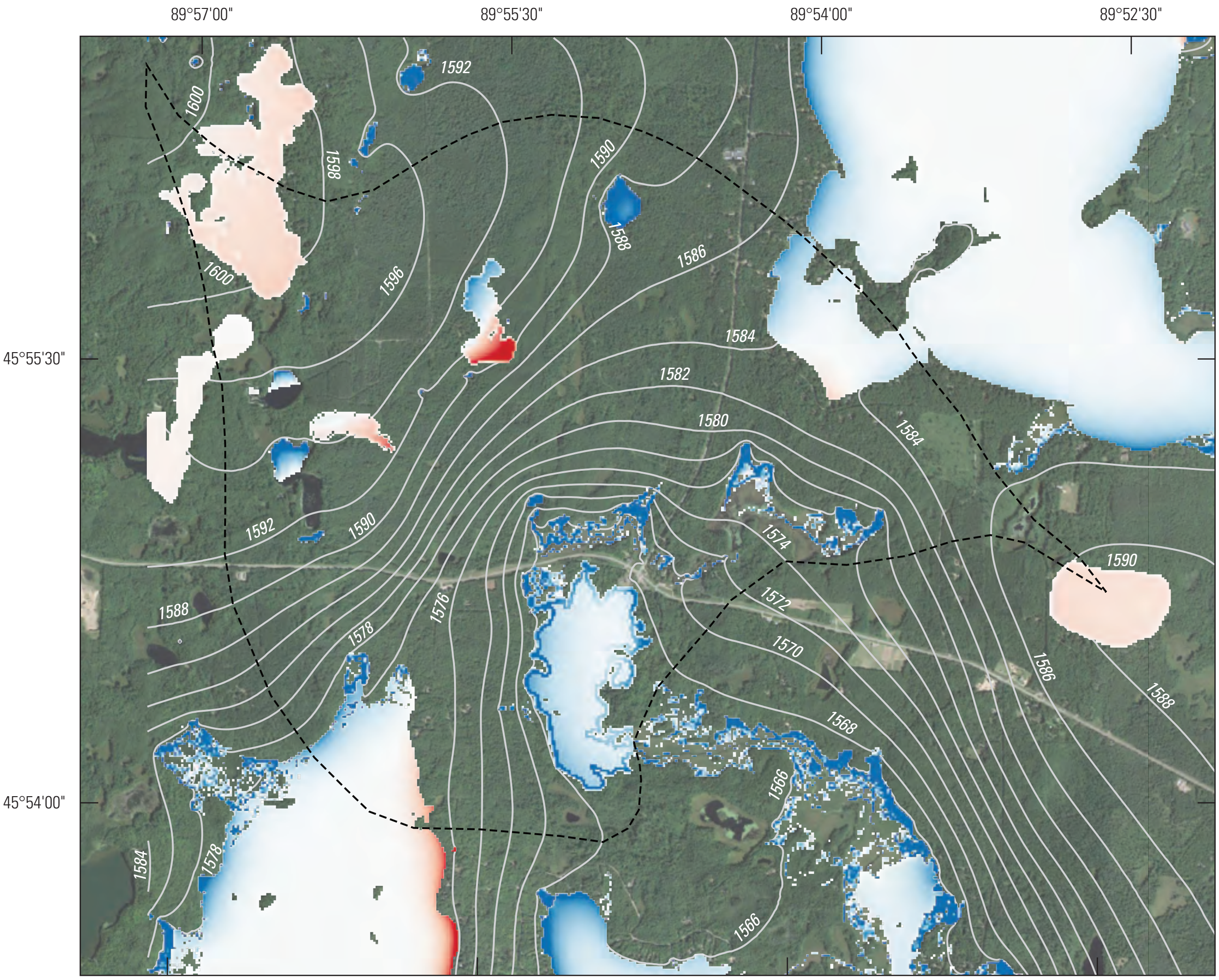

Base-map data from Google, 2018
Hillshade base map modified from Vilas County Land Information and Mapping Department (2016)

0 20 40 FEET
0 20 40 METERS

EXPLANATION

[≤, less than or equal to; ≥, greater than or equal to]

Leakage, in cubic feet per day in each model cell

≤ –100
–66.7
–33.3
0
33.3
66.7
≥ 100

Estimated groundwatershed

1570 **Contour of water table elevation, with elevation label**

Figure 21. Simulated steady-state water table elevation, groundwater/surface-water interactions, and groundwatershed. The light gray lines are contours of equal water table elevation at 2-foot intervals. Groundwater flow occurs in the direction of steepest decent, perpendicular to the equal elevation contour lines. Groundwater/surface-water interactions are indicated by the red and blue shaded cells from the Lake, Unsaturated-Zone Flow, and Streamflow-Routing Packages. Blue hues (negative values) indicate groundwater discharge; red hues indicate leakage of surface water into groundwater. The dashed outline indicates the approximate extent of the area contributing groundwater flow to Haskell Lake and the upstream portion of Tower Creek. The steady-state simulation represents average conditions between July 26, 2016, and November 30, 2017.

flow is thought to be lower because of thin or absent sapropel sediments. Concentrated discharge near the shore, where hydraulic head gradients are highest, is also consistent with first principals of groundwater theory (for example, Haitjema, 1995; McBride and Pfannkuch, 1975). Groundwater discharge is also simulated in myriad wetland areas along Tower Creek and in kettle depressions dispersed throughout the groundwatershed.

Haskell Lake Water Budget and Hydraulic Residence Time

The water budget for Haskell Lake, as simulated by the MODFLOW LAK Package, is presented in table 1. Linear-based posterior uncertainty estimates computed by PEST++ for each component (expressed as percentages of the total flow) are also shown. The posterior uncertainties reflect uncertainty in the model inputs (prior uncertainty) and the effects of the history matching to observed data, which can reduce uncertainty by constraining the model input parameters. All uncertainties presented reflect the 95-percent confidence interval of an assumed normal distribution.

Flow to and from Tower Creek is the largest component of the water budget, accounting for about 61 percent (± 10 percent) of the total flow into the lake and 95 percent of flow out of the lake. Groundwater inflow is second largest, at about 22 percent (± 11 percent), which compares favorably to the estimate from the stable isotope analysis (table 1). Direct precipitation constitutes most of the remaining inflow, with a minor amount of discharge from riparian wetlands to the lake simulated by the UZF Package. In reality, much of the lake is surrounded by wetlands that receive groundwater discharge but are well connected to the lake, making the riparian component difficult to distinguish from the groundwater inflow component. Most riparian wetlands are simulated as part of Haskell Lake, using LAK Package cells. The riparian component of discharge to Haskell Lake includes similar adjacent wetlands that are outside the footprint of the Lake Package cells and were simulated with the UZF Package instead, with simulated flow being routed into Haskell Lake.

A large groundwater inflow component in the Haskell Lake water budget (almost double precipitation) is consistent with the large groundwater contributing area (fig. 21), high terrestrial recharge rates (fig. 20), and the position of Haskell Lake within the Tower Creek drainage, which is a hydrographic low point in a landscape with few streams. Allequash Lake, another drainage lake about 16 miles to the northeast (fig. 1), has a similar groundwater component, receiving just under 2 meters (79 inches) of groundwater annually (Hunt and others, 2013).

Using the computed lake stage and lake bathymetry defined in the layer 1 bottom elevations, the LAK Package computes a lake volume, which can be used to determine a hydraulic residence time. Hydraulic residence time is the lake volume divided by the flow through the lake and represents the

Table 1. Water budget for Haskell Lake, with uncertainty estimates for the percentage of each component.

[in/yr, inch per year; --, no data]

Component	MODFLOW Lake Package: Inflow (in/yr)	MODFLOW Lake Package: Percent	MODFLOW Lake Package: Uncertainty[1] (percent)	Stable isotope analysis: Inflow (in/yr)	Stable isotope analysis: Percent	Stable isotope analysis: Uncertainty[2] (percent)
Precipitation	43.7	12.1	2.3	43.7	--	--
Groundwater discharge to riparian wetlands	19.3	5.3	7.0	0.0	--	--
Groundwater inflow	79.6	22.0	11.5	103.9	27.4	65.0
Inflow from Tower Creek	219.3	60.6	10.4	231.9	--	--
Total	362.0	100.0	--	379.5	--	--
Component	**MODFLOW Lake Package: Inflow (in/yr)**	**MODFLOW Lake Package: Percent**	**MODFLOW Lake Package: Uncertainty[1] (percent)**	**Stable isotope analysis: Inflow (in/yr)**	**Stable isotope analysis: Percent**	**Stable isotope analysis: Uncertainty[2] (percent)**
Evaporation	19.5	5.4	0.9	19.5	--	--
Unsaturated leakage	0.0	0.0	7.0	--	--	--
Outflow to Tower Creek	342.4	94.6	0.9	360.0	--	--
Total	362.0	100.0	--	379.5	--	--

[1]Posterior uncertainty estimated by the linear uncertainty method in PEST++; represents a 95-percent confidence interval or two standard deviations.

[2]Uncertainty from first-order error analysis.

average amount of time that a particle of water spends in the lake. The hydraulic residence time for Haskell Lake, under the average conditions reflected in the steady-state model simulation, is about 64 days (± 12 days).

Groundwater Discharge through the Petroleum Contamination Plume

Simulated groundwater discharge in the lake cells receiving particles from the plume footprint (fig. 2) is about 1.4 percent (with an uncertainty range of 0 to 8.5 percent) of total groundwater discharge to Haskell Lake, or about 0.3 percent (uncertainty range of 0 to 1.8 percent) of the total Haskell Lake water budget. This number was relatively consistent among exploratory model runs (completed prior to parameter estimation) with different input parameters. This estimate of the fraction of groundwater discharge passing through the plume area does not represent an actual contaminant load to the lake because the distribution of contaminant concentrations in the discharging water are not well known. In addition, by assuming that the plume occupies the entire volume of aquifer beneath its areal footprint, this estimate is likely higher than the actual quantity of contaminated groundwater discharge. Although information on the vertical extent of the plume is limited, field investigations indicate that contaminant concentrations vary vertically throughout the plume footprint. For example, near the source area, contamination is concentrated in the vadose zone and upper interval of aquifer; near the lake, there is more contamination at depth (Weston Solutions, Inc., 2016).

Some experimental model runs during the trial-and-error phase of model calibration prior to parameter estimation simulated a minor amount of groundwater discharge from the plume area to Tower Creek. Although the calibrated model does not simulate any discharge from the plume area to Tower Creek and the monitoring data (fig. 7) do not indicate gradients in this direction, the location of the contamination source near the groundwater divide between Haskell Lake and Tower Creek raises the possibility of occasional gradients from the plume source area towards the creek.

Extent of the Petroleum Contamination Plume Beneath Haskell Lake

Figure 22 shows the particle traces from the model cells within the areal plume footprint to discharge locations in Haskell Lake. The particles represent the migration of a conservative solute—a solute that does not lose mass to the processes of biodegradation and sorption to aquifer materials. Petroleum contamination plumes are affected by biodegradation and sorption, which tend to reduce plume length in comparison to a conservative solute (for example, Chapelle and others, 2003). Analysis of biodegradation and sorption requires an accurate understanding of contaminant concentration trends in space and time and is beyond the scope of this study. These factors may or may not be important to the plume at Haskell Lake, but would only serve to reduce the extent shown by the particle tracking. The particle traces also do not consider dispersion—a site-specific parameter that describes the spreading of a contaminant caused by small-scale heterogeneities in the aquifer. Although consideration of dispersion might result in a wider simulated plume extent in comparison to the particles, dispersion would not be expected to appreciably lengthen the simulated plume, which already terminates at the lake. With these caveats in mind, the simulated particle traces are referred to as the simulated plume extent for convenience.

The simulated areal extent of the plume beneath the lake is sensitive to the local distribution of hydraulic conductivity and lakebed leakance in the plume vicinity. Different spatial distributions of these parameters can move the simulated extent of the plume beneath the lakebed to the east or west. Lakebed leakance is a resistance term that accounts for both the thickness of the lakebed (in length units) and its permeability (in units of length/time). The units of (1/time) for leakance therefore represent a total resistance to groundwater flow. Lower values of lakebed leakances would be expected to increase the length of the groundwater discharge zone away from shore (for example, Haitjema, 2006), thereby lengthening the simulated plume. Lakebed leakances used in the groundwater flow model were estimated on the basis of the field data collected for this study and a prior knowledge of reasonable values from the work of Hunt and others (2013) in the nearby Trout Lake area. Average values of about 0.10 1/days and about 0.019 1/days (table 10.3) estimated for the littoral (near-shore) and profundal (away from shore) zones in Haskell Lake are higher than the means of 0.039 1/days and 0.000292 1/days reported by Hunt and others (2013), but are within the ranges reported by that study. The average values reported by Hunt and others (2013) represent conditions in 30 lakes; Haskell Lake may not be average in comparison to this population.

Experimental model runs with lower values of littoral and profundal lakebed leakance (down to the minimum of 0.0001 1/days reported by Hunt and others [2013]) resulted in unrealistically high simulated gradients between the lake and the mini-piezometers and between the lake and contamination site monitoring wells. A run also was completed with only profundal lakebed leakance lowered to one posterior standard deviation below the estimated values, as calculated by the linear uncertainty analysis. Although this resulted in a somewhat improved fit to the field observations compared to the minimum leakance case, the overall objective function was still more than 40 times higher than the calibrated model (table 10.2). More importantly, this adjustment did not result in a longer plume than that shown in figure 22. Instead of causing the plume to extend farther out into the lake, the reduced lakebed leakance caused the plume to curve westward and discharge in the higher-leakance littoral zone near the western shore. This result is similar to the field situation observed by Sebok and others (2013), who noted flow paths

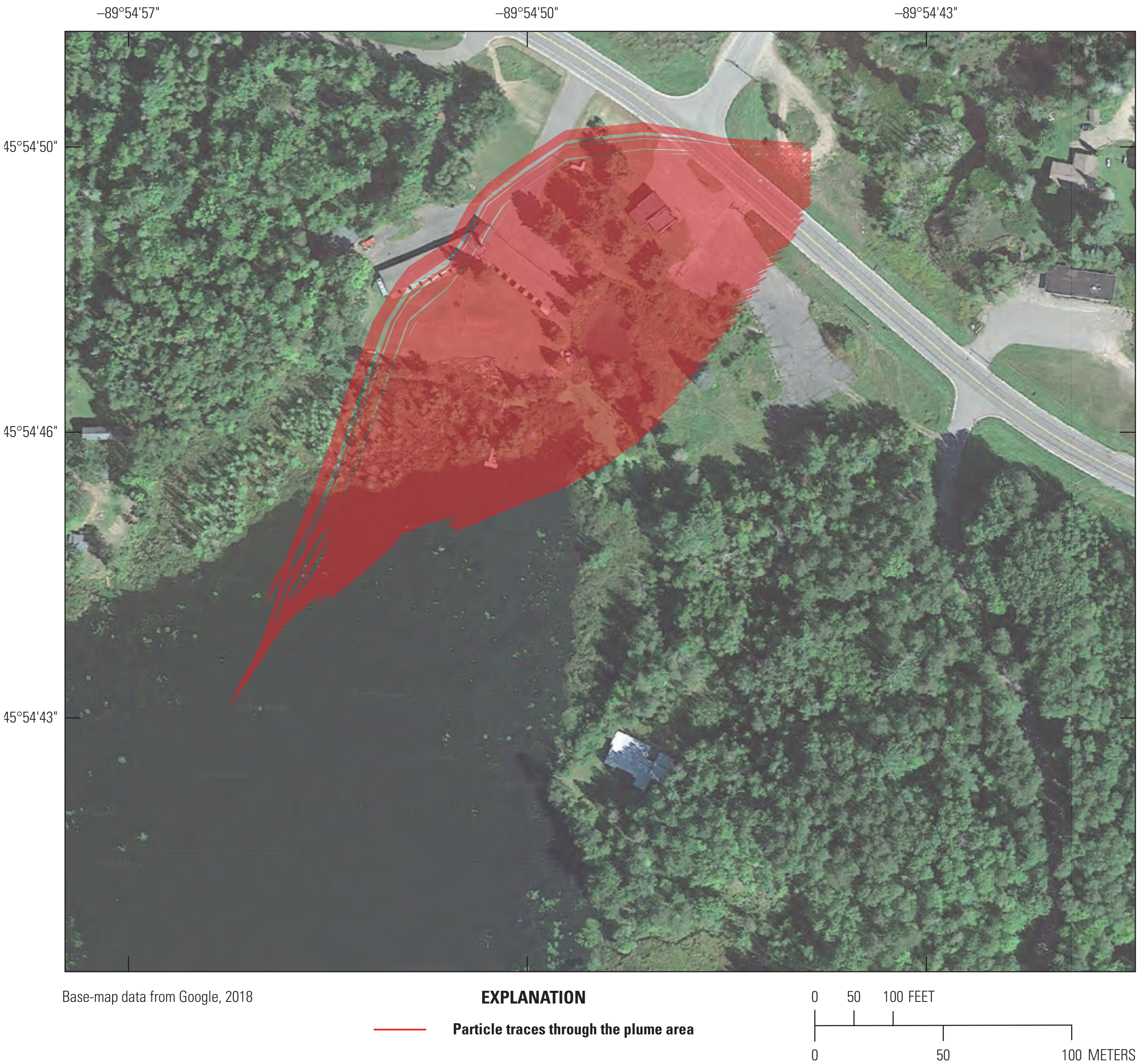

Figure 22. Particle traces representing groundwater discharge through the plume area, as simulated with the calibrated model parameters. The actual extent of the plume beneath the lake may vary between the western and eastern shores, but the total length is unlikely to be appreciably longer than the particle traces shown.

crossing a lake underlain by low permeability sediments in a hydrogeologic setting similar to Haskell Lake. Field observations support a higher lakebed leakance near shore where sapropel is absent and exposed sand and gravel are visible.

Although some combinations of model input parameters may exist that could lengthen the particle traces somewhat beyond those shown in figure 22, the model results indicate that the actual plume beneath Haskell Lake is unlikely to be appreciably longer than the simulated particle tracks shown in figure 22. Other studies that have summarized data from hundreds of similar sites support the simulated plume length (figure 22) as an upper limit. For example, Connor and others (2015) reviewed 13 studies summarizing data from hundreds of underground storage tank-related petroleum contamination plumes distributed throughout the United States. They reported median plume lengths that were all less than 200 feet and 90th percentile lengths that were all less than 500 feet. In a review of 10 Wisconsin sites, Evanson and others (2009) reported plume lengths ranging up to 400 feet; one-half of the plumes were less than 100 feet. For comparison, the plume shown in figure 22 is approximately 850 feet, as measured in a straight line from the MW20 well nest near the source area to the most distant particle endpoints. The actual plume is likely to be shorter than 850 feet because of biodegradation, sorption, and the vertical distribution of contamination indicated by the field data. The most distal particles in figure 22 originated near the bottom of the surficial aquifer beneath the source area, which has relatively low levels of contamination (Weston Solutions, Inc., 2014).

Groundwatershed and Sources of Groundwater Discharge to Haskell Lake

The outline of the groundwatershed boundary in figure 21 is sensitive to the hydraulic conductivity values used in the simulation. Hydraulic conductivity affects groundwater levels and directions of groundwater flow, as well as simulated groundwater discharge to depressions in the land surface when the water table is high. The groundwatershed boundary is uncertain in many areas of the model where groundwater levels (fig. 10.4) or other information about aquifer hydraulic conductivity is sparse. In general, lower aquifer hydraulic conductivities produce more localized mounding of the water table between Haskell Lake and neighboring lakes, resulting in a smaller groundwatershed for Haskell Lake and Tower Creek. For example, lower values of hydraulic conductivity near Buckskin and Crawling Stone Lakes can result in a simulated groundwater divides that place those features out of the Haskell Lake/Tower Creek groundwatershed. Conversely, higher hydraulic conductivities tend to flatten the water table, resulting in a large groundwatershed and larger contributions from neighboring lakes. High hydraulic conductivities are indicated by well construction report records near Buckskin and Crawling Stone Lakes that indicate leakage from those features and groundwater flow towards Haskell Lake.

Although Haskell Lake receives some water from neighboring lakes, approximately 94 percent of groundwater inflow was simulated as originating from terrestrial recharge (uncertainty range of 80 to 100 percent). Flow-weighted average traveltimes also were computed for each groundwater source to Haskell Lake. The age of groundwater discharge to Haskell Lake varies from less than 1 year for groundwater that originated as terrestrial recharge near the lake to more than 60 years for groundwater sourced near the edges of the groundwatershed. The average age of groundwater sourced from terrestrial recharge is about 20 years, with an upper uncertainty bound of 120 years. Average traveltimes from the neighboring lakes ranged from about 14 years for Unnamed Lake 2, to approximately 60 years or more for lakes near the model perimeter.

Assumptions and Limitations

The Haskell Lake model, like all models, is a simplified representation of a natural system of unknowable complexity. Although an effort was made to include all available information in the model, information on the groundwater system properties (for example, heterogeneity in the hydraulic conductivity field) or the system state (transient water levels and flows), is limited across much of the model domain. Therefore, the model is not only simplified but also conditioned on an incomplete set of data. These two factors contribute to “structural error” in the model (Doherty and Welter, 2010), which can cause inaccuracies in areas where the model predictions are sensitive to the uncertain input parameters. An effort was made to limit the effects of structural error to localized areas by distributing the parameterization of hydraulic conductivity across the model grid using pilot points.

Steady-State Assumption

A key assumption of the model is that the groundwater system can be represented as steady state and that the key model predictions are independent of the time period chosen (October 2016 through November 2017). Given the large amount of precipitation (and recharge) that occurred during this period, the flows and hydraulic heads simulated by the model are likely greater than longer term averages. Experimentation with the model using boundary fluxes and recharge rates from the model of Juckem and others (2014), which are assumed to represent average conditions, indicates that the percentage of groundwater inflow in the Haskell Lake water budget is relatively steady with time. Extending the model to simulate transient conditions could provide a more definitive answer about how groundwater discharge to Haskell Lake varies with time.

Limitations in the Simulation of the Petroleum Contamination Plume

Although the model is suitably discretized to simulate the water budget, spatial distribution of groundwater/surface-water interactions, and groundwater contributing area for Haskell Lake, the 50-foot cell size cannot represent the petroleum contamination plume in detail. The estimate of groundwater discharge through the plume area is intended to provide an approximate, conservative (overestimate) of this quantity, because summed discharges are not weighted by the number of particles terminating in their respective cells, and the contamination is not uniformly distributed beneath the plume footprint. For example, a single particle terminating in a cell on the edge of the plume causes all of the discharge in that cell to be included. A finer grid spacing or a mass transport simulation (for example, with the MT3D program; Zheng, 2010) would probably result in a smaller estimate. Such a simulation would still be limited, however, by the accuracy of supporting information about the spatial extent and mass of the remaining hydrocarbon source.

Similarly, the particle traces from the plume area are intended to give an estimate of the possible extent of the plume beneath the lake. However, the particle traces may overestimate plume length because advective particle tracking does not account for the processes of biodegradation and sorption that can reduce plume length compared to a conservative solute. Consideration of these factors would require detailed information about VOC concentration trends in space and time, as well as an understanding of the source area.

Slug test results, calibrated hydraulic conductivity values, and knowledge of the Quaternary geology indicate that the shallow aquifer is not homogenous across the contamination site. Specifically, the slug test results indicate a transition in material in the upper 30 feet from a relatively silt-rich sand in the western portion of the site to a coarser, perhaps poorly sorted sand and gravel in the eastern portion of the site near the MW20 well nest. The silt-rich sand across the western portion of the site may be associated with debris flow deposits from the remnant ice block that created the Haskell Lake watershed. Pilot points were used to represent this local heterogeneity in the groundwater model, but the location of the geologic contact between the two material types is unknown. Similarly, the path and discharge of the plume could be controlled by uncharacterized preferential flow paths similar to those encountered by Krabbenhoft and Anderson (1986) at nearby Trout Lake (fig. 1). Regardless, the estimated hydraulic conductivity field is probably at best a crude representation of reality and also nonunique. As a result, the shapes of the path lines representing the plume are uncertain.

Uncertainty in the Groundwatershed Boundary

The groundwatershed of Haskell Lake and the upstream portion of Tower Creek is constrained by the locations and elevations of surrounding water bodies, the base flow in Tower Creek, and the groundwater inflow to Haskell Lake. Low water levels in well construction reports provide some evidence of leakage from Crawling Stone and Buckskin Lakes. Leakage from these features constrains the possible ranges of reasonable aquifer hydraulic conductivity values and, therefore, the groundwatershed boundary.

Simulation of land surface depressions (kettles) with the UZF Package creates some uncertainty in the delineation of groundwatershed, because the kettles are treated as drains that only remove water from the groundwater system when the water table reaches their bottom elevations, which were estimated from the lidar survey (Vilas County Land Information & Mapping Department, 2016). This assumption does not account for precipitation, evaporation, or leakage back to groundwater. In reality, the kettles may behave like Unnamed Lake 2, with groundwater discharge on one side and leakage on the other. The implication for delineation of the groundwatershed is that kettles near the edge may be in the groundwatershed in reality but simulated as outside of the groundwatershed. This issue was mitigated somewhat by the adjustment of model top elevations at these features to account for higher water levels during the study period (see the Boundary Conditions section).

Limitations of the Linear Uncertainty Analysis

The linear uncertainty calculation uses parameter sensitivities and uncertainty bounds to estimate forecast uncertainties. Parameter sensitivities are assumed to be constant with respect to the parameter values, which may not be realistic. For example, an experimental run with lower profundal lakebed leakage values (discussed in "Extent of the Petroleum Contamination Plume Beneath Haskell Lake") resulted in a small number of plume particles discharging to Tower Creek. Sensitivities computed from the calibrated parameter sets, where no plume discharge to Tower Creek is simulated, can never anticipate such a shift. In addition, the linear projection of uncertainty bounds often results in unrealistic values; for example, negative traveltimes or discharge fractions. The uncertainty bounds presented with the model results should, therefore, be viewed as approximate.

Summary and Conclusions

Haskell Lake has long been valued by the Lac du Flambeau Band of Lake Superior Chippewa Indians for historical abundance of wild rice, game fish, and other natural resources. In recent decades, wild rice has mostly disappeared from the lake and the fishery has declined. A petroleum contamination plume discovered in the 1990s in the shallow aquifer upgradient from the northern end of the lake poses a threat to the ecological health of the lake and the surficial aquifer, which is the sole drinking water source for nearby residents and businesses. Understanding of the lake's hydrology is important to the Lac du Flambeau Band of Lake Superior Chippewa Indians as they seek to restore wild rice and maintain the ecological health to the Haskell Lake/Tower Creek watershed. An improved understanding of lithology in the area of the contamination plume and documentation of a contamination pathway from groundwater in the plume area to Haskell Lake are needed to advance remediation efforts. Evaluation of the portion of groundwater discharge that is contaminated relative to the overall lake water budget was desired as a first step towards determining the extent of ecological impacts from the plume. A cooperative study between the U.S. Geological Survey and the Lac du Flambeau Band of Lake Superior Chippewa Indians was initiated to quantify the lake water budget and the sources of water to the lake, to provide a rough estimate of the maximum quantity of groundwater discharge to the lake that may be contaminated, and to improve the conceptual understanding of the plume extent and subsurface materials in the area of contamination.

The hydrology of Haskell Lake and its contributing groundwater flow system were investigated using field data and a three-dimensional (MODFLOW–NWT) groundwater flow model of the Haskell Lake/Tower Creek watershed. Field data included continuous measurements of Tower Creek streamflow, Haskell Lake water levels, and groundwater levels in nested wells near the lake; seasonal measurements of groundwater levels around Haskell Lake and the water levels of neighboring lakes; slug testing in monitoring wells at the contamination site, measurements of lakebed temperature, shallow geophysics, and surface-water samples analyzed for stable isotopes of oxygen. Field data were used to inform the structure and properties of the MODFLOW model and evaluate simulated groundwater levels, lake levels, and base flow in Tower Creek. Particle tracking was performed with the MODFLOW solution to estimate groundwater flux through the petroleum contamination plume, the possible extent of the plume beneath Haskell Lake, and the groundwater contributing area (groundwatershed) for Haskell Lake and Tower Creek. Linear uncertainty estimates for model results were computed during model parameter estimation using PEST++. The key findings are as follows:

- Groundwater discharge into Haskell Lake was measured and simulated around the entire perimeter of the lake, including the area downgradient from the petroleum contamination plume.

- Groundwater accounts for about 22 (± 11.5) percent of the water budget of Haskell Lake, with inflow from Tower Creek (61 percent) and precipitation (about 12 percent) as the remaining two components. A large groundwater inflow component in the Haskell Lake water budget (roughly double precipitation) is consistent with the large groundwater contributing area, high terrestrial recharge rates, and the position of Haskell Lake within the Tower Creek drainage, which is a hydrographic low point in a landscape with few streams.

- A stable isotope-derived estimate of groundwater inflow to Haskell Lake compared favorably to the MODFLOW model results. However, this estimate is uncertain because of isotopic similarity between Haskell Lake/Tower Creek and the groundwater. The stable isotope water balance method is best suited to lakes with more distinguishable input sources.

- Field data, the MODFLOW model, and basic principles of groundwater flow indicate that the entire contamination plume discharges to Haskell Lake (with the possible exception of minor discharge to Tower Creek). The exact locations where contaminated water is entering the lake remain unclear, but could extend up to approximately 700 feet from shore, based on detection of appreciable benzene at depths of approximately 36 feet below the lakebed 70 feet from shore, and particle tracking using the groundwater flow model. The length of the plume is ultimately limited by natural attenuation processes that degrade petroleum contamination and the driving hydraulic head gradients between the lake and groundwater system, which decrease with distance from shore. Previous analyses of hundreds of other sites with contamination from leaking underground storage tanks have generally reported plume lengths that are much shorter than the 850-foot length shown in figure 22.

- The difficulties encountered with sampling the lakebed sapropel sediments present a fundamental challenge to defining the downgradient extent of the plume in the field. A customized coring method that preserves pore water in situ within the sapropel would probably be required.

- Particle tracking and simulated groundwater discharge to Haskell Lake indicate that, at most, contaminated groundwater from the petroleum plume accounts for about 1.4 percent of groundwater discharge, or 0.3 percent of the total water budget of Haskell Lake. Most groundwater discharge to Haskell Lake (about 95 percent) originates as terrestrial recharge; the remainder originates as leakage from neighboring lakes. The average age of terrestrial recharge discharging to Haskell Lake is about 20 years; ages of discharging groundwater range from less than 1 year for groundwater that recharged near the lake to more than 60 years for groundwater sourced near the edges of the groundwatershed.

- Slug test results and model parameter estimation indicate that hydraulic conductivities in the upper 30 feet of material across much of the contamination site, with the exception of the area around MW20, are less than 10 feet per day, indicative of an appreciable silt content. Higher values of hydraulic conductivity near the MW20 well nest and in the deep interval of MW16 indicate poorly sorted sand and gravel. These results indicate heterogeneity at the contamination site, possibly explained by the presence of debris flow deposits associated with the remnant ice block that melted out to form the Haskell Lake Basin. This heterogeneity would need to be considered carefully in future remediation system design.

References Cited

Agency for Toxic Substances and Disease Registry, 1989, Public Health Statement for 1,1,2-trichloroethane: CAS# 79–00–5, 3 p., Agency for Toxic Substances and Disease Registry web site, accessed July 16, 2019, at https://www.atsdr.cdc.gov/phs/phs.asp?id=794&tid=155.

Anderson, M.P., and Lowry, C.S., 2007, Transient functioning of groundwater wetland complex, Allequash Basin, Wisconsin: Water Resources Institute University of Wisconsin Report WR05R007, 16 p., accessed December 14, 2017, at https://www.wri.wisc.edu/wp-content/uploads/Final-WR05R007.pdf.

Attig, J.W., 1985, Pleistocene geology of Vilas County, Wisconsin: Wisconsin Geological and Natural History Survey Information Circular 50, 32 p., accessed September 26, 2017, at https://wgnhs.uwex.edu/pubs/download_ic50/.

Attig, J.W., and Rawling, J.E., 2016, Quaternary geology of Oneida County, Wisconsin: Wisconsin Geological and Natural History Survey Open-File Report 2016–01, Plate 1, 1 p., accessed February 28, 2017, at https://wgnhs.uwex.edu/pubs/download_wofr201601/.

Batten, W.G., and Lidwin, R.A., 1996, Water resources of the Lac du Flambeau Indian Reservation, Wisconsin, 1981–86: U.S. Geological Survey Water-Resources Investigation Report 94–4025, 47 p.

Born, S.M., Smith, S.A., and Stephenson, D.A., 1979, Hydrogeology of glacial-terrain lakes, with management and planning applications, *in* Back, W., and Stephenson, D.A., eds., Contemporary hydrogeology—The George Burke Maxey memorial volume: Journal of Hydrology, no. 43, no. 1–4, p. 7–43.

Bristol Environmental Remediation Services, LLC, 2016a, EPA Contract No. EP–W–12–009, EPA Contract No. EP–W–12–009, Task Order (TO) 2012 Tower Standard Site, Lac du Flambeau Reservation, Wisconsin March and April 2016 Site Investigation, Rev 0: Technical memorandum, April 18, 2016, 42 p.

Bristol Environmental Remediation Services, LLC, 2016b, EPA Contract No. EP–W–12–009, Task Order (TO) 3012 Tower Standard Site, Lac du Flambeau Reservation, Wisconsin August 2016 Site Investigation, Rev 0: Technical memorandum, September 23, 2016, 167 p.

Bujewski, G., and Rutherford, B., 1997, The Rapid-Optical Screening Tool (ROST) Laser-Induced Fluorescence (LIF) system for screening of petroleum hydrocarbons in subsurface soils: Technical Report, U.S. Environmental Protection Agency, 104 p., accessed June 20, 2018, at https://nepis.epa.gov/Exe/ZyPURL.cgi?Dockey=30003JAJ.TXT.

Cascade Technical Services, 2016, MIHPT Site Investigation 14267 State Highway 70 West: Wisconsin, Lac Du Flambeau, 79 p.

Chandler, V.W., and Lively, R.S., 2016, Utility of the horizontal-to-vertical spectral ratio passive seismic method for estimating thickness of Quaternary sediments in Minnesota and adjacent parts of Wisconsin: Interpretation, v. 4, no. 3, SH71–SH90, https://doi.org/10.1190/INT-2015-0212.1.

Chapelle, F.H., Widdowson, M.A., Brauner, J.S., Mendez, E., and Casey, C.C., 2003, Methodology for estimating times of remediation associated with monitored natural attenuation: U.S. Geological Survey Water-Resources Investigations Report 2003–4057, 51 p., https://doi.org/10.3133/wri034057.

Connor, J.A., Kamath, R., Walker, K.L., and McHugh, T.E., 2015, Review of quantitative surveys of the length and stability of MTBE, TBA, and benzene plumes in groundwater at UST sites: Groundwater, v. 53, no. 2, p. 195–206, https://doi.org/10.1111/gwat.12233.

Cunningham, W.L., and Schalk, C.W., comps., 2011, Groundwater technical procedures of the U.S. Geological Survey, GWPD 17—Conducting instantaneous change in head (slug) test with mechanical slug and submersible pressure transducer: U.S. Geological Survey Techniques and Methods, book 1, chap. A1, 151 p., https://pubs.usgs.gov/tm/1a1/pdf/tm1-a1.pdf.

Dakota Technologies Company, Inc., 2016, High resolution site characterization report—Ultra-violet optical screening tool, 53 p.

Doherty, J., 2003, Ground water model calibration using pilot points and regularization: Ground Water, v. 41, no. 2, p. 170–177, https://doi.org/10.1111/j.1745-6584.2003.tb02580.x.

Doherty, J.E., and Hunt, R.J., 2010, Approaches to highly parameterized inversion—A guide to using PEST for groundwater-model calibration: U.S. Geological Survey Scientific Investigations Report 2010–5169, 59 p., https://doi.org/10.3133/sir20105169.

Doherty, J., and Welter, D., 2010, A short exploration of structural noise: Water Resources Research, v. 46, no. 5, 14 p., https://doi.org/10.1029/2009wr008377.

Dripps, W., Hunt, R., and Anderson, M., 2006, Estimating recharge rates with analytic element models and parameter estimation: Ground Water, v. 44, no. 1, p. 47–55, https://doi.org/10.1111/j.1745-65284.2005.00115.x.

Emeis, K.C., 2009, Sapropels, in Gornitz, V., ed., Encyclopedia of Paleoclimatology and Ancient Environments, Encyclopedia of Earth Sciences Series: Dordrecht, Springer, p. 867–877, https://link.springer.com/referenceworkentry/10.1007%2F978-1-4020-4411-3_204.

Evanson, T., Pelayo, A., and Bahr, J., 2009, Wisconsin closure protocol study—A retrospective study of LUST site closures between 1999 and 2000: Madison, Wis., Wisconsin Department of Natural Resources Report PUB–RR–805.

Fetter, C.W., 1994, Contaminant hydrogeology (2d ed.): New York, Macmillan College Publishing, Inc., 458 p.

Gebert, W.A., Walker, J.F., and Kennedy, J.L., 2011, Estimating 1970–99 average annual groundwater recharge in Wisconsin using streamflow data: U.S. Geological Survey Open–File Report 2009–1210, 14 p., plus appendixes, http://pubs.usgs.gov/ofr/2009/1210/.

Haitjema, H.M., 1995, Analytic element modeling of groundwater: San Diego, Calif., Academic Press, 394 p.

Haitjema, H., 2006, The role of hand calculations in ground water flow modeling: Ground Water, v. 44, no. 6, p. 786–791, https://doi.org/10.1111/j.1745-6584.2006.00189.x.

Heck, J., Rodysill, J., and Woods, P., 2013, Preliminary core sampling project for The Lac du Flambeau Band of Lake Superior Chippewa Indians: Minneapolis, Minn., LacCore, National Lacustrine Core Facility, Department of Earth Sciences, University of Minnesota, 84 p.

Hunt, R.J., Walker, J.F., Selbig, W.R., Westenbroek, S.M., and Regan, R.S., 2013, Simulation of climate-change effects on streamflow, lake water budgets, and stream temperature using GSFLOW and SNTEMP, Trout Lake Watershed, Wisconsin: U.S. Geological Survey Scientific Investigations Report 2013–5159, 118 p., https://doi.org/10.3133/sir20135159.

Institute of Hydrology, 1980, Low flow studies report no. 3—Research report: Wallingford, Oxon, United Kingdom, Institute of Hydrology Report no. 3, p. 12–19.

Irvine, D.J., Briggs, M.A., Lautz, L.K., Gordon, R.P., McKenzie, J.M., and Cartwright, I., 2017, Using diurnal temperature signals to infer vertical groundwater-surface water exchange: Groundwater, v. 55, no. 1, p. 10–26, https://doi.org/10.1111/gwat.12459.

Irvine, D.J., Lautz, L.K., Briggs, M.A., Gordon, R.P., and McKenzie, J.M., 2015, Experimental evaluation of the applicability of phase, amplitude, and combined methods to determine water flux and thermal diffusivity from temperature time series using VFLUX 2: Journal of Hydrology (Amsterdam), v. 531, no. 3, p. 728–737, https://doi.org/10.1016/j.jhydrol.2015.10.054.

Juckem, P.F., Fienen, M.N., and Hunt, R.J., 2014, Simulation of groundwater flow and interaction of groundwater and surface water on the Lac du Flambeau Reservation, Wisconsin: U.S. Geological Scientific Investigations Report 2014–5020, 34 p., https://dx.doi.org/10.3133/sir20145020.

Kenoyer, G.J., 1986, Groundwater/lake dynamics and chemical evolution in a sandy silicate aquifer in northern Wisconsin: Madison, Wis., University of Wisconsin-Madison, Department of Geology, Wis., Ph.D. thesis, 174 p.

Krabbenhoft, D.P., 1988, Hydrologic and geochemical investigations of aquifer-lake interactions at Sparkling Lake Wisconsin: Madison, Wis., University of Wisconsin-Madison, Ph.D. thesis, 213 p.

Krabbenhoft, D.P., and Anderson, M.P., 1986, Use of a numerical ground-water flow model for hypothesis testing: Ground Water, v. 24, no. 1, p. 49–55, https://doi.org/10.1111/j.1745-6584.1986.tb01458.x.

Krabbenhoft, D.P., Bowser, C.J., Anderson, M.P., and Valley, J.W., 1990, Estimating groundwater exchange with lakes—1. The stable isotope mass balance method: Water Resources Research, v. 26, no. 10, p. 2445–2453, https://doi.org/10.1029/WR026i010p02445.

Leaf, A.T., 2020, A distributed temperature sensing investigation of groundwater discharge to Haskell Lake, Lac du Flambeau Reservation, Wisconsin, July 27–August 1, 2016: U.S. Geological Survey Scientific Investigations Report 2020–5005, 17 p., https://doi.org/10.3133/sir20205005.

Leaf, A.T., Fienen, M.N., Hunt, R.J., and Buchwald, C.A., 2015, Groundwater/surface-water interactions in the Bad River watershed, Wisconsin: U.S. Geological Survey Scientific Investigations Report 2015–5162, 110 p., https://doi.org/10.3133/sir20155162.

Leaf, A.T., and Haserodt, M.J., 2020, MODFLOW–NWT and MODPATH models, data from aquifer tests and temperature profilers, and groundwater flux estimates used to assess groundwater/surface-water interactions in Haskell Lake, Wisconsin: U.S. Geological Survey data release, https://doi.org/ 10.5066/P9ZQGGHY.

McBride, M.S., and Pfannkuch, H.O., 1975, The distribution of seepage within lakebed: Journal of Research of the U.S. Geological Survey, v. 3, no. 5, p. 505–512, accessed January 7, 2020, at https://pubs.usgs.gov/journal/1975/vol3issue5/report.pdf.

Meeker, J.E., 1996, Wild-rice and sedimentation processes in a Lake Superior coastal wetland: Wetlands, v. 16, no. 2, p. 219–231, https://doi.org/10.1007/BF03160695.

Meeker, J.E., 1999, The Ecology of "wild" wild-rice (*Zizania palustris* var. *palustris*) in the Kakagon Sloughs, a riverine wetland on Lake Superior, *in* Williamson, L.S., Dlutkowski, L.A., and McCammon Soltis, A.P., eds., Proceedings of the Wild River Research and Management Conference: Carlton, Minn., July 7–8, 1999, p. 68–83.

Merritt, M.L., and Konikow, L.F., 2000, Documentation of a computer program to simulate lake-aquifer interaction using the MODFLOW ground-water flow model and the MOC3D solute-transport model: U.S. Geological Survey Water-Resources Investigations Report 00–4167, 146 p.

M.H.E. Products, 2003, PushPoint Sampler (US Pat. # 6,470,967)—Operators manual and applications guide, version 2.01: East Tawas, Mich., M.H.E. Products web page, accessed March 23, 2020, at http://mheproducts.com/downloads.html.

National Archives and Records Administration, 1911, Map of the Lac du Flambeau Reservation: U.S. Department of Interior, Office of Indian Affairs, National Archives and Records Administration, Record Group 75, Lac du Flambeau Agency, civilian Conservation Corps- Indian Division, Lac du Flambeau Unit, Undescribed Materials Box 387867, Maps Projects LDF 1009.

National Atlas of the United States, 2014, 1:1,000,000-scale state boundaries of the United States: accessed March 20, 2014, at http://nationalatlas.gov/atlasftp-1m.html. [Also available at https://geodata.lib.berkeley.edu/catalog/stanford-wj635fh1294.]

National Oceanic and Atmospheric Administration (NOAA), 2018a, Daily summaries station details for Minocqua, WI, station GHCND, USC00475516: accessed March 19, 2018, at https://www.ncdc.noaa.gov/cdo-web/datasets/GHCND/stations/GHCND:USC00475516/detail.

National Oceanic and Atmospheric Administration (NOAA), 2018b, Local climatological data station details for Lakeland Noble Lee Memorial Field Airport, WI, station WBAN, 04865: accessed May 29, 2018, at https://www.ncdc.noaa.gov/cdo-web/datasets/LCD/stations/WBAN:04865/detail.

Niswonger, R.G., Panday, S., and Ibaraki, M., 2011, MODFLOW–NWT—A Newton formulation for MODFLOW–2005: U.S. Geological Survey Techniques and Methods, book 6, chap. A37, 44 p.

Niswonger, R.G., and Prudic, D.E., 2005, Documentation of the Streamflow-Routing (SFR2) Package to include unsaturated flow beneath streams—A modification to SFR1: U.S. Geological Survey Techniques and Methods book 6, chap. A13, 50 p., https://doi.org/10.3133/tm6A13.

Niswonger, R.G., Prudic, D.E., and Regan, R.S., 2006, Documentation of the Unsaturated-Zone Flow (UZF1) Package for modeling unsaturated flow between the land surface and the water table with MODFLOW–2005: U.S. Geological Survey Techniques and Methods book 6, chap. A19, 62 p., https://doi.org/10.3133/tm6A19.

Northern Lake Service, Inc., 2016, Analytical Results: VOC's by P&T/GCMS-Water-(VarSat2000), project 264654 Haskell Lake Pore Water Sample, August 18, 5 p.

Northern Lake Service, Inc., 2017, Analytical Results: VOC's by P&T/GCMS-Water-(VarSat2000), project 286136 Sub Lake Sampling, September 14, 6 p.

Özaydin, V., Şendil, U., and Altinbilek, D., 2001, Stable isotope mass balance method to find the water budget of a lake: Turkish Journal of Engineering and Environmental Sciences, v. 15, p. 329–344.

Pastor, J., Dewey, B., Johnson, N.W., Swain, E.B., Monson, P., Peters, E.B., and Myrbo, A., 2017, Effects of sulfate and sulfide on the life cycle of *Zizania palustris* in hydroponic and mesocosm experiments: Ecological Applications, v. 27, no. 1, p. 321–336, https://doi.org/10.1002/eap.1452.

Patterson, G.L., 1989, Water resources of Vilas County, Wisconsin: U.S. Geological Survey Miscellaneous Paper 89–1, 46 p., accessed January 7, 2020, at https://wgnhs.wisc.edu/pubs/mp891/.

Pollock, D.W., 2012, User guide for MODPATH version 6—A particle-tracking model for MODFLOW: U.S. Geological Survey Techniques and Methods book 6, chap. A41, 58 p., https://doi.org/10.3133/tm6A41.

REI Engineering Inc., 2016, Current conditions report tower standard, 506 p.

Schreüder, W.A., 2009, Running BeoPEST, *in* PEST Conference 2009, Potomac, Md., November 2–4, 2009, Proceedings: Bethesda, Md., S.S. Papadopulos & Associates, Inc., 304 p.

Schwartz, F.W., and Zhang, H., eds., 2003, Fundamentals of ground water: New York, John Wiley and Sons, 621 p.

Sebok, E., Duque, C., Kazmierczak, J., Engesgaard, P., Nilsson, B., Karan, S., and Frandsen, M., 2013, High-resolution distributed temperature sensing to detect seasonal groundwater discharge into Lake Væng, Denmark: Water Resources Research, v. 49, no. 9, p. 5355–5368, https://doi.org/10.1002/wrcr.20436.

Solinst, 2013, Drive-point piezometer instructions: accessed May 17, 2018, at http://www.forestry-suppliers.com/Documents/2212_msds.pdf.

Turnipseed, D.P., and Sauer, V.B., 2010, Discharge measurements at gaging stations: U.S. Geological Survey Techniques and Methods, book 3, chap. A8, 87 p., https://doi.org/10.3133/tm3A8.

U.S. Department of Commerce, 2014, TIGER/Line shapefile, 2014, state, Wisconsin, primary and secondary roads state-based shapefile: accessed December 20, 2017, at https://catalog.data.gov/dataset/tiger-line-shapefile-2014-state-wisconsin-primary-and-secondary-roads-state-based-shapefile.

U.S. Department of Commerce and U.S. Census Bureau, Geography Division, Cartographic Products and Services Branch, 2017, 2016 cartographic boundary file, current American Indian/Alaska Native/Native Hawaiian areas for United States 1:500,000: accessed December 20, 2017, at https://www2.census.gov/geo/tiger/GENZ2016/shp/cb_2016_us_aiannh_500k.zip.

U.S. Geological Survey, 2004, USGS Small-scale dataset—Cities and towns of the United States 200402 shapefile: U.S. Geological Survey: accessed August 11, 2004, at http://nationalatlas.gov/atlasftp.html.

U.S. Geological Survey, 2013, National elevation dataset: accessed December 20, 2017, at https://nationalmap.gov.

U.S. Geological Survey, 2018, USGS water data for the Nation: U.S. Geological Survey National Water Information System database, accessed November 15, 2018, at https://doi.org/10.5066/F7P55KJN.

Vilas County Land Information & Mapping Department, 2016, Bare earth lidar DEM tiles: provided to the USGS on December 6, 2016.

Wahl, K.L., and Wahl, T.L., 1988, Effects of regional groundwater level declines on streamflow in the Oklahoma Panhandle: Proceedings of Symposium on Water-Use Data for Water Resources Management, American Water Resources Association, August 1988, Tucson, Arizona, p. 239–249.

Weaver, T.L., Neff, B.P., and Ellis, J.M., 2005, Water quality and hydrology of the Lac Vieux Desert Watershed, Gogebic County, Michigan, and Vilas County, Wisconsin, 2002–04: U.S. Geological Survey Scientific Investigations Report 2005–5237, 42 p., https://doi.org/10.3133/sir20055237.

Welter, D.E., White, J.T., Hunt, R.J., and Doherty, J.E., 2015, Approaches in highly parameterized inversion—PEST++ Version 3, a Parameter ESTimation and uncertainty analysis software suite optimized for large environmental models: U.S. Geological Survey Techniques and Methods, book 7, chap. C12, 54 p., https://doi.org/10.3133/tm7C12.

Westenbroek, S.M., Kelson, V.A., Dripps, W.R., Hunt, R.J., and Bradbury, K.R., 2010, SWB—A Modified Thornthwaite-Mather Soil-Water-Balance code for estimating groundwater recharge: U.S. Geological Survey Techniques and Methods book 6, chap. A31, 60 p.

Weston Solutions, Inc., 2011, Final phase II environmental site assessment for the highway 70 former fireworks stand site Lac Du Flambeau, Vilas County, Wisconsin: Report prepared for U.S. Environmental Protection Agency on behalf of the Lac Du Flambeau Band of Lake Superior Chippewa Indians, 173 p.

Weston Solutions, Inc., 2014, Summary of findings June 2014 vertical aquifer sampling Haskell Lake area groundwater investigation, 89 p.

Weston Solutions, Inc., 2016, Investigation results summary map 2014–2015—Total VOCs in groundwater: Obtained from Kristen Hanson (LDF Tribe) on August 3, 2018.

Weston Solutions, Inc., 2017, Extent of mid-depth (5–15 ft) soil contamination soil boring maximum PID measurements Haskell Lake Area Lac du Flambeau, Vilas County, Wisconsin: Obtained from Kristen Hanson (LDF Tribe) on August 18, 2018.

White, J.T., 2017, Forecast first—An argument for groundwater modeling in reverse: Groundwater, v. 55, no. 5, p. 660–664, https://doi.org/10.1111/gwat.12558.

White, J.T., Fienen, M.N., and Doherty, J.E., 2016, A python framework for environmental model uncertainty analysis: Environmental Modelling & Software, v. 85, p. 217–228, https://doi.org/10.1016/j.envsoft.2016.08.017.

Wisconsin Department of Natural Resources (WDNR), 2015a, Wisconsin Beaver Management Plan 2015–2025: Wisconsin Department of Natural Resources, accessed Jan 7, 2020, at https://dnr.wi.gov/files/PDF/pubs/wm/WM0610.pdf.

Wisconsin Department of Natural Resources (WDNR), 2015b, WDNR 24K Hydro Geodatabase, 1:24,000: accessed June 8, 2016, at ftp://dnrftp01.wi.gov/geodata.

Wisconsin Department of Natural Resources (WDNR), 2017a, Haskell Lake: accessed February 28, 2017, at http://dnr.wi.gov/lakes/lakepages/LakeDetail.aspx?wbic=1538000.

Wisconsin Department of Natural Resources (WDNR), 2017b, BRRTs on the web: accessed February 28, 2017, at http://dnr.wi.gov/botw/GetActivityDetail.do?siteId=5170900&adn=0364127899.

Wisconsin Department of Transportation, 2015, Wisconsin airport reference points: accessed Jan 7, 2020, at https://wiscon-sindot.gov/Pages/doing-bus/aeronautics/resources/arp.aspx.

Zheng, C., 2010, MT3DMS v. 5.3 Supplemental user's guide, technical report to the U.S. Army Engineer Research and Development Center: Department of Geological Sciences, University of Alabama, 220 p.

Appendixes 1–10

Appendix 1. Monitoring Well Information and Groundwater Elevation Measurements

Figure 2 shows monitoring wells that were previously installed at the study site as part of the ongoing groundwater contamination investigation. This existing well network was used in this study to measure groundwater elevations (hydraulic head) and perform slug tests. Site access issues limited the ability to regularly access four of the well pairs (MW18, MW18D, MW19, MW19D, MW21, MW21D, MW21M, MW22, and MW22D). A summary of well locations and depths, as reported in REI Engineering, Inc. (2016); Weston Solutions, Inc. (2011); and Bristol Environmental Remediation Services, LLC (2016), is presented in table 1.1. Tables 1.2 through 1.11 present detailed well completion information and lithology (as reported by REI Engineering, Inc. [2016]; Weston Solutions, Inc. [2011]; and Bristol Environmental Remediation Services, LLC [2016]) for wells where slug tests were completed (appendix 5).

Field Methods

Groundwater elevation measurements were collected in the monitoring well network (figs. 2, 7) with an electric water level meter and from established measurement points on the well casing following standard U.S. Geological Survey procedures (Cunningham and Schalk, 2011). The depth to groundwater in the full set of wells was measured on March 1, 2017. Depths to groundwater in a partial set of wells was regularly measured between July 2016 and November 2017.

Hourly groundwater elevation data were collected in the MW16 well nest (wells MW16, MW16D, and MW16E) using submersible absolute pressure transducers (Cunningham and Schalk, 2011). Continuous groundwater elevation data were collected from July 27, 2016, to February 7, 2018, in wells MW16 and MW16D and from October 26, 2016, to February 7, 2018, in well MW16E.

Data Analysis

The continuous data from the absolute pressure transducers include the following two pressure components: (1) the pressure from the water column above the pressure sensor and (2) the atmospheric pressure. To compute a groundwater elevation, atmospheric pressure was subtracted from the absolute pressure. Water level records can be compensated for atmospheric pressure using a barometric pressure transducer at the site or with pressure data from a nearby weather station. Site barometric pressure transducers failed for the initial data collection effort and were used when quality data were available. When site pressure data were not available, pressure data from the Minocqua/Woodruff National Weather Service Lakeland Airport/Noble F. Lee Memorial Field weather station (National Oceanic and Atmospheric Administration [NOAA], 2018a) and the Manitowish Waters Airport weather station (NOAA, 2018b) were used. Atmospheric pressure data were resampled to hourly values to compensate the hourly groundwater level data. Gaps when both weather stations were missing pressure data and no site pressure data were available, are gaps in the groundwater level record for the wells.

The groundwater level record was converted to groundwater elevations using manual depth to water measurements with the electric water level meter and the surveyed elevations of the well casing measurement points. Changes in pressure sensor elevation were prorated evenly between visits unless a known event, like the removal and replacement of the transducer to download data, caused a change in the transducer position.

Results

The depths to groundwater data are presented in table 1.12, and quarterly groundwater elevations are shown spatially in figure 7. Hourly groundwater elevation data for the wells in the MW16 well nest are in the U.S. Geological Survey National Water Information System (NWIS) database (U.S. Geological Survey, 2018) under U.S. Geological Survey site numbers 455448089545001 (MW16), 455448089545002 (MW16D), and 455448089545003 (MW16E). The continuous groundwater elevation data and vertical hydraulic gradients between the wells in the MW16 nest are shown in figure 8. A negative vertical hydraulic gradient indicates upward movement of water and a positive gradient indicates downward movement of water. The vertical gradients between the shallow MW16 well and the mid-depth MW16D well were almost always negative, upward flow, with notable changes in magnitude during recharge events. The vertical gradient between the mid-depth MW16D well and the deepest MW16E well was almost zero, indicating little to no vertical flow at depth. The following tables are presented in Microsoft Excel files available at https://dx.doi.org/10.3133/sir20205024:

Conclusion

Synoptic groundwater elevation data show consistent groundwater flow toward Haskell Lake across the site and a likely groundwater divide between the lake and Tower Creek (fig. 7). Continuous water level data from the MW16 well nest indicate relatively quick responses at all well depth to recharge events and a consistent upward gradient between the two deeper wells and the shallowest well (fig. 8). This upward gradient and the spatial groundwater elevation distribution indicates groundwater from the site is likely discharging into the nearby Haskell Lake.

References Cited

Bristol Environmental Remediation Services, LLC, 2016, EPA Contract No. EP–W–12–009, Task Order (TO) 3012 Tower Standard Site, Lac du Flambeau Reservation, Wisconsin August 2016 Site Investigation, Rev 0: Technical memorandum, September 23, 2016, 167 p.

Cunningham, W.L., and Schalk, C.W., comps., 2011, Groundwater technical procedures of the U.S. Geological Survey, GWPD 17—Conducting instantaneous change in head (slug) test with mechanical slug and submersible pressure transducer: U.S. Geological Survey Techniques and Methods, book 1, chap. A1, 151 p., https://pubs.usgs.gov/tm/1a1/pdf/tm1-a1.pdf.

National Oceanic and Atmospheric Administration (NOAA), 2018a, Local climatological data station details for Lakeland Noble Lee Memorial Field Airport, WI, station WBAN, 04865, accessed May 29, 2018, at https://www.ncdc.noaa.gov/cdo-web/datasets/LCD/stations/WBAN:04865/detail.

National Oceanic and Atmospheric Administration (NOAA), 2018b, Local climatological data station details for Manitowish Water Airport, WI, station WBAN, 00297, accessed March, 19, 2018, at https://www.ncdc.noaa.gov/cdo-web/datasets/LCD/stations/WBAN:00297/detail.

REI Engineering Inc., 2016, Current conditions report tower standard, 506 p.

U.S. Geological Survey, 2018, USGS water data for the Nation: U.S. Geological Survey National Water Information System database, accessed November 15, 2018, at https://doi.org/10.5066/F7P55KJN.

Weston Solutions, Inc., 2011, Final phase II environmental site assessment for the highway 70 former fireworks stand site Lac Du Flambeau, Vilas County, Wisconsin: Report prepared for U.S. Environmental Protection Agency on behalf of the Lac Du Flambeau Band of Lake Superior Chippewa Indians, 173 p.

Appendix 2. Lake Elevations

Synoptic lake elevations were surveyed using a survey-grade Global Positioning System (GPS). Regular measurements were made between July 2016 and November 2017 at Squirrel, Crawling Stone, Booth, and Buckskin Lakes and at two unnamed lakes northwest of Haskell Lake (fig. 13). One-time measurements were collected at Jerms, Broken Bow, and Tippecanoe Lakes and at ponds adjacent to the northeast shore of Haskell Lake (fig. 9); measurement dates are presented in table 2.1. An established survey benchmark was measured during each survey to assess the accuracy of each survey. The National Geodetic Survey marker DO6241 (https://www.ngs.noaa.gov/cgi-bin/ds_mark.prl?PidBox=DO6241) on State Highway 70, east of Haskell Lake and north of Squirrel Lake was used for all of the surveys.

Lake elevations are summarized in table 2.1, displayed graphically in figure 10, and an average elevation is shown in figure 13. An estimated error for each lake elevation is included in table 2.1 and is the greater of either twice the standard deviation of the measured elevations at benchmark DO6241 or the vertical root mean square reported by the GPS receiver for each data point. The vertical root mean square is an estimate of the precision in the collected vertical coordinate and is output by the GPS software. The following table is presented in a Microsoft Excel file available at https://dx.doi.org/10.3133/sir20205024:

Table 2.1. Measured lake elevations.

Appendix 3. Installation and Collection of Data from the Mini-Piezometer Network

A network of 10 miniature piezometers (mini-piezometers) was established around Haskell Lake (fig. 9) to assess vertical hydraulic gradients between the lake and the shallow aquifer.

Field Methods and Data Analysis

Mini-piezometers were constructed from 0.5-inch high-density polyethylene (HDPE) tubing with a 0.5- to 1-foot screen made of HDPE tubing with drilled holes wrapped in porous cloth to prevent sediment from clogging the holes of the screen. The mini-piezometers were installed at depths of 3.8–7.5 feet around the periphery of the lake in the lakebed and along the lake shore and at depths of up to 26 feet into the lakebed sediment along the dock by the Haskell Lake study site (fig. 19). The depth to groundwater was measured in the mini-piezometers using an electric water level meter or using a steel tape if the groundwater conductance was too low to get a signal from the electric water level meter following methods by Cunningham and Schalk (2011). Measurements were made from a measuring point marked on the mini-piezometer tubing. A top of casing elevation was established for each mini-piezometer by surveying the height of the measuring point relative to the stage of Haskell Lake, the elevation of which was measured at the U.S. Geological Survey site 455430089550001. A summary of mini-piezometer construction and location information is listed in table 3.1.

Results

Tables 3.2 through 3.6 provide measured depths to groundwater and computed gradients for the mini-piezometer network. Mini-piezometer data can be downloaded from the National Water Information System (NWIS) database (U.S. Geological Survey, 2018) using the NWIS site numbers presented in table 3.1. Hydraulic gradients measured at the mini-piezometers are presented in fig. 15, with average gradients shown spatially in figure 14. The November 2, 2017, measurement in PZ8 (fig. 15) was a large positive value (downward groundwater flow) and was inconsistent with all other measurements at this location and in nearby mini-piezometers; this reading was likely erroneous. The following tables are presented in Microsoft Excel files available at https://dx.doi.org/10.3133/sir20205024:

Table 3.1. Mini-piezometer construction information and surveyed locations.

Table 3.2. Depth to groundwater measurements in mini-piezometers on May 4, 2017, and calculated vertical hydraulic gradients.

Table 3.3. Depth to groundwater measurements in mini-piezometers on May 15, 2017, and calculated vertical hydraulic gradients.

Table 3.4. Depth to groundwater measurements in mini-piezometers on May 16, 2017, and calculated vertical hydraulic gradients.

Table 3.5. Depth to groundwater measurements in mini-piezometers on August 30, 2017, and calculated vertical hydraulic gradients.

Table 3.6. Depth to groundwater measurements in mini-piezometers on November 2–3, 2017, and calculated vertical hydraulic gradients.

Conclusion

The measured gradients indicate groundwater discharge (negative gradient) to Haskell Lake around most of its perimeter (fig. 14), with the possible exception of the area near the outlet, which was not measured. Larger gradients on the western side of the lake are consistent with a steeper gradient in the water table between Buckskin and Haskell Lakes (fig. 13). Measured gradients near the petroleum contaminant plume (fig. 2) indicate groundwater discharge to Haskell Lake downgradient from the plume source area.

References Cited

Cunningham, W.L., and Schalk, C.W., comps., 2011, Groundwater technical procedures of the U.S. Geological Survey, GWPD 17—Conducting instantaneous change in head (slug) test with mechanical slug and submersible pressure transducer: U.S. Geological Survey Techniques and Methods, book 1, chap. A1, 151 p., https://pubs.usgs.gov/tm/1a1/pdf/tm1-a1.pdf.

U.S. Geological Survey, 2018, USGS water data for the Nation: U.S. Geological Survey National Water Information System database, accessed November 15, 2018, at https://doi.org/10.5066/F7P55KJN.

Appendix 4. Synoptic Flow Survey

A synoptic streamflow survey was completed on November 2, 2017, along Tower Creek upstream and downstream from Haskell Lake (fig. 9). Streamflow measurements to the south of Haskell Lake were made using an acoustic Doppler current profiler (ADCP) on a raft and a pulley system setup across the channel (Mueller and others, 2013). The ADCP on a pulley system minimizes disturbances from being in the channel or using a boat and can be useful at low-velocity sites. Streamflow downstream from the culvert on Peace Pipe Lane (figs. 2, 9) was measured with a handheld acoustic Doppler velocimeter where the water depth was too shallow and the channel was too narrow for the ADCP raft. A routine streamflow measurement was made on November 6, 2017, at the Tower Creek streamgage (U.S. Geological Survey streamgage 05392187) using methods of Turnipseed and Sauer (2010). Gage height at the creek was within 0.02 foot between the afternoon of the synoptic survey on November 2 and when the routine streamflow measurement at the streamgage was made on November 6. Despite being several days after the synoptic streamflow survey, the routine streamflow measurement was considered valid for inclusion in the synoptic streamflow survey results because of the similar creek stage on November 2 and 6. Streamflows measured during the synoptic streamflow survey and estimated uncertainties are summarized in table 4.1 and are available in the National Water Information Services (NWIS) database (U.S. Geological Survey, 2018) using the NWIS site numbers listed in table 4.1. Tower Creek was determined to be gaining base flow between all measurement points, consistent with the results of the updated GFLOW model of Juckem and others (2014), described in appendix 10. The following table is presented in Microsoft Excel files available at https://dx.doi.org/10.3133/sir20205024:

Table 4.1. Summary of synoptic flow survey results along Tower Creek, ordered from upstream to downstream locations.

References Cited

Juckem, P.F., Fienen, M.N., and Hunt, R.J., 2014, Simulation of groundwater flow and interaction of groundwater and surface water on the Lac du Flambeau Reservation, Wisconsin: U.S. Geological Scientific Investigations Report 2014–5020, 34 p., https://dx.doi.org/10.3133/sir20145020.

Mueller, D.S., Wagner, C.R., Rehmel, M.S., Oberg, K.A, and Rainville, Francois, 2013, Measuring discharge with acoustic Doppler current profilers from a moving boat (ver. 2.0, December 2013): U.S. Geological Survey Techniques and Methods, book 3, chap. A22, 95 p., https://doi.org/10.3133/tm3A22.

Turnipseed, D.P., and Sauer, V.B., 2010, Discharge measurements at gaging stations: U.S. Geological Survey Techniques and Methods, book 3, chap. A8, 87 p., https://doi.org/10.3133/tm3A8.

U.S. Geological Survey, 2018, USGS water data for the Nation: U.S. Geological Survey National Water Information System database, accessed November 15, 2018, at https://doi.org/10.5066/F7P55KJN.

Appendix 5. Slug Test Methods and Results

Slug tests are a relatively simple method for estimating the horizontal hydraulic conductivity of an aquifer near a well. A volume of water is displaced in the well and the recovery of the water level monitored. Slug tests were completed in all wells at the Haskell Lake contamination site where access was permitted. The estimates of hydraulic conductivity from the slug tests provide information on the relative heterogeneity of the unconsolidated materials at the study site and guided the bounds for hydraulic conductivity parameters used in the parameter estimation process.

Field Methods

On August 30 and 31, 2017, slug-in and slug-out tests were performed in monitoring wells MW1, MW2, MW3, MW16, MW16D, MW16E, MW17, MW17D, MW20, and MW20D. Figure 2 shows the location of these wells and table 1.1 provides coordinates and surveyed casing elevations for each well. Slug tests were completed using a solid, cylindrical, plastic slug that was 5-feet long and had a 0.115-foot diameter. Wells were instrumented with a submersible pressure transducer set to collect pressure data at a 0.5-second interval. Slug tests were completed using the standards and methods outlined in Cunningham and Schalk (2011). Data were collected until at least 90-percent recovery relative to the initial measured groundwater elevation.

Data Analysis

Slug test results were analyzed using the Bouwer and Rice (1976) solution for unconfined aquifers in AQTESOLV (Duffield, 2007), version 4.50, software (HydroSOLVE, 2017). An aquifer thickness of 50 feet was assumed for all wells based on depth to bedrock data from the wells in and near the Haskell Lake contamination site; a manual sensitivity analysis of aquifer thickness determined the results to be insensitive to this parameter. As recommended in Butler (1998), a correction for drainage from the filter pack was used for test results from wells screened across the water table; for this correction, the effective porosity of the filter pack was assumed to be 0.32, equivalent to a medium sand. Drainage from the filter pack manifests as a double straight line in a plot of normalized water levels recorded in the well versus time, with a steeper initial test response when drainage from the filter pack dominates followed by a less-steep response that represents flow conditions in the aquifer. For tests in water table wells that exhibited a double straight line effect, the middle portion (after the initial steep response and before the expected deviation from straight line conditions toward the end of the test) of the response curve was analyzed, as recommended in Bouwer (1989). For wells screened across the water table, slug-in tests typically overestimate the hydraulic conductivity; slug-out test results are more accurate (Bouwer, 1989).

Available well completion and lithologic data for MW1, MW2, MW3, MW16, MW16D, MW16E, MW17, MW17D, MW20, and MW20D, as recorded by REI Engineering, Inc. (2016), Weston Solutions Inc. (2011), and Bristol Environmental Remediation Services, LLC (2016) when the wells were installed, are summarized in tables 1.1 through 1.11. Lithologic data were only recorded for the shallow wells; all deep, “D”, wells were drilled without collecting lithology samples. All of the monitoring wells were constructed from 2-inch, schedule 40 polyvinyl chloride PVC casing and screens. The shallow wells (MW1, MW2, MW3, MW16, MW17, and MW20) were screened across the water table; the deeper wells were screened below the water table.

Results

The results from the slug test analysis are summarized in table 5.1. Raw and processed slug test data, including AQTESOLVE output files, have been archived in the aquifer test archive at the Upper Midwest Water Science Center and are included in the ancillary directory of the data release (Leaf and Haserodt, 2020). Estimated hydraulic conductivity at the site was generally less than 10 feet per day (within the literature range of fine to well-sorted sands; table 3.7 in Fetter, 1994), with some locations (the MW17 well nest and MW2) as low as 1 foot per day (within the literature range of silty sands; Fetter, 1994). Hydraulic conductivity was high-est (>50 feet per day) at the MW20 nest, with values in the literature range for well-sorted sands and glacial outwash (table 3.7 in Fetter, 1994). The following table is presented in a Microsoft Excel file available at https://dx.doi.org/10.3133/sir20205024:

Table 5.1. Summary of hydraulic conductivity estimates from slug tests in contamination site wells.

Conclusion

The estimated hydraulic conductivities from the slug tests indicate substantial heterogeneity in the unconsolidated materials at the Haskell Lake contamination site. The low hydraulic conductivities encountered at the MW17 well nest and the hydraulic conductivities of less than 10 feet per day at wells MW1, MW2, MW3, and the upper two wells in the MW16 well nest, are indicative of a moderate to high silt content and may indicate the predominance of debris flow and possibly till deposits in the upper 30 feet of sediments west of the plume center line (fig. 2). Higher hydraulic conductivity values for the unconsolidated sediments at the MW20 well nest and MW16E may indicate outwash of the Wildcat Lake Member near the source area and sands and gravels predating the Wildcat Lake Member at depth.

References Cited

Bouwer, H., 1989, The Bouwer and Rice slug test—An update: Ground Water, v. 27, no. 3, p. 304–309, https://doi.org/10.1111/j.1745-6584.1989.tb00453.x.

Bouwer, H., and Rice, R.C., 1976, A slug test for determining hydraulic conductivity of unconfined aquifers with completely or partially penetrating wells: Water Resources Research, v. 12, no. 3, p. 423–428, https://doi.org/10.1029/WR012i003p00423.

Bristol Environmental Remediation Services, LLC, 2016, EPA Contract No. EP–W–12–009, Task Order (TO) 3012 Tower Standard Site, Lac du Flambeau Reservation, Wisconsin August 2016 Site Investigation, Rev 0: Technical memorandum, September 23, 2016, 167 p.

Butler, J.J., 1998, The design, performance, and analysis of slug tests: New York, Lewis Publishers, 252 p.

Cunningham, W.L., and Schalk, C.W., comps., 2011, Groundwater technical procedures of the U.S. Geological Survey, GWPD 17—Conducting instantaneous change in head (slug) test with mechanical slug and submersible pressure transducer: U.S. Geological Survey Techniques and Methods, book 1, chap. A1, 151 p., https://pubs.usgs.gov/tm/1a1/pdf/tm1-a1.pdf.

Duffield, G.M., 2007, AQTESOLV for Window User's Guide, version 4.5, HydroSOLVE, Inc., 530 p., accessed Jan 7, 2019 at http://www.aqtesolv.com/manual.asp.

Fetter, C.W., 1994, Contaminant hydrogeology (2d ed.): New York, Macmillan College Publishing, Inc., 458 p.

HydroSOLVE, Inc., 2017, AQTESOLV: Reston, Va., HydroSolve, Inc., web page: accessed August 25, 2017, at http://www.aqtesolv.com/.

Leaf, A.T., and Haserodt, M.J., 2020, MODFLOW–NWT and MODPATH models, data from aquifer tests and temperature profilers, and groundwater flux estimates used to assess groundwater/surface-water interactions in Haskell Lake, Wisconsin: U.S. Geological Survey data release, https://doi.org/10.5066/P9ZQGGHY.

REI Engineering Inc., 2016, Current conditions report tower standard, 506 p.

Weston Solutions, Inc., 2011, Final phase II environmental site assessment for the highway 70 former fireworks stand site Lac Du Flambeau, Vilas County, Wisconsin: Report prepared for U.S. Environmental Protection Agency on behalf of the Lac Du Flambeau Band of Lake Superior Chippewa Indians, 173 p.

Appendix 6. Vertical Temperature Profiles

Temperature time-series data were collected in vertical profiles within the top foot of lakebed sediment to estimate the groundwater flux to or from Haskell Lake near the Haskell Lake contamination site. The temperature data are available in the ancillary directory of Leaf and Haserodt (2020). Heat has been widely used as a tracer for quantifying surface-water/groundwater exchanges (for example, Irvine and others 2017; Gordon and others, 2012; Anderson, 2005; Stonestrom and Constantz, 2003; Lapham, 1989; Bredehoeft and Papadopoulos, 1965), and many different numerical and analytical methods of analysis are available. Analytical models based on the downward propagation of the diurnal temperature signal can be fit to time-series temperature data to estimate the vertical pore-water fluid flux between surface water and groundwater for upwelling and downwelling conditions (Irvine and others, 2017). In the case of downwelling, diurnal temperature signals are transported downward by advection and conduction from the surface-water interface into the underlying sediment to depths that typically exceed 1.5 feet. Conversely, in upwelling zones heat is only transported downward by conduction; data from upwelling zones indicate a muted diurnal signal with depth, with a loss in signal as shallow as 0.3 foot (Irvine and others, 2017). Analysis of thermal data from upwelling zones can be challenging because diurnal signal phase shifts can be small relative to measurement error, and signal amplitudes are attenuated rapidly with depth (Irvine and others, 2017). Furthermore, thermal gradients in areas with upwelling are easy to miss because the gradients can occur in such a limited zone beneath the sediment-water interface. Custom-made temperature profilers with small sensor spacing were deployed near the sediment-water interface to best capture the thermal gradients under upwelling conditions.

Field Methods

Vertical temperature profilers were constructed from four Thermochron iButton DS1922L temperature sensors (± 0.0625 degree Celsius resolution) placed horizontally in a notched, hollow steel rod at a spacing of 1.2 inches. Silicon caulk held the temperature sensors in place and protected them from water damage. Profilers were pounded into the lakebed until the top sensor was below the lakebed/water interface, ensuring the vertical spacing between sensors was known and not affected by bed scour/deposition, assuming the upper sensor remained buried. Temperature data were recorded simultaneously at all four sensors at a sampling interval of either 15 minutes or 1 hour.

Profilers were deployed at two locations (VTP3 and VTP4; shown on fig. 9), from September 18, 2016, to October 26, 2016, and at two locations (VTP1 and VTP2) from August 31, 2017, to September 27, 2017. Two additional deployments from May 4, 2017, to August 2, 2017, failed to collect any data because of water damage.

Data Analysis

The collected temperature data were analyzed for vertical groundwater flux using the MATLAB (MathWorks, Inc., Natick, MA) computer program VFLUX, version 2 (Gordon and others, 2012). The temperature data can be accessed in the data release associated with this publication (Leaf and Haserodt, 2020). VFLUX resamples temperature time series from sensors in a vertical profile to a common time increment and identifies the diurnal phase and amplitude using the dynamic harmonic regression signal processing technique. The signal phase lag or amplitude attenuation between two depths in the vertical is used in analytical solutions to estimate vertical water flux. The analytical solutions to the heat transport equations implemented by VFLUX require several simplifying assumptions including steady, one-dimensional vertical groundwater flow; homogeneous lakebed sediments; and a groundwater temperature equal to the average temperature in the stream or lakebed (Irvine and others, 2015; Briggs and others, 2014). The steady-state assumption limits the ability to apply this method to data with abrupt changes in fluxes; errors have been found to be minimal where fluxes vary slowly. Varying fluxes that change slowly over time may be estimated with VFLUX; however, rapid changes in the groundwater flux from activities like groundwater pumping or sudden changes in lake/stream stage can result in errors in the estimated groundwater flux from VFLUX (Lautz, 2012). VFLUX implements the temperature phase or amplitude methods of Hatch and others (2006) and Keery and others (2007) and the combined phase and amplitude methods of McCallum and others (2012) and Luce and others (2013). For upwelling zones, phase lag or combined amplitude and phase lag methods are less reliable than amplitude only methods (Briggs and others, 2014). The Hatch amplitude method (Hatch and others, 2006) was used for this study.

Inputs to VFLUX include time-series temperature data at multiple depths, sediment porosity, thermal dispersivity (assumed negligible), thermal conductivity, the volumetric heat capacity of the sediment, the volumetric heat capacity of water, and the sensor depths. In addition to flux estimates, VFLUX allows for estimation of the saturated sediment thermal diffusivity (ratio of saturated thermal conductivity to saturated heat capacity) using combined phase and amplitude transport characteristics (Irvine and others, 2015, 2017). Assuming sediment composition does not change, the estimated thermal diffusivity should be constant during the modeled time period; highly variable thermal diffusivity values within a given time series indicate potential errors in the associated fluid flux estimates and provide a qualitative check on flux estimates. Similar to flux, estimates of thermal diffusivity may be difficult in zones with strong upwelling because of rapid attenuation of the diurnal signal with depth and short phase lags that are difficult to accurately characterize (Briggs and others, 2014). The magnitude of the temperature amplitude and quality of the diurnal signal can affect the accuracy of computed fluxes; better defined diurnal signals and larger temperature amplitudes can improve flux estimates.

Advantages of VFLUX versus other thermal modeling methods include the ability to easily estimate fluxes at a high temporal resolution and the ability to assess data quality by looking at the time series of estimated thermal diffusivity. Disadvantages include the number of assumptions used for the analytical solutions, the requirement of a clear, discernable diurnal signal, and the cost of MATLAB software.

The temperature data were also modeled numerically with the 1DTempPro software (Koch and others, 2015) to estimate groundwater fluxes. 1DTempPro simulates one-dimensional vertical groundwater flux and heat transport using the numerical U.S. Geological Survey program VS2DH (Healy and Ronan, 1996). Temperatures simulated by VS2DH are then matched (inverted) to temperature profile data to estimate vertical groundwater flux through the stream or lakebed. Inputs to the program include temperature time series at a minimum of three depths, porosity, saturated thermal conductivity, saturated sediment heat capacity, and thermal dispersivity (Koch and others, 2016). The magnitude of the temperature gradient impacts the accuracy of the flux estimates. A published threshold for high-quality temperature signals does not exist, but ideally data should have a minimum difference of 2 degrees Celsius between the top and bottom temperature series or a 1 degree Celsius difference in sensor amplitude between the top and bottom temperature series. Advantages of using 1DTempPro include a free and user-friendly graphical user interface (GUI), and less simplifying assumptions compared to the analytical methods. However, 1DTempPro only estimates a single average flux for a given period of analysis, making estimation of changing fluxes during longer periods cumbersome and the quality (uncertainty) of flux estimates can be unclear.

The thermal input parameters needed for VFLUX and 1DTempPro are often poorly constrained in the absence of sediment analyses but have small ranges of realistic values (Anderson, 2005). For the Haskell Lake data, no sediment analyses were done and sediment was assumed to be a fine sand with the average literature properties presented in table 6.1. To estimate the effects of uncertainty in the sediment thermal properties on the estimated groundwater fluxes, a Monte Carlo analysis was done in VFLUX using 1,000 realizations (Gordon and others, 2012). For each realization, VFLUX was run with a randomly sampled combination of thermal parameter values based on the user-supplied mean and standard deviation of each parameter listed in table 6.1 (Gordon and others, 2012).

For the Haskell Lake thermal data, where thermal gradients and amplitudes were often small, the period of analysis was sufficiently long, and no large, abrupt changes in flux were expected; VFLUX produced more consistent flux estimates. The estimated thermal diffusivity from VFLUX was used as a basic check on the quality of flux estimate, and the ability to run a Monte Carlo analysis across a range of thermal properties allowed an estimate of the uncertainty resulting from unknown lakebed sediment thermal properties. Therefore, only the VFLUX results are presented. Although fluxes were estimated between each adjacent pair of thermometers in the profiles, only the shallowest pair at each location (with the largest diurnal thermal amplitudes) were used. Following Gordon and others (2012), the 2–3 days of flux data at the beginning and end of the analysis period were discarded because they could have edge effects from the digital filtering (Gordon and others, 2012); figures 6.1, 6.2, and 6.3 present the reduced analysis period without edge effects.

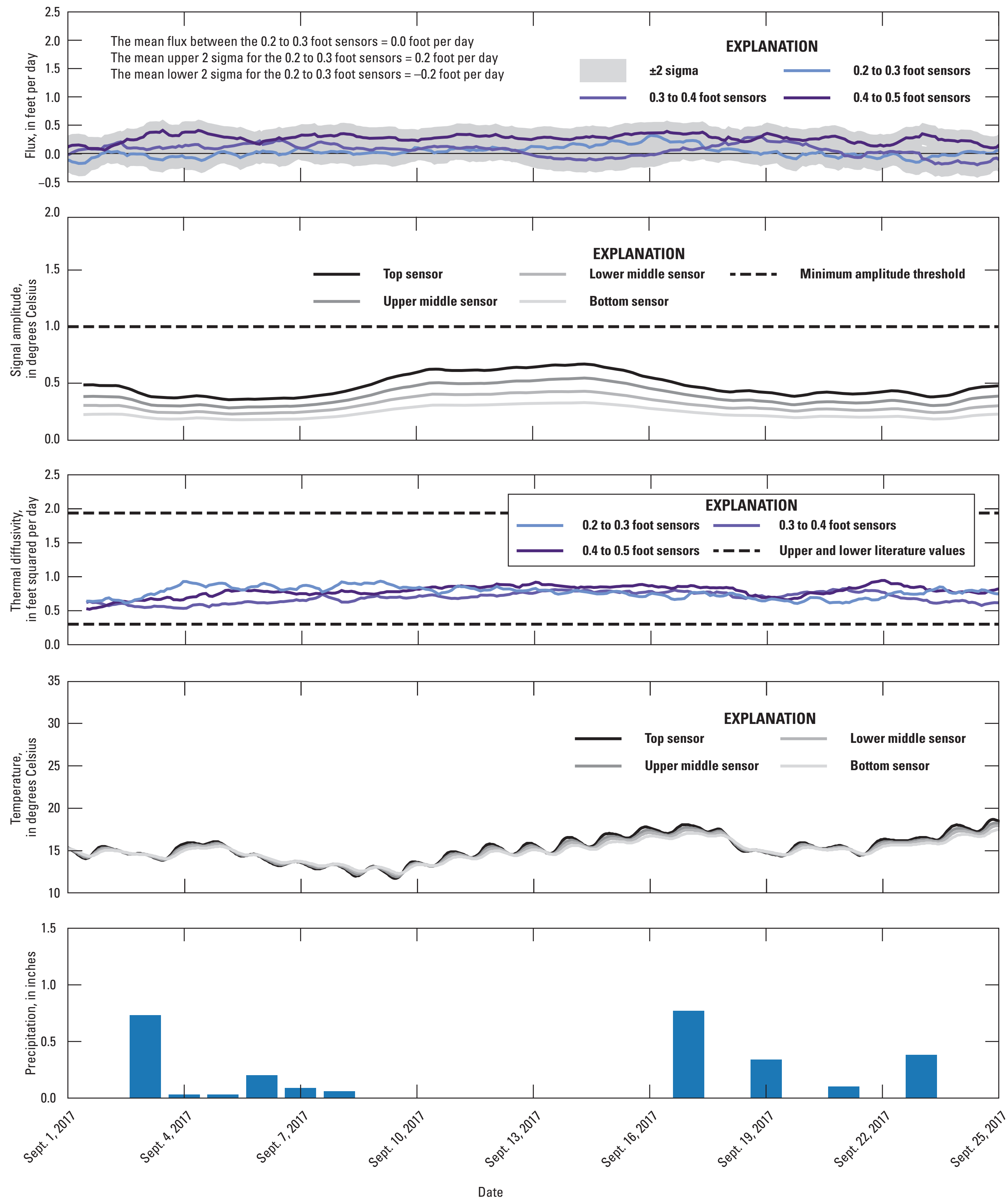

Figure 6.1. Estimated groundwater flux at site VTP2 from VFLUX2, with signal amplitude, estimated thermal diffusivity, recorded temperatures, and precipitation from the Minocqua weather station (National Oceanic and Atmospheric Administration, 2018). A negative flux indicates upward groundwater flow into the lake and a positive flux indicates downward groundwater flow.

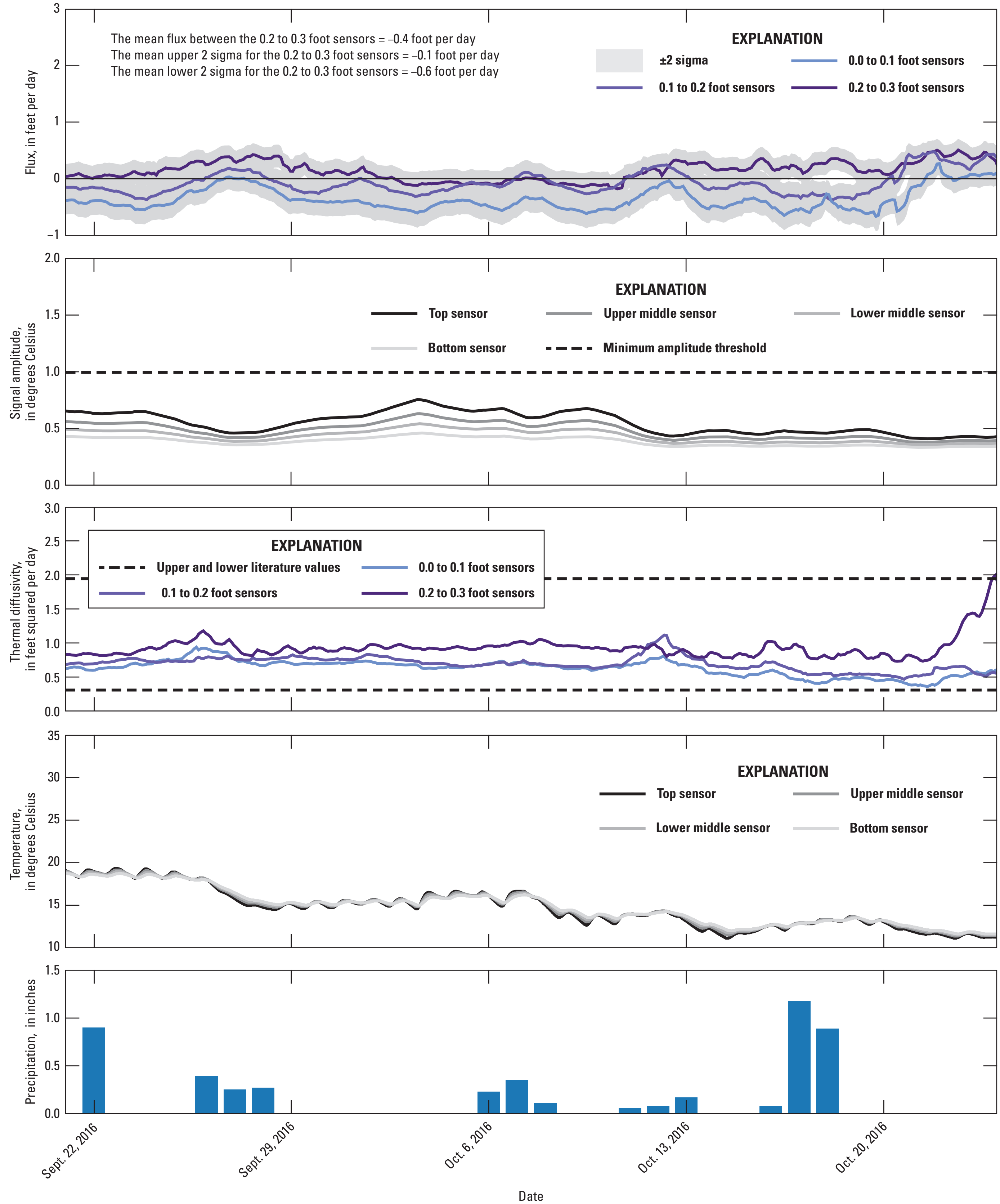

Figure 6.2. Estimated groundwater flux at site VTP3 from VFLUX2, with signal amplitude, estimated thermal diffusivity, recorded temperatures, and precipitation from the Minocqua weather station (National Oceanic and Atmospheric Administration, 2018). A negative flux indicates upward groundwater flow into the lake and a positive flux indicates downward groundwater flow.

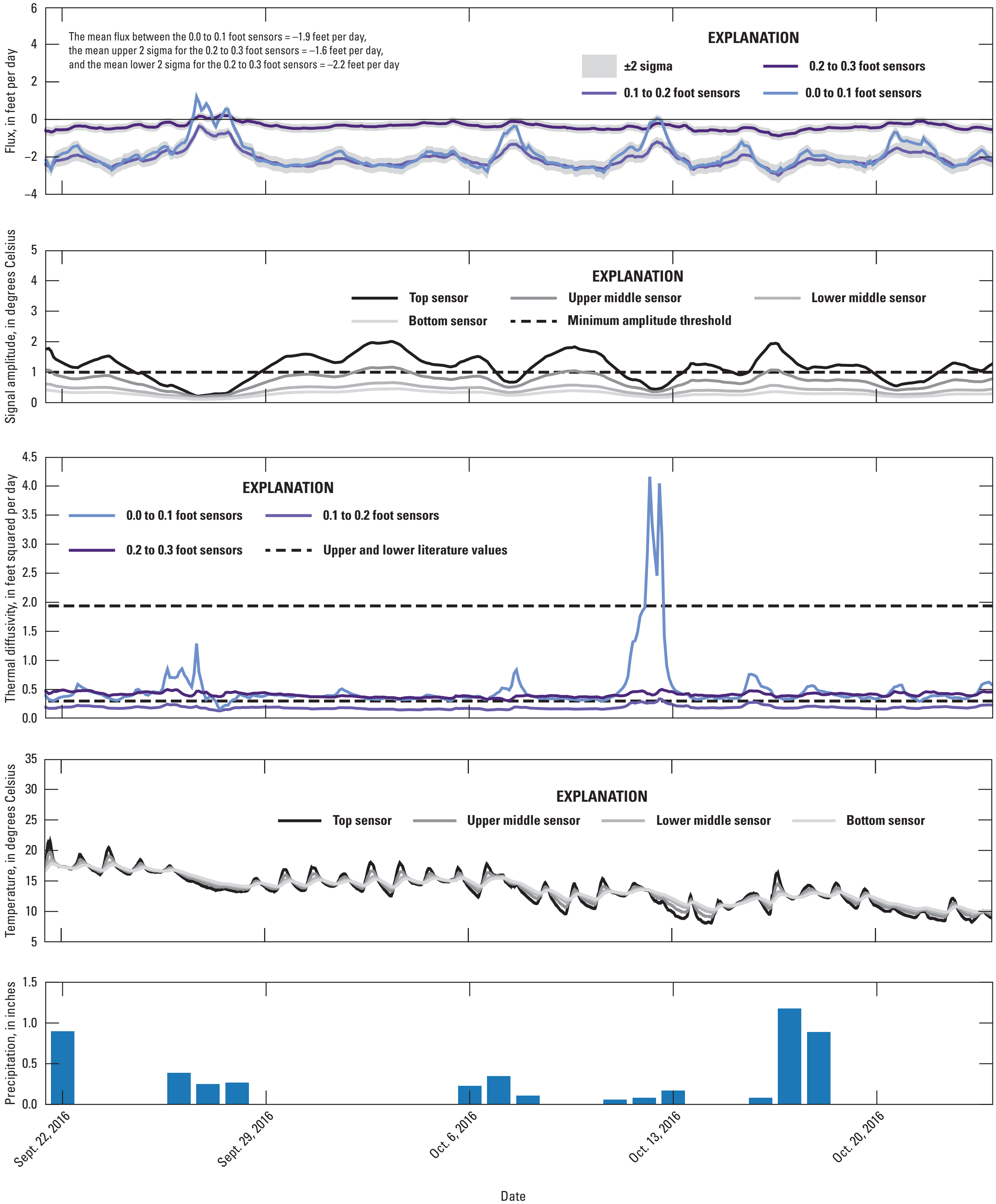

Figure 6.3. Estimated groundwater flux at site VTP4 from VFLUX2, with signal amplitude, estimated thermal diffusivity, recorded temperatures, and precipitation from the Minocqua weather station (National Oceanic and Atmospheric Administration, 2018). A negative flux indicates upward groundwater flow into the lake and a positive flux indicates downward groundwater flow.

Results

Flux, thermal diffusivity, temperature, and amplitude results from the VFLUX analysis for VTP2, VTP3, and VTP4 are presented with precipitation data from the Minocqua weather station (National Oceanic and Atmospheric Administration [NOAA], 2018) in figures 6.1, 6.2, and 6.3. Results from VTP1 are not presented; no clear diurnal signals were apparent in the VTP1 data because the profiler was likely installed too deep in the lake sapropel. Lake sapropel flocculates easily, making it difficult to achieve a seal around the profiler at shallower depths.

VTP4 had the largest temperature amplitudes and best-defined diurnal temperature signals and was assumed to have the highest quality flux estimate of the three VTPs. The estimated average flux at VTP4 was −1.9 feet per day (negative sign indicates an upward groundwater flux) with an upper bound of −2.2 feet per day and a lower bound of −1.6 feet per day from the Monte Carlo analysis (table 6.2).

VTP2 and VTP3 had lower temperature amplitudes and weak diurnal signals (figs. 6.1, 6.2). With temperature amplitudes below 1 degree Celsius; the flux estimates from these locations a poorly constrained. In particular, the relatively steady flux and thermal diffusivity estimates for VTP2 (compared to VTP4) likely indicate a poor fit to the data during the dynamic harmonic regression analysis in VFLUX (M. Briggs, U.S. Geological Survey, oral commun., 2017). The average groundwater flux estimated for VTP2 was zero foot per day (neutral) with bounds of 0.2 and −0.2 foot per day from the Monte Carlo analysis, which is inconsistent with the upward gradient observed in nearby mini-piezometer PZ8 (fig. 15). The average groundwater flux for VTP3 was −0.4 foot per day (upward) with bounds of −0.1 and −0.6 foot per day from the Monte Carlo analysis. The upward flux at VTP3 agrees with the upward gradients observed in mini-piezometers PZ0 and PZ1.

An effective vertical hydraulic conductivity of the lakebed sediments can be calculated by dividing estimated groundwater flux by vertical hydraulic gradients measured at the mini-piezometers. The effective vertical hydraulic conductivities for VTP2, VTP3, and VTP4 using the average groundwater flux and the minimum and maximum bounds from the Monte Carlo analysis are presented in table 6.2. VTP4 had an estimated vertical hydraulic conductivity that ranged from 27 to 37 feet per day. VTP2 and VTP3 had much smaller and similar estimated vertical hydraulic conductivities that ranged from 1 to 7 feet per day. Lakebed sediment appeared similar at both sites, but no formal sediment analysis was done and there may be subtle differences in the sediment composition between locations VTP4 and VTP2 or VTP3. The following tables are presented in Microsoft Excel files available at https://dx.doi.org/10.3133/sir20205024:

Table 6.1. Sensitivity analysis of thermal parameters for 1DTempPro using site VTP3 data.

Table 6.2. Summary of estimated groundwater fluxes and effective vertical hydraulic conductivities.

Conclusion

Temperature amplitudes and diurnal signals were well defined at one location, VTP4, where a strong upward groundwater gradient was observed. Flux estimates from the other two locations, VTP2 and VTP3, are more uncertain because of the low signal amplitudes and weak diurnal signals during the fall data collection. VTP1 was not analyzed because no discernable diurnal temperature signal was measured, thereby preventing analysis by VFLUX. Natural diurnal temperature signals are often reduced in lake waters compared to flowing streams, because of less mixing in the water column. However, temperature data collected during summer, when the thermal contrast between lake and groundwater and diurnal temperature amplitude are maximized, would likely provide more robust flux estimates. The loose consistency and poorly defined sediment/water interface in the sapropel lakebed sediment presented a challenge for the collection of meaningful temperature profiles. Nonetheless, the collected data that were amenable for analysis and the associated vertical flux estimates are consistent with measured water levels in wells and mini-piezometers, in that the computed vertical fluxes indicate groundwater discharge to Haskell Lake along the shoreline downgradient of the petroleum plume.

References Cited

Anderson, M.P., 2005, Heat as a ground water tracer: Ground Water, v. 43, no. 6, p. 951–968, https://doi.org/10.1111/j.1745-6584.2005.00052.x.

Bredehoeft, J.D., and Papadopoulos, I.J., 1965, Rates of vertical groundwater movement estimated from the Earth's thermal profile: Water Resources Research, v. 1, no. 2, p. 325–328, https://doi.org/10.1029/WR001i002p00325.

Briggs, M.A., Lautz, L.K., Buckley, S.F., and Lane, J.W., 2014, Practical limitations on the use of diurnal temperature signals to quantify groundwater upwelling: Journal of Hydrology (Amsterdam), v. 519, p. 1739–1751, https://doi.org/10.1016/j.jhydrol.2014.09.030.

Gordon, R.P., Lautz, L.K., Briggs, M.A., and McKenzie, J.M., 2012, Automated calculation of vertical pore-water flux from field temperature time series using the VFLUX method and computer program: Journal of Hydrology (Amsterdam), v. 420–421, p. 142–158, https://doi.org/10.1016/j.jhydrol.2011.11.053.

Hatch, C.E., Fisher, A.T., Revenaugh, J.S., Constantz, J., and Ruehl, C., 2006, Quantifying surface water–groundwater interactions using time series analysis of streambed thermal records—Method development: Water Resources Research, v. 42, no. 10, 14 p., https://doi.org/10.1029/2005WR004787.

Healy, R.W., and Ronan, A.D., 1996, Documentation of computer program VS2Dh for simulation of energy transport in variably saturated porous media—Modification of the U.S. Geological Survey's computer program VS2DT: U.S. Geological Survey Water-Resources Investigations Report 96–4230, 36 p., https://doi.org/10.3133/wri964230.

Irvine, D.J., Briggs, M.A., Lautz, L.K., Gordon, R.P., McKenzie, J.M., and Cartwright, I., 2017, Using diurnal temperature signals to infer vertical groundwater-surface water exchange: Groundwater, v. 55, no. 1, p. 10–26, https://doi.org/10.1111/gwat.12459.

Irvine, D.J., Lautz, L.K., Briggs, M.A., Gordon, R.P., and McKenzie, J.M., 2015, Experimental evaluation of the applicability of phase, amplitude, and combined methods to determine water flux and thermal diffusivity from temperature time series using VFLUX 2: Journal of Hydrology (Amsterdam), v. 531, no. 3, p. 728–737, https://doi.org/10.1016/j.jhydrol.2015.10.054.

Keery, J., Binley, A., Crook, N., and Smith, J.W.N., 2007, Temporal and spatial variability of groundwater–surface water fluxes—Development and application of an analytical method using temperature time series: Journal of Hydrology (Amsterdam), v. 336, no. 1-2, p. 1–16, https://doi.org/10.1016/j.jhydrol.2006.12.003.

Koch, F.W., Voytek, E.B., Day-Lewis, F.D., Healy, R., Briggs, M.A., Lane, J.W., Jr., and Werkema, D., 2016, 1DTempPro V2—New features for inferring groundwater/surface-water exchange: Groundwater, v. 54, no. 3, p. 434–439, https://doi.org/10.1111/gwat.12369.

Koch, F.W., Voytek, E.B., Day-Lewis, F.D., Healy, R., Briggs, M.A., Werkema, D., and Lane, J.W., Jr., 2015, 1DTempPro—A program for analysis of vertical one-dimensional (1D) temperature profiles v2.0: U.S. Geological Survey Software Release, http://dx.doi.org/10.5066/F76T0JQS.

Lapham, W.W., 1989, Use of temperature profiles beneath streams to determine rates of vertical ground-water flow and vertical hydraulic conductivity: U.S. Geological Survey Water-Supply Paper 2337, 35 p., https://pubs.usgs.gov/wsp/2337/report.pdf.

Lautz, L.K., 2012, Observing temporal patterns of vertical flux through streambed sediments using time-series analysis of temperature records: Journal of Hydrology, v. 464–465, p. 199–215, https://doi.org/10.1016/j.jhydrol.2012.07.006.

Leaf, A.T., and Haserodt, M.J., 2020, MODFLOW–NWT and MODPATH models, data from aquifer tests and temperature profilers, and groundwater flux estimates used to assess groundwater/surface-water interactions in Haskell Lake, Wisconsin: U.S. Geological Survey data release, https://doi.org/10.5066/P9ZQGGHY.

Luce, C.H., Tonina, D., Gariglio, F., and Applebee, R., 2013, Solutions for the diurnally forced advection-diffusion equation to estimate bulk fluid velocity and diffusivity in streambeds from temperature time series: Water Resources Research, v. 49, no. 1, p. 488–506, https://doi.org/10.1029/2012WR012380.

McCallum, A.M., Andersen, M.S., Rau, G.C., and Acworth, R.I., 2012, A 1-D analytical method for estimating surface water–groundwater interactions and effective thermal diffusivity using temperature time series: Water Resources Research, v. 48, no. 11, 8 p., https://doi.org/10.1029/2012WR012007.

National Oceanic and Atmospheric Administration (NOAA), 2018, Daily summaries station details for Minocqua, WI, station GHCND, USC00475516: accessed March 19, 2018, at https://www.ncdc.noaa.gov/cdo-web/datasets/GHCND/stations/GHCND:USC00475516/detail.

Stonestrom, D.A., and Constantz, J., eds., 2003, Heat as a tool for studying the movement of ground water near streams: U.S. Geological Survey Circular 1260, 96 p., https://doi.org/10.3133/cir1260.

Appendix 7. Summary of Geophysical Data Collection and Results

Wisconsin Geological and Natural History Survey (WGNHS) staff led a geophysical investigation at the Haskell Lake contamination site on May 15–16, 2017, and June 27–28, 2017. The primary goal of the investigation was to improve understanding of the bedrock surface elevations at the contamination site and throughout the greater MODFLOW model domain. A secondary goal was to gain additional qualitative understanding of the hydraulic conductivity structure and plume extent at the contamination site. A complete description of the geophysical methods and results is provided in an unpublished memorandum, available from the WGNHS on request (Carolyn Streiff and Dave Hart, WGNHS, written commun., 2017). This appendix includes an overview of the collection of depth to bedrock geophysical data that were used to refine the bedrock surface for the groundwater flow model, as discussed in appendix 10.

Data were collected using the horizontal-to-vertical spectral ratio (HVSR) passive seismic (Chandler and Lively, 2016), refraction seismic, electrical resistivity imaging (ERI), and EM31 ground conductivity methods (for example, Burger and others, 2006). Bedrock surface elevations were successfully estimated using the HVSR passive seismic and refraction seismic methods; however, the bedrock surface was too deep for the ERI method. Although the contamination plume and lithologic contrasts between coarse and fine deposits may be visible in the ERI and EM31 data, the confounding interplay between these factors and possible additional influences from road salt and buried utilities preclude any definite conclusions. Only the seismic methods are presented here.

Horizontal-to-Vertical Spectral Ratio Passive Seismic Methods

The HVSR method uses naturally occurring vibrations in the subsurface from ambient sources such as waves, wind, or human activity to estimate the depths of lithologic contacts. A common application of HVSR, used in this study, is estimation of depth to bedrock (thickness of overlying soft sediment) from the peak frequencies of natural vibrations. For a uniform material, the thickness (y) is proportional to the S-wave (shear wave) velocity (Vs) divided by the HVSR peak frequency (x). In reality, Vs in soft sediments increases logarithmically with depth because of compaction and other factors. Previous work has indicated that soft sediment thickness can be estimated by the power-law relation $y = ax^b$, where a and b are empirical coefficients that are determined by collecting HVSR data at locations where the depth to bedrock is known (Chandler and Lively, 2016).

In investigations of Quaternary sediments in the upper Midwest, it is common practice to use a single set of a and b coefficients across a study area, provided the lithology is understood to be sufficiently similar, and appropriate attention is applied to potentially problematic conditions or anomalous results. Conditions that can cause poor HVSR results include shallow depth to bedrock, weathered bedrock, the presence of gravel layers, and local heterogeneity that deviates from the average seismic velocity conditions reflected in the a and b coefficients (Chandler and Lively, 2016; Carolyn Streiff and Dave Hart, WGNHS, written commun., 2017).

Refraction Seismic Methods

Refraction seismic requires the creation of seismic waves via a sound source such as a hammer hitting a metal plate, and then recording the refracted seismic wave arrivals along a transect of geophones. Two transects were used, with several noise perturbation “shots” on each line. Not all shots were successful, possibly because of complicating factors such as the ground being too soft or too hard to transmit the shot, or noise introduced into the data from other sources such as road traffic.

Results and Discussion

The depths to bedrock estimated from the HVSR and the refraction seismic methods are presented in table 7.1, with a map of the resulting estimated bedrock surface in shown in figure 18. The map also incorporates the interpretation of Batten and Lidwin (1996, plate 1) in areas of sparse HVSR data. Depths to bedrock ranged from 46 to 178 feet. Bedrock surface elevations are highest to the east and west of Haskell Lake and lowest within the Haskell Lake/Tower Creek corridor, indicating that Tower Creek occupies a historical valley in the bedrock surface that predates the most recent glaciation.

Two HVSR data points were not used in the creation of the bedrock surface. The apparent depth to bedrock of 103.3 feet at HVSR–28 (table 1; near the boat landing for Haskell Lake Lodge in fig. 18 but not shown) is likely indicative of local heterogeneity. Previous drilling (Weston Solutions, Inc., 2014; boring VAS–02; Cascade Technical Services, 2016; boring MIHPT–14) as well as the ERI survey (Carolyn Streiff and Dave Hart, WGNHS, written commun., 2017) indicate the possible presence of finer-grained or organic sediments in this location. Both of these materials have lower seismic velocities relative to the sand and gravel that predominate across the study area, which would result in overestimation of bedrock depth.

Point HVSR–3 had a lower quality comment in the measurement notes of WGNHS staff and did not agree with other nearby data. The HVSR results were used to help refine a bedrock surface for the groundwater flow model (appendix 10). The following table is presented in Microsoft Excel files available at https://dx.doi.org/10.3133/sir20205024:

Table 7.1. Results from horizontal-to-vertical spectral ratio (HVSR) and refraction seismic surveys.

References Cited

Batten, W.G., and Lidwin, R.A., 1996, Water resources of the Lac du Flambeau Indian Reservation, Wisconsin, 1981–86: U.S. Geological Survey Water-Resources Investigation Report 94–4025, 47 p.

Burger, H. R., Sheehan, A. F., Jones, C. H., 2006, Introduction to applied geophysics: Exploring the shallow subsurface: New York, W.W. Norton, 554 p.

Cascade Technical Services, 2016, MIHPT Site Investigation 14267 State Highway 70 West: Wisconsin, Lac Du Flambeau, 79 p.

Chandler, V.W., and Lively, R.S., 2016, Utility of the horizontal-to-vertical spectral ratio passive seismic method for estimating thickness of Quaternary sediments in Minnesota and adjacent parts of Wisconsin: Interpretation, v. 4, no. 3, SH71–SH90, https://doi.org/10.1190/INT-2015-0212.1.

Vilas County Land Information & Mapping Department, 2016, Bare earth lidar DEM tiles: provided to the USGS on December 6, 2016.

Weston Solutions, Inc., 2014, Summary of findings June 2014 vertical aquifer sampling Haskell Lake area groundwater investigation, 89 p.

Appendix 8. Stable Isotope Mass Balance Method

The ratio between the stable isotopes of oxygen ($^{18}O/^{16}O$) has been used with the mass balance method to estimate groundwater inflow and outflow in lakes (Krabbenhoft and others, 1990; Özaydin and others, 2001; Krabbenhoft and Babiarz, 1992). This method combines known or computable hydrologic fluxes into and out of the lake with assumed or measured stable isotope concentrations to estimate the unknown hydrologic flux of groundwater inflow (GW_{in}) at steady state conditions. The flux is estimated by combining the water mass balance (eq. 8.1) with the isotope mass balance (eq. 8.2) to isolate the groundwater influx term (eq. 8.3).

$$\frac{dV}{dt} = GW_{in} + P + S_{in} - GW_{out} - E - SW_{out} = 0 \qquad (8.1)$$

$$\frac{d(V\delta_L)}{dt} = GW_{in}\delta_{GWin} + P\delta_P + SW_{in}\delta_{SWin} - GW_{out}\delta_L - E\delta_E - SW_{out}\delta_L = 0 \qquad (8.2)$$

$$GW_{in} = \frac{P(\delta_L - \delta_P) + SW_{in}(\delta_L - \delta_{SI}) + E(\delta_E - \delta_L)}{\delta_{GWin} - \delta_L} \qquad (8.3)$$

where

- $\frac{dV}{dt}$ is the change in lake (storage) volume, in cubic length per time units;
- GW_{in} is groundwater inflow rate, in cubic length per time units;
- P is precipitation rate, in cubic length per time units;
- SW_{in} is surface-water inflow rate, in cubic length per time units;
- GW_{out} is groundwater outflow rate, in cubic length per time units;
- E is evaporation rate, in cubic length per time units;
- SW_{out} is surface-water outflow rate, in cubic length per time units;
- δ_L isotopic concentration of lake water, in delta notation;
- δ_{GWin} is isotopic concentration of groundwater inflow, in delta notation;
- δ_P is isotopic concentration of precipitation, in delta notation;
- δ_{SWin} isotopic concentration of surface water, in delta notation;
- δ_E isotopic concentration of evaporated lake water, in delta notation.

Under a steady-state assumption, the water mass balance ($\frac{dV}{dt}$) and the isotope mass balance ($\frac{d(V\delta_L)}{dt}$) can be set equal to zero. Equation 8.1 can be rearranged to solve for the groundwater inflow rate in terms of the groundwater outflow rate and substituted into equation 8.2 to estimate the groundwater inflow rate, independent of the groundwater outflow rate, as indicated in equation 8.3 and demonstrated in Krabbenhoft and others (1990). The flux and concentration terms in equation 8.3 were calculated using a variety of methods and data sources.

Field Methods

Following the sample collection methods suggested by the U.S. Geological Survey (USGS) (2018a), stream and lake stable isotope samples were collected in 20-milliliter glass vials with Polyseal caps. After the sample was collected, the vial was wrapped in Parafilm to prevent leaking or evaporation through the cap seal and then stored at room temperature. Samples were analyzed at the USGS Reston Stable Isotope Laboratory. Results from the laboratory were reported as per mil (‰), where ‰ is per mil or delta notation relative to the Vienna Standard Mean Ocean Water and normalized to oxygen values of Standard Light Antarctic Precipitation according to methods in Coplen (1994).

Twelve stream samples were collected at the Tower Creek streamgage (USGS site 05392187) between October 2016 and February 2018. The measured isotope concentrations for the stream samples can be downloaded from https://nwis.waterdata.usgs.gov/wi/nwis/qwdata/, USGS site number 05392187 (U.S. Geological Survey, 2018b). Three lake samples (October 2016, May 2017, and November 2017) were collected from Haskell Lake during the spring and fall turnovers when the lake was assumed to be well mixed. Results from the lake samples are available at https://nwis.waterdata.usgs.gov/wi/nwis/qwdata/, USGS site number 455430089550001 (U.S. Geological Survey, 2018b).

Data Analysis and Results

Monthly values used in the mass balance computation are presented in table 8.1. Monthly data were estimated using climate data from November 1, 2016, to October 31, 2017.

Monthly precipitation (P) was calculated by summing daily precipitation data recorded at the Tower Creek precipitation site (USGS site 455452089551701) for periods with temperatures above freezing; winter periods were calculated by summing the precipitation recorded at the Minocqua weather station (National Oceanic and Atmospheric Administration [NOAA], 2018a) supplemented by the St. Germain weather station (NOAA, 2018b) where data were missing. Because the Haskell Lake residence time is thought to be on the order of a few months, isotopic concentrations in the lake should reflect precipitation inputs from recent months; precipitation data from the same time period that stream and lake isotope data were collected were deemed appropriate.

Collecting and analyzing precipitation samples for stable oxygen isotope concentrations was beyond the scope of this study. Krabbenhoft and others (1990) collected monthly precipitation concentrations from November 1985 to August 1987 at Sparkling Lake, approximately 12.5 miles northeast of

Haskell Lake (fig. 1). Variation in precipitation concentrations between sampling years was minimal and these monthly average precipitation isotope concentrations (δ_P) were used for the Haskell Lake stable isotope mass balance budget.

Average monthly evaporation rates (E) were calculated using open water evaporation estimates from the unmodified Hamon method (Harwell, 2012) with Minocqua weather station (NOAA, 2018a) air temperature data. Following Krabbenhoft and others (1990), the monthly evaporation rate for December, January, February, and March, when lake ice cover is likely, was assumed to be zero.

Monthly isotope concentrations for the lake evaporate (δ_E) were calculated using equations 8–14 in Özaydin and others (2001). Inputs included the relative humidity, lake surface-water temperature, isotopic composition of the precipitation (δ_P), and isotopic concentration of the lake water (δ_L). The monthly precipitation isotopic concentrations (δ_P) came from Krabbenhoft and others (1990), and the lake isotopic concentration was the average (−9.30 ‰) of the two lake samples (May 2017 and November 2017) collected during the study. The October 2016 lake sample was not used in the lake average because the sample likely reflected inputs from several months prior to the start of the study. Humidity data from the Lakeland Lee Memorial weather station at the Lakeland airport (fig. 1) were downloaded from www.weatherunderground.com (Weather Underground, 2018) and averaged to monthly values. Average monthly humidity was normalized to lake surface temperatures using the relative humidity equation in Różański (2000), with lake surface temperatures estimated from average air temperature data from the Minocqua weather station (NOAA, 2018a) and applying the difference between average monthly air and lake temperatures reported in Krabbenhoft and others (1990). The water temperature recorded at the Haskell Lake precipitation site (USGS site 455430089550001) was considered for the humidity calculations but was not used because it reflected the lake temperature several feet below the water surface, which is different from the surface temperature.

Monthly surface-water inflow (S_i) was calculated from the discharge record for the Tower Creek streamgage (USGS site 05392187); changes in base flow between the streamgage and Haskell Lake inlet were assumed to be sufficiently small that the streamflows observed at the streamgage represented the lake surface-water inflow rate.

The monthly isotopic concentrations for the Tower Creek inflow to Haskell Lake (δ_{Si}) are estimated from 12 samples collected at the Tower Creek streamgage between March 2017 and February 2018. Ideally, stream samples would have been collected between November 1, 2016, and October 31, 2017; however, the assumption was that the isotope ratios in samples collected during November 2017, December 2017, January 2018, and February 2018 were representative for those months during the prior year. No stream water sample was collected in April; the April isotropic concentration for Tower Creek inflow was estimated as the average of the March and May samples. Oxygen-18 isotopic concentrations for Tower Creek ranged from −8.99 to −10.94 ‰.

An average oxygen-18 concentration (δ_{GWin}) of −11.5 ‰ was assumed for groundwater inflow to Haskell Lake, based on an average of 57 samples collected over 2 years from water table wells near Sparkling Lake (Krabbenhoft and others, 1990). Oxygen-18 concentrations in groundwater are generally understood to be uniform through time and space (within an area of similar environmental conditions), because of mixing in the unsaturated zone that homogenizes temporally variable precipitation. Oxygen-18 conditions at Sparkling Lake are assumed to be representative of the area around Haskell Lake because of its close proximity, similar land cover, and same surficial geology.

The isotopic concentration of the lake (δ_L) was estimated by averaging values from two Haskell Lake samples; one sample during fall turnover (November 2, 2016) and one sample during spring turnover (May 4, 2017) when the lake was assumed to be well mixed.

Each monthly water flux term was summed across the study months to get an annual flux term. Weighted isotope concentrations associated with each water flux term were calculated using the fraction of the total annual flux term represented by each monthly value, as reported in table 8.1. Using the estimated and calculated values for each mass balance term in equation 8.3, the average annual groundwater inflow rate was determined to be 8.7 feet per year (ft/yr).

A first-order sensitivity analysis was used to estimate the 95 percent confidence interval for the predicted groundwater inflow rate, following the methods of Krabbenhoft and others (1990) and Krabbenhoft (1988). Standard deviations were estimated for each term in the isotope mass balance equation following Krabbenhoft (1988) unless better estimates of standard deviations were available. Additional uncertainty was assumed for the estimated evaporation flux rate and stable isotope concentration in the lake evaporate because of the added assumptions used to calculate these terms that Krabbenhoft (1988) had measured. The estimated standard deviation for each term is presented in table 8.1. From the first-order analysis, the estimated uncertainty of the groundwater inflow rate was 5.6 feet (GW_{in} = 8.7 ± 5.6 ft/yr).

For comparison, a mass balance estimate assuming no groundwater outflow from the lake, a surface-water outflow 1.7 times the surface-water inflow (based on the measurements from the synoptic streamflow survey in appendix 4), and the other hydrologic fluxes reported in table 8.1, would estimate a groundwater inflow rate of 11.5. ft/yr. The average

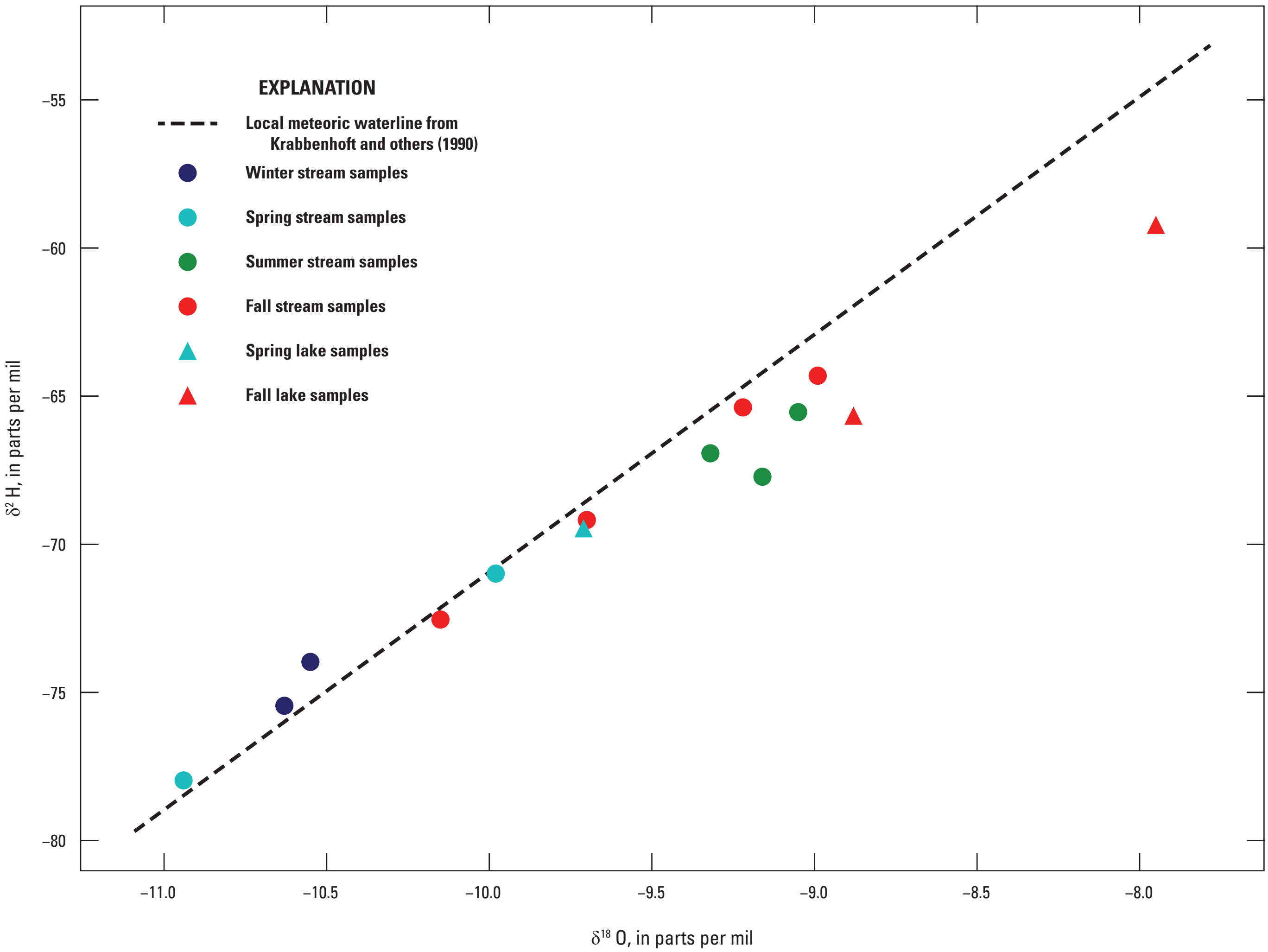

Figure 8.1. Stable isotope results from site samples plotted on the local meteoric waterline from Krabbenhoft and others (1990).

groundwater flux estimated from the VTP4 and VTP3 vertical temperature profilers (1.1 ft/yr) and assuming a 5-foot wide groundwater discharge zone around the lake perimeter with the lake geometry used in the MODFLOW model, would predict 9.2 ft/yr of groundwater discharge. Both of these estimates (9.2 ft/yr and 11.5 ft/yr) are within the 95 percent confidence interval (14.3 – 3.1 ft/yr) for the estimated groundwater inflow using the stable isotope mass balance method.

In addition to oxygen stable isotopes, lake and stream samples were analyzed for hydrogen stable isotopes to allow for comparison with the local meteoric waterline ($\delta^2H = 8.02\ \delta^{18}O + 9.26$) presented in Krabbenhoft and others (1990).

Water samples should generally plot on the meteoric waterline unless evaporation has occurred. Samples that plot to the right of the meteoric waterline are interpreted as having evaporative influences (Krabbenhoft and others, 1990). Comparing sample isotope ratios with the meteoric waterline can be a quality check on the measured isotope ratios. All site water samples (fig. 8.1) plotted on or near the meteoric waterline, with summer and early fall lake and stream water samples plotting slightly to the right of the meteoric waterline, indicating an evaporative signature. The following table is presented in a Microsoft Excel file available at https://dx.doi.org/10.3133/sir20205024:

Table 8.1. Summary of isotopic mass balance terms.

Conclusions

The stable isotope method indicates that Haskell Lake receives substantial groundwater discharge and provides an independent comparison for groundwater inflows to Haskell Lake estimated by the groundwater flow model.

References Cited

Coplen, T.B., 1994, Reporting of stable hydrogen, carbon, and oxygen isotopic abundances: Pure and Applied Chemistry, v. 66, p. 273–276.

Harwell, G.R., 2012, Estimation of evaporation from open water—A review of selected studies, summary of U.S. Army Corps of Engineers data collection and methods, and evaluation of two methods for estimation of evaporation from five reservoirs in Texas: U.S. Geological Survey Scientific Investigations Report 2012–5202, 96 p., https://doi.org/10.3133/sir20125202.

Krabbenhoft, D.P., 1988, Hydrologic and geochemical investigations of aquifer-lake interactions at Sparkling Lake Wisconsin: Madison, Wis., University of Wisconsin-Madison, Ph.D. thesis, 213 p.

Krabbenhoft, D.P., and Babiarz, C.L., 1992, The role of groundwater transport in aquatic mercury cycling: Water Resources Research, v. 28, no. 12, p. 3119–3128, https://doi.org/10.1029/92WR01766.

Krabbenhoft, D.P., Bowser, C.J., Anderson, M.P., and Valley, J.W., 1990, Estimating groundwater exchange with lakes—1. The stable isotope mass balance method: Water Resources Research, v. 26, no. 10, p. 2445–2453, https://doi.org/10.1029/WR026i010p02445.

National Oceanic and Atmospheric Administration (NOAA), 2018a, Daily summaries station details for Minocqua, WI, station GHCND, USC00475516: accessed March 19, 2018, at https://www.ncdc.noaa.gov/cdo-web/datasets/GHCND/stations/GHCND:USC00475516/detail.

National Oceanic and Atmospheric Administration (NOAA), 2018b, Daily summaries station details for St. Germain, WI, station GHCND, USC00477480: accessed March 19, 2018, at https://www.ncdc.noaa.gov/cdo-web/datasets/GHCND/stations/GHCND:USC00477480/detail.

Özaydin, V., Şendil, U., and Altinbilek, D., 2001, Stable isotope mass balance method to find the water budget of a lake: Turkish Journal of Engineering and Environmental Sciences, v. 15, p. 329–344.

Różański, K., Froehlich, K., and Mook, W.G., 2000, Environmental isotopes in the hydrological cycle—Principles and applications, vol. 3: International Atomic Energy Agency and United Nations Educational, Scientific and Cultural Organization, 73 p., accessed May 18, 2018, at http://businessdocbox.com/Green_Solutions/75062476-Environmental-isotopes-in-the-hydrological-cycle.html.

U.S. Geological Survey, 2018a, Instructions for collecting samples: U.S. Geological Survey, Reston Stable Isotope Laboratory web page, accessed May 16, 2016, at http://isotopes.usgs.gov/lab/instructions.html.

U.S. Geological Survey, 2018b, USGS water data for the Nation: U.S. Geological Survey National Water Information System database, accessed November 15, 2018, at https://doi.org/10.5066/F7P55KJN.

Weather Underground, 2018, Weather history for Arbor Vitae, WI, Lakeland Lee Memorial: accessed April 9, 2018, at https://www.wunderground.com/history/airport/KARV/.

Appendix 9. Lakebed Pore Water Sampling

Lakebed pore water samples were collected August 3, 2016, and August 29–30, 2017. The objective was to better characterize the petroleum plume discharging into Haskell Lake and to qualitatively guide the Haskell Lake contamination site conceptual model in support of the remediation goals of the Lac du Flambeau Band of Lake Superior Chippewa Indians (LDF Tribe). Samples were collected by U.S. Geological Survey personnel and were submitted to Northern Lake Service, Inc. (Crandon, Wisconsin) by the LDF Tribe for analysis. Water samples were analyzed for volatile organic compounds (VOCs), sulfide, metals, alkalinity, nitrate, nitrite, sulfate, and dissolved organic carbon. This appendix describes the sampling and analytical methods, and summarizes the results for contaminants of concern that exceed standards or screening levels of the LDF Tribe, the Wisconsin Department of Natural Resources, and the U.S. Environmental Protection Agency (EPA).

Sample Locations

The selection of sample locations was guided by the results of the distributed temperature sensing survey of lakebed temperatures (fig. 16; Leaf, 2020), the interpreted plume extent (fig. 2), and the detection of appreciable benzene concentration in groundwater at depth near the MW16 well nest, which would indicate at least some discharge of contaminated groundwater away from shore. Locations where lakebed temperatures were consistently cooler in the early morning were interpreted to have concentrated groundwater discharge. Final locations were selected based on where lakebed sediments could yield sufficient pore water for sampling. Of the 13 sample locations, 7 were successfully sampled and 6 could not be sampled because the presence of fine sediments limited production of sample water. All sample locations, including those that were attempted, are shown on figure 19A.

Methodology

During sampling, U.S. Geological Survey and EPA procedures for groundwater and pore water sampling (U.S. Geological Survey, variously dated; U.S. Environmental Protection Agency, Region 4, 2013) were followed to the extent feasible.

Equipment

Samples were collected with a peristaltic pump connected to stainless steel PushPoint (Henry) sampling devices (M.H.E. Products, 2003) for shallow locations and stainless steel drive-point piezometers (Solinst, 2013) for deeper locations. Several studies (for example, Zimmerman and others, 2005; Pitz, 2009) have determined these samplers to be effective for obtaining representative pore water samples free of surface-water contamination, including VOCs.

The PushPoint samplers were inserted into the lakebed sediment to a depth of at least 0.5 foot. The sampler was connected with 0.25-inch, high-density polyethylene (HDPE) tubing using a short piece of platinum-cured silicone tubing. The HDPE tubing was attached to the peristaltic pump with another piece of platinum-cured silicone tubing.

The stainless-steel drive-point samplers have a threaded screen with a barb to connect tubing inside of metal drive pipes. The sampler is advanced by adding metal pipe sections to the piezometer point; the tubing connected to the piezometer screen runs inside the pipe sections and keeps the water sample free from any contamination in the pipe. A silicone tube was used to connect one end of the HDPE tubing to the stainless steel barb on the drive point. The other end of the HDPE tubing was connected to platinum-cured silicone connected to the peristaltic pump. Field blanks were collected to ensure that equipment did not contaminate samples.

Sample Collection

For both samplers, a flow-through cell with a calibrated water-quality meter was used to collect field water-quality properties prior to and after sampling. The water-quality meter was connected to the outflow tubing from the peristaltic pump. Water-quality properties included specific conductance, temperature, pH, and dissolved oxygen.

Samplers were purged at a low-flow rate (within the peristaltic pump range). Samples were collected when at least three volumes of the sampler had been evacuated, field water-quality properties were stable (readings within the tolerances described by the U.S. Geological Survey (2006, p. 106), and the values of the field water-quality properties were indicative of pore water (were chemically distinct from the lake water field properties). Specific conductance was the main property used to distinguish lake water and pore water. The specific conductance of pore water ranged from 347 to 709 microsiemens per centimeter at 25 degrees Celsius, and the lake water had values less than 200 microsiemens per centimeter at 25 degrees Celsius. These differences in specific conductance indicated that the sampled pore water was chemically distinct from the lake water.

Water samples were collected directly from the tubing upstream from the water-quality meter flow-through cell. Appropriate glassware (with any necessary preservatives) for the desired sample analysis was furnished by the LDF Tribe through Northern Lakes Service, Inc. Sample vials were filled so that there was a meniscus with no headspace or bubbles once the vial lid was fastened. Following collection, samples were immediately preserved in an ice-filled cooler and transferred to the LDF Tribe. Sample analysis was performed by Northern Lake Service, Inc. (2016, 2017) for the VOCs (EPA method 8260), 1,2–dibromoethane (ethylene dibromide; EPA method 504.1), arsenic, cadmium, lead, nitrate/nitrite, iron, manganese, sulfate/sulfide, alkalinity, and dissolved organic carbon. A chain of custody form was used to document sample collection by the U.S. Geological Survey and subsequent transfer of the samples.

The PushPoint and stainless steel samplers were cleaned between the collection of each sample following the procedures outlined in Wilde (2004). The samplers were scrubbed with Alconox detergent and then rinsed (in the following order) with tap water, methanol, and volatiles-grade blank water (Wilde, 2004, p. 14). New tubing was used for each sample. Staff collecting the samples wore nitrile gloves, which were discarded after collecting each water sample.

Field blanks were collected from each sampler type during both sampling trips (August 3, 2016, and August 29–30, 2017) to verify the integrity of the sampling equipment and decontamination procedures for the sampling analytical goals. Field blanks were collected by running volatiles-grade blank water through cleaned sampling equipment and new tubing, per the sampling protocol, after all samples had been collected. A trip blank was collected during the first sampling round (August 3, 2016). In general, the blank samples showed results below the detection limit except for acetone in field blank 1 and Methyl ethyl ketone in field blank 3. The detects in the field blanks indicate that for these two constituents the cleaning procedure may have left or introduced some residual material. For these two constituents found in the field blanks, detections in the samples collected the same day as the field blanks are inconclusive where results are below the field blank detections.

Results

Analytical results were provided to the LDF Tribe by Northern Lake Service, Inc. and shared with the U.S. Geological Survey to aid in the site conceptual model. Results for benzene, which is carcinogenic and relatively volatile (and, therefore, indicative of slow degradation or a residual LNAPL source), are shown spatially on figure 19A, in a cross section in figure 19B, and summarized in table 9.1. Results for lead, 1,1,2-trichloroethane, and naphthalene are also summarized in figure 19*B* and table 9.1.

Benzene was detected in the three deepest samples collected along the dock, at depths of 11–36 feet, with the highest concentrations below 30 feet. Shallow samples collected near the shore had no detectable benzene. These results indicate that the fine lakebed sediments are limiting vertical discharge of the plume despite upward groundwater gradients between the lake and shallow aquifer, as noted in the mini-piezometers along the dock. How far the plume continues under the lake is unknown. If the lakebed sediment composition or thickness is variable, the plume could discharge at discrete locations where preferential groundwater discharge occurs. Homogeneity in the lakebed sediments would cause the plume to discharge diffusely across a broad area. Improved characterization of the lakebed sediment could aid in guiding future pore water sampling efforts for plume characterization. The following table is presented in a Microsoft Excel file available at https://dx.doi.org/10.3133/sir20205024:

Table 9.1. Pore water sampling locations and selected analytical results.

Summary

Samples were successfully collected at one-half of the locations attempted. Sample results indicate that the petroleum plume is present at a depth of 30 feet below the lakebed, approximately 70 feet away from shore, near the dock for Haskell Lake Lodge. Pore water sampling at the Haskell Lake contamination site presented many challenges. Areas more than a few feet from shore were generally unwadable because of thick and loose sapropel sediments. Dense but unstable floating bog vegetation precluded boat access to much of the rest of the nearshore areas downgradient of the plume (floating bog can be seen along the dock at PZ7, PZ8, and PZ9 in the inset on fig. 9). The sapropel sediments typically did not yield water, especially at shallow depths where loose, fine organic fragments clogged the sampling screens. Manual installation and retrieval of a temporary piezometer to depths greater than 15 feet was generally not feasible from a small boat because of limited opposing force available for retrieving the pipes. A specially designed sampling platform would be required for future sampling efforts from the lake. These difficulties limited the number and locations of sites that could be sampled.

References Cited

Leaf, A.T., 2020, A distributed temperature sensing investigation of groundwater discharge to Haskell Lake, Lac du Flambeau Reservation, Wisconsin, July 27–August 1, 2016: U.S. Geological Survey Scientific Investigations Report 2020–5005, 17 p., https://doi.org/10.3133/sir20205005.

M.H.E. Products, 2003, PushPoint Sampler (US Pat. #6,470,967)—Operators manual and applications guide, version 2.01: East Tawas, Mich., M.H.E. Products web page, accessed March 23, 2020, at http://mheproducts.com/downloads.html.

Northern Lake Service, Inc., 2016, Analytical Results: VOC's by P&T/GCMS-Water-(VarSat2000), project 264654 Haskell Lake Pore Water Sample, August 18, 5 p.

Northern Lake Service, Inc., 2017, Analytical Results: VOC's by P&T/GCMS-Water-(VarSat2000), project 286136 Sub Lake Sampling, September 14, 6 p.

Pitz, C.F., 2009, High-resolution porewater sampling near the groundwater/surface water interface: Washington State Department of Ecology, Publication No. 09–03–017, 43 p., accessed January 7, 2020, at https://fortress.wa.gov/ecy/publications/documents/0903017.pdf.

Solinst, 2013, Drive-point piezometer instructions: accessed May 17, 2018, at http://www.forestry-suppliers.com/Documents/2212_msds.pdf.

U.S. Environmental Protection Agency, Region 4, 2013, SESD operating procedure for pore water sampling, SESDPROC–513–R2: assessed January 7, 2020, at https://19january2017snapshot.epa.gov/sites/production/files/2015-06/documents/Porewater-Sampling.pdf.

U.S. Geological Survey, variously dated, National field manual for the collection of water-quality data: U.S. Geological Survey Techniques of Water-Resources Investigations, book 9, chaps. A1–A10, http://pubs.water.usgs.gov/twri9A.

U.S. Geological Survey, 2006, Collection of water samples (ver. 2.0): U.S. Geological Survey Techniques of Water-Resources Investigations, book 9, chap. A4, accessed, September 2006, at https://pubs.water.usgs.gov/twri9A4/.

Wilde, F.D., ed., 2004, Cleaning of equipment for water sampling (version 2.0): U.S. Geological Survey Techniques of Water-Resources Investigations, book 9, chap. A3, accessed May 18, 2018, at http://pubs.water.usgs.gov/twri9A3/.

Zimmerman, M.J., Massey, A.M., and Campo, K.W., 2005, Pushpoint sampling for defining spatial and temporal variations in contaminant concentrations in sediment pore water near the ground-water/surface-water interface: U.S. Geological Survey Scientific Investigations Report 2005–5036, 70 p., https://doi.org/10.3133/sir20055036.

Appendix 10. Additional Description of Groundwater Flow Model

This appendix provides some additional description of the groundwater flow model. Model files are available in the accompanying data release for this report (Leaf and Haserodt, 2020).

Creation of Model Layer Surfaces

Four primary surfaces are represented in the layering of the MODFLOW model:

- the land surface (including lake bathymetries) constitutes the top of the model;
- the top and bottom of the fine-grained sediments of the Wildcat Lake Member constitute the bottoms of layers 2 and 3; and
- the bedrock surface forms a no-flow boundary at the bottom of the model.

Top elevations in layer 1 were calculated from the 1-meter lidar digital elevation model (Vilas County Land Information & Mapping Department, 2016) as the average of the elevation values contained in each model cell. At the locations of lakes, the lidar elevations represent the lake surface at the time of the lidar survey. At the locations of lakes represented by the General-Head Boundary (GHB) Package, layer 1 top elevations were set to represent the lake bottoms by subtracting off lake depths derived from Wisconsin Department of Natural Resources (WDNR) lake maps (http://dnr.wi.gov/lakes/). Figure 10.1 illustrates the model layer configuration in cross section.

Layer 1 bottom elevations were set to be halfway between the model top and bottom of layer 2, except for model cells containing the Lake (LAK) Package (Haskell Lake, Unnamed Lakes 1 and 2, and Jerms and Tippecanoe Lakes). Layer 1 bottom elevations in the LAK Package cells were set to represent lake bottoms using depths derived from WDNR lake maps (so that the volume of the lake was contained in layer 1). No bathymetric map was available for Haskell Lake. Bathymetry for Haskell Lake was developed from lake depths provided by the Lac du Flambeau Band of Lake Superior Chippewa Indians. The lake depths were measured during a 2010 field survey of aquatic vegetation on a regular grid spaced approximately every 100 feet throughout the lake.

The bottoms of layers 2 and 3, which represent the top and bottom of the finer-grained deposits of the Wildcat Lake Member, were interpolated from the upper and lower contacts of fine-grained lithologic intervals reported in well construction reports (WDNR, 2017). The bottom of layer 4 was set to be halfway between the bottom of layer 3 and the bottom of layer 5 representing the bedrock surface.

The bedrock surface was developed from the surface presented by Batten and Lidwin (1996, plate 1), depth to bedrock data from well construction reports (WDNR, 2017), bedrock elevation data from the passive seismic surveys presented in appendix 7, and geologic interpretation. Contours from Batten and Lidwin (1996, plate 1) were digitized to a point layer and combined with the well construction report and geophysical data. An initial raster surface was created using the natural neighbor interpolation method in ArcGIS (Sibson, 1981). Additional "dummy" points were then added to sparse areas of the bedrock dataset to create a final surface consistent with the interpretation of a buried valley running beneath Tower Creek (fig. 18).

Boundary Conditions

Recharge

Input data sources for Soil-Water-Balance (SWB) simulation are listed in table 10.1. A single weather station approach, versus gridded precipitation data, is appropriate for the small Haskell Lake model domain where large consistent spatial variation in precipitation and temperature are not expected. Daily temperature data came from the Minocqua, Wis., weather station (National Oceanic and Atmospheric Administration [NOAA], 2018a) with missing data filled with data from the St. Germain, Wis., weather station (NOAA, 2018b), east of Minocqua. Precipitation data came from the Tower Creek precipitation site (U.S. Geological Survey site 455452089551701) for nonwinter months and from the Minocqua weather station (NOAA, 2018a) and St. Germain weather station (NOAA, 2018b; about 10 miles east of Woodruff, Wis.; fig. 1) for winter months.

Extraction of Perimeter Fluxes from the Analytic Element Model of Juckem and Others (2014)

Groundwater flow into and out of the MODFLOW model domain was represented with a specified flux boundary along the model perimeter. Perimeter fluxes were extracted from a modified version of the analytic element (GFLOW) model documented by Juckem and others (2014) and included in the MODFLOW Well Package (fig. 10.2), following established procedures (for example, appendix 1 in Leaf and others, 2015; Hunt and others, 1998). Perimeter fluxes were distributed between layers based on their transmissivities. A detailed description of the analytic element method and the computer program GFLOW is given by Haitjema (1995).

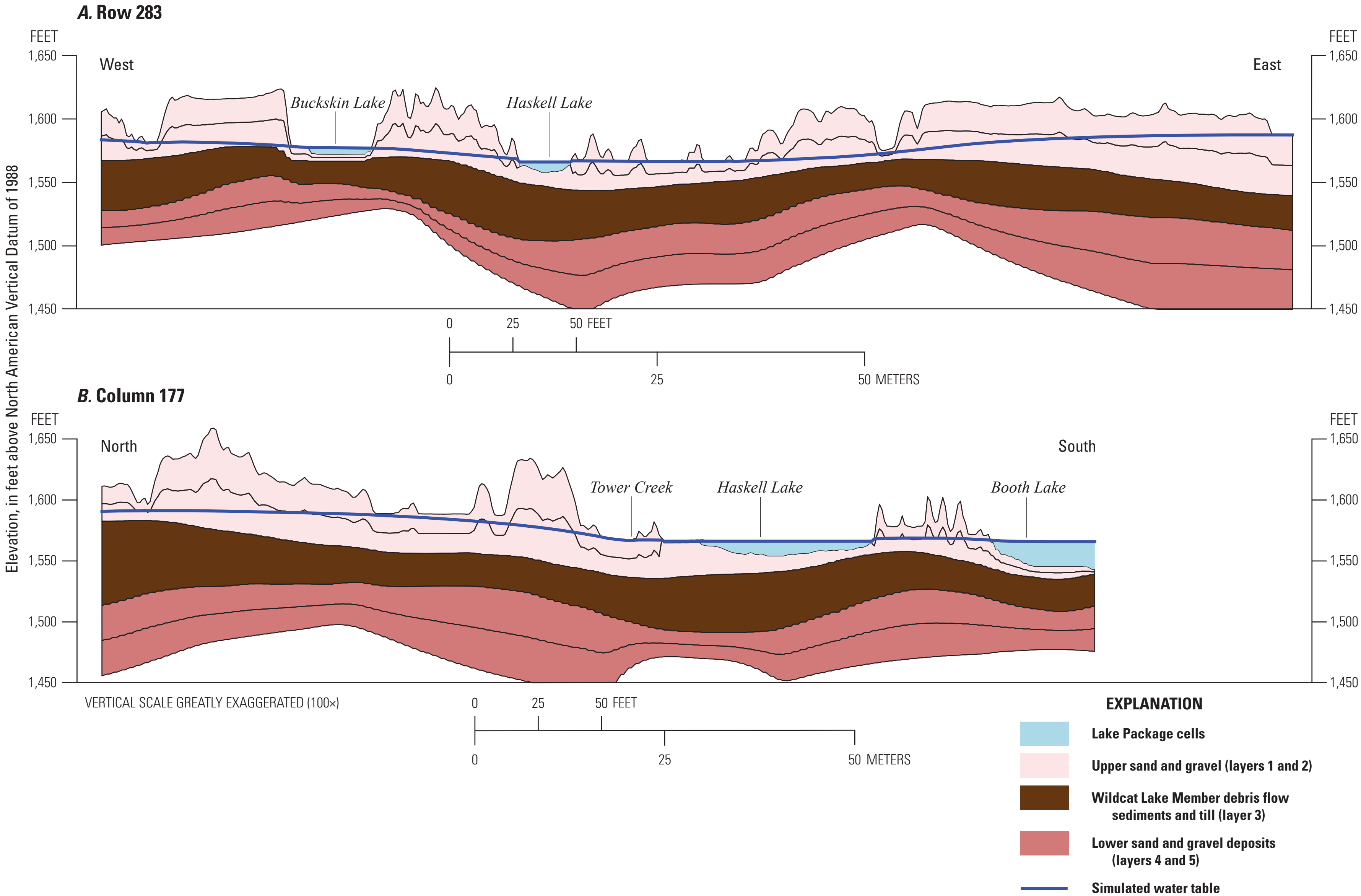

Figure 10.1. Cross sections through Haskell Lake showing model layering. *A*, along a (west to east) row of model cells intersecting Haskell Lake; *B* along, along a (north to south) column of model cells intersecting Haskell Lake. Haskell Lake is shown in light blue, indicating the extent of the Lake Package cells contained in layer 1. At Booth and Buckskin Lakes, (represented with the General-Head Boundary Package), the top of layer 1 represents the lake bottom. The blue line represents the simulated water table.

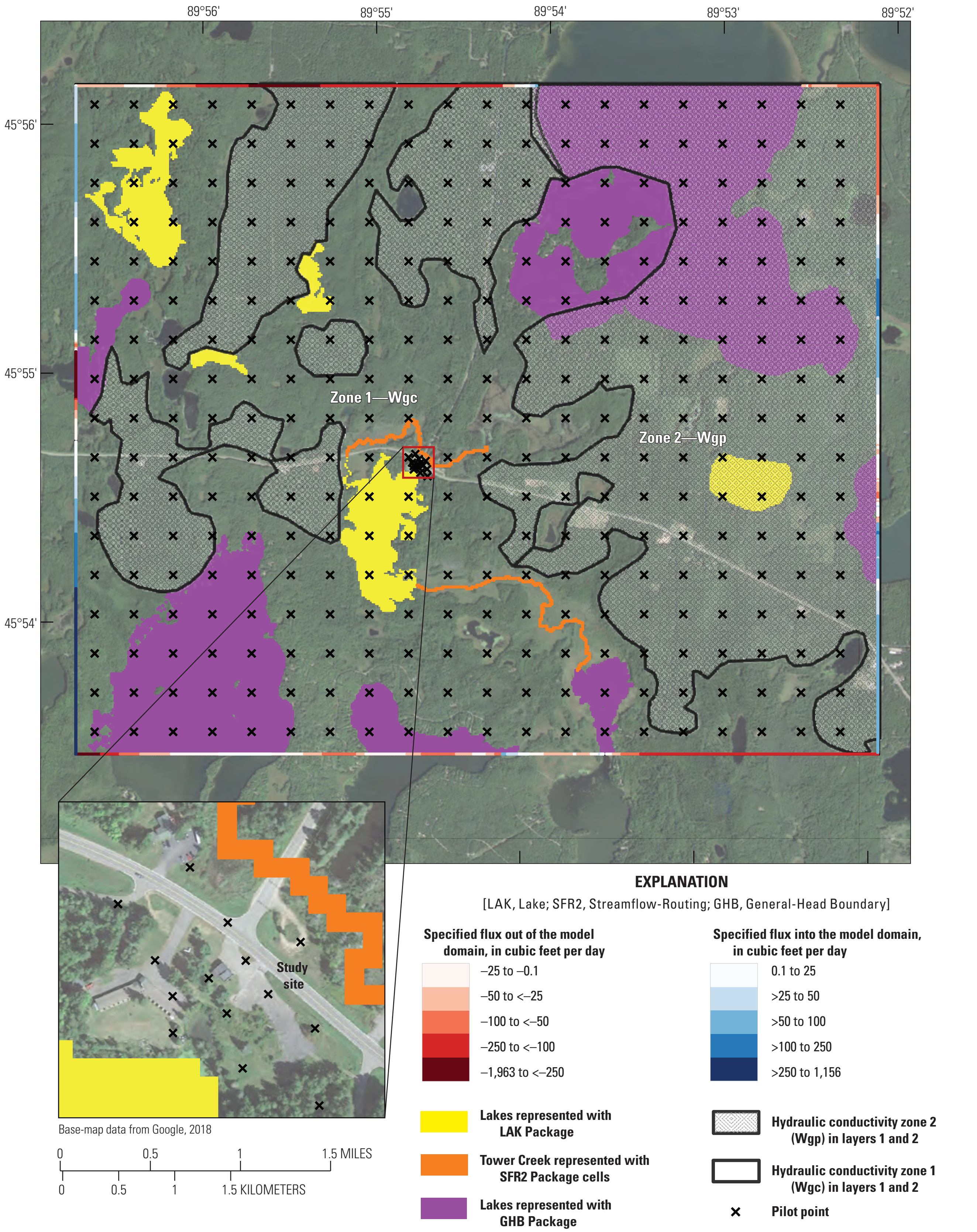

Figure 10.2. Boundary conditions, pilot points, and hydraulic conductivity zones representing the braided (Wgp) and collapsed (Wgc) stream deposits. Perimeter boundary cells are colored by flux specified to the MODFLOW Well Package (reds denote outflows, blues denote inflows; white would indicate groundwater flow parallel to the boundary [no flow across the boundary]).

Modifications to the GFLOW Model of Juckem and Others (2014)

Modifications were made to the GFLOW model of Juckem and others (2014) to incorporate new data and increase the level of detail in the linesink features defining the groundwatershed for Haskell Lake and Tower Creek. The modifications are as follows:

- increasing the level of detail in the linesinks representing Tower Creek and Haskell Lake;
- updating the linesink elevations for surrounding lakes using the surveyed lake elevations presented in table 2.1;
- converting Buckskin Lake from a far-field (zero resistance) to near-field linesink with a resistance of 1 day (same as other drainage lakes in the model);
- adding additional linesink elements to expand the model southward beyond Haskell Lake;
- adjusting the areal recharge rate from 9.2 to 13.7 inches per year, so that base flow simulated by the GFLOW model at the Bear River streamgage (site 05357335; fig. 1) matched average base flow for July 26, 2016, through November 30, 2017 (spanning the complete set of collected field data and climate inputs to the SWB deep infiltration model), as determined by hydrograph separation of daily streamflow values (Wahl and Wahl, 1988; Institute of Hydrology, 1980).

Files for the modified GFLOW model are available in the model archive for this report (Leaf and Haserodt, 2020).

Representation of Surface-Water Bodies

Figure 10.2 shows the lakes represented in the model by the GHB and LAK Packages, as well as the Streamflow-Routing (SFR2) Package cells representing Tower Creek.

Aquifer Properties

Figure 10.2 shows the network of pilot points that was used to estimate aquifer hydraulic conductivity on the basis of the observation data. Hydraulic conductivity values were interpolated to individual cells between pilot points via kriging. Interpolation was done within zones representing the braided (Wgp; zone 2) and collapsed (Wgc; zone 1) stream deposits. A higher density of pilot points was used to represent the Haskell Lake contamination site, commensurate with a higher density of data and a conceptual model of lithologic heterogeneity consisting of coarse and fine subsurface deposits of unknown extent.

Parameter Estimation

Observation data were grouped by type of observation and the source of the data. Within each group, observations were weighted based on the inverse of their estimated uncertainty. For example, a hydraulic head measurement with an uncertainty of 10 feet would have an initial weight of 0.1. Weights were then multiplied by observation group to emphasize or deemphasize the representation of each group in the overall calibration objective function. For example, the weights on hydraulic head measurements at the Haskell Lake contamination site were reduced to limit their influence, because the 50-foot grid spacing of the model does not carry enough resolution to represent fine-scale differences in the water table between these wells. The observation groups and their weights are summarized in table 10.2.

Fit to Observed Data

Overall, a good correspondence was achieved between the observation data and their simulated model equivalents (figs. 10.3*A*–*H*). Somewhat greater scatter in the observation residuals around the Haskell Lake contamination site reflects the 50-foot grid resolution not being able to capture fine-scale variation in hydraulic heads across the site. Differences between simulated and observed hydraulic head gradients in the MW16 and MW17 well nests also may reflect local vertical heterogeneity in the subsurface that is not well represented in the model. Scatter in the observation residuals of hydraulic heads for the well construction report group (fig. 10.3*H*) reflects a larger amount of uncertainty in these measurements (5–10 feet) relative to a total range in hydraulic head of less than 60 feet.

Despite these discrepancies, the model captures the salient aspects of the system. At the Haskell Lake contamination site, the model reproduces the overall trend in hydraulic heads across the site (fig. 10.3*E*), as well as the gradients at the MW16 well nest and between MW16 and Haskell Lake (point mw16slakedh_ss in fig. 10.3*A*). At the lake scale, the observed gaining conditions around the lake are reproduced in the simulated mini-piezometers gradients (fig. 10.3*B*). Base flow gain in Tower Creek upstream from Haskell Lake is well simulated (fig. 10.3*G*; points tc1_ss and tc2_ss); some scatter in the base flow residuals between Haskell and Squirrel Lakes may reflect greater uncertainty in those measurements. Most of the Tower Creek channel between Haskell and Squirrel Lakes is characterized by a soft bottom and low velocities that are difficult to measure accurately, even with the methods described in appendix 4. Regionally, generally well-mixed positive and negative well construction report residuals indicate a lack of spatial bias in the model solution (fig. 10.4).

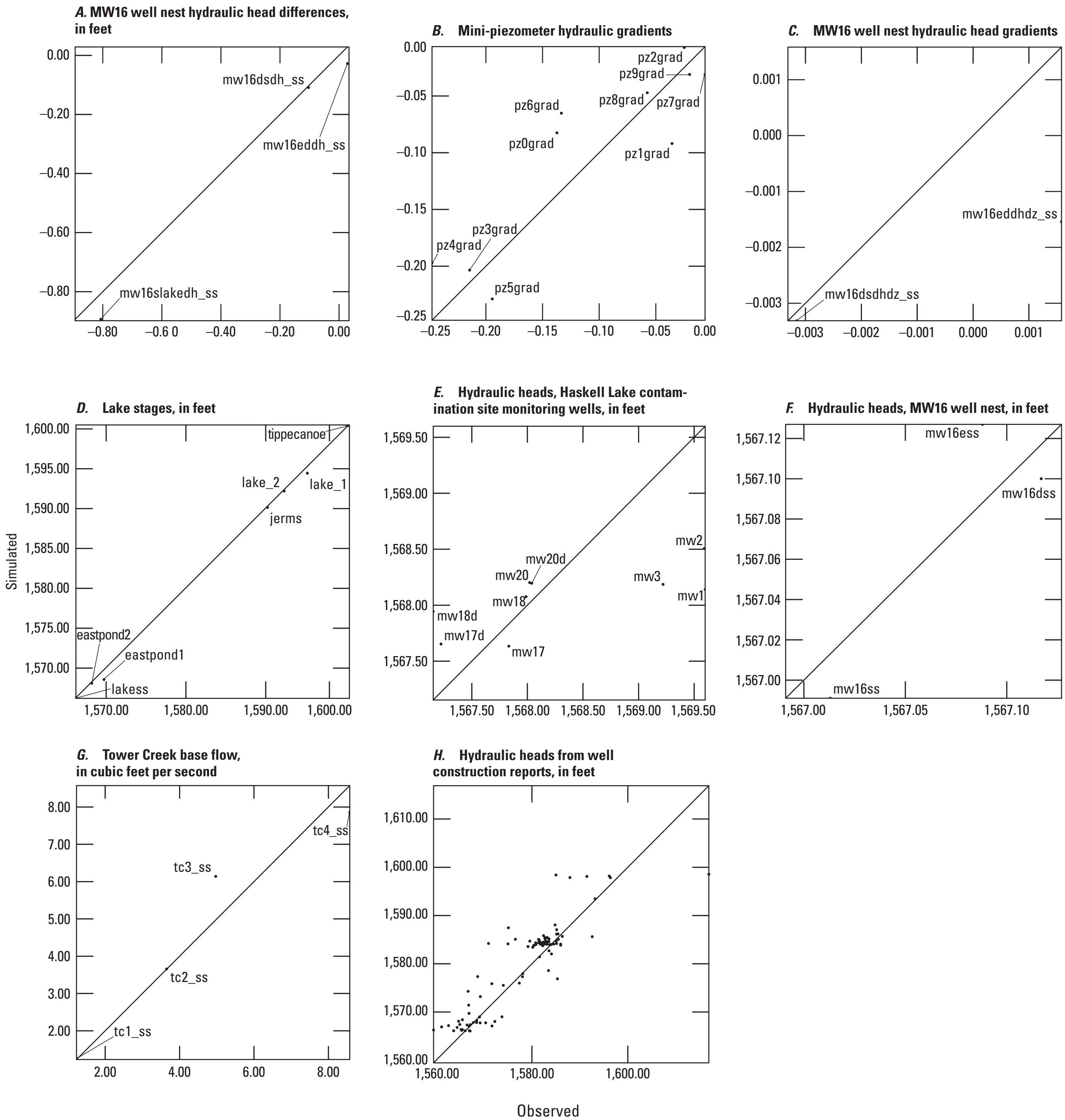

Figure 10.3. Comparison of simulated model outputs to field observations.

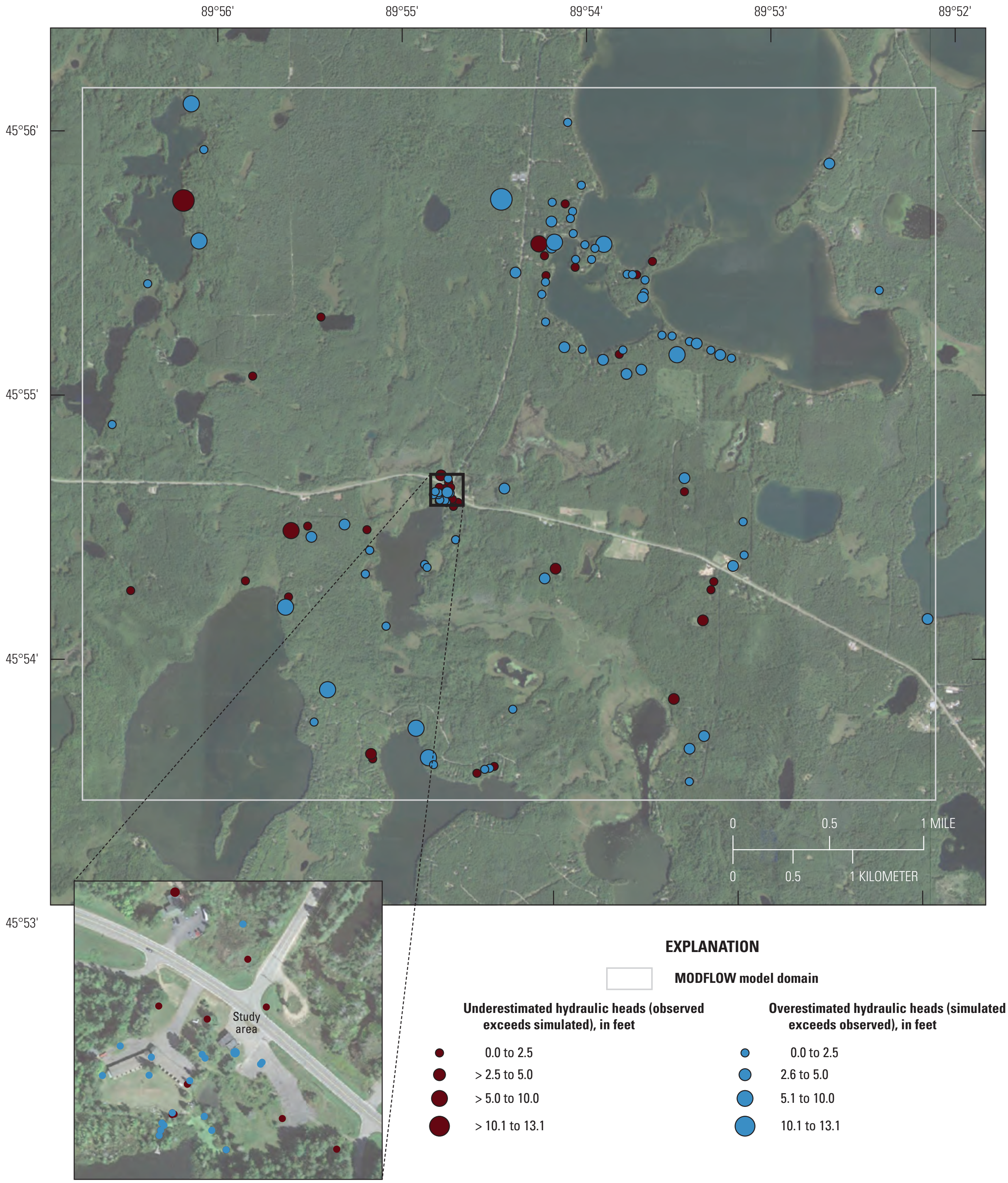

Base-map data from Google, 2018

Figure 10.4. Map of hydraulic head observation residuals.

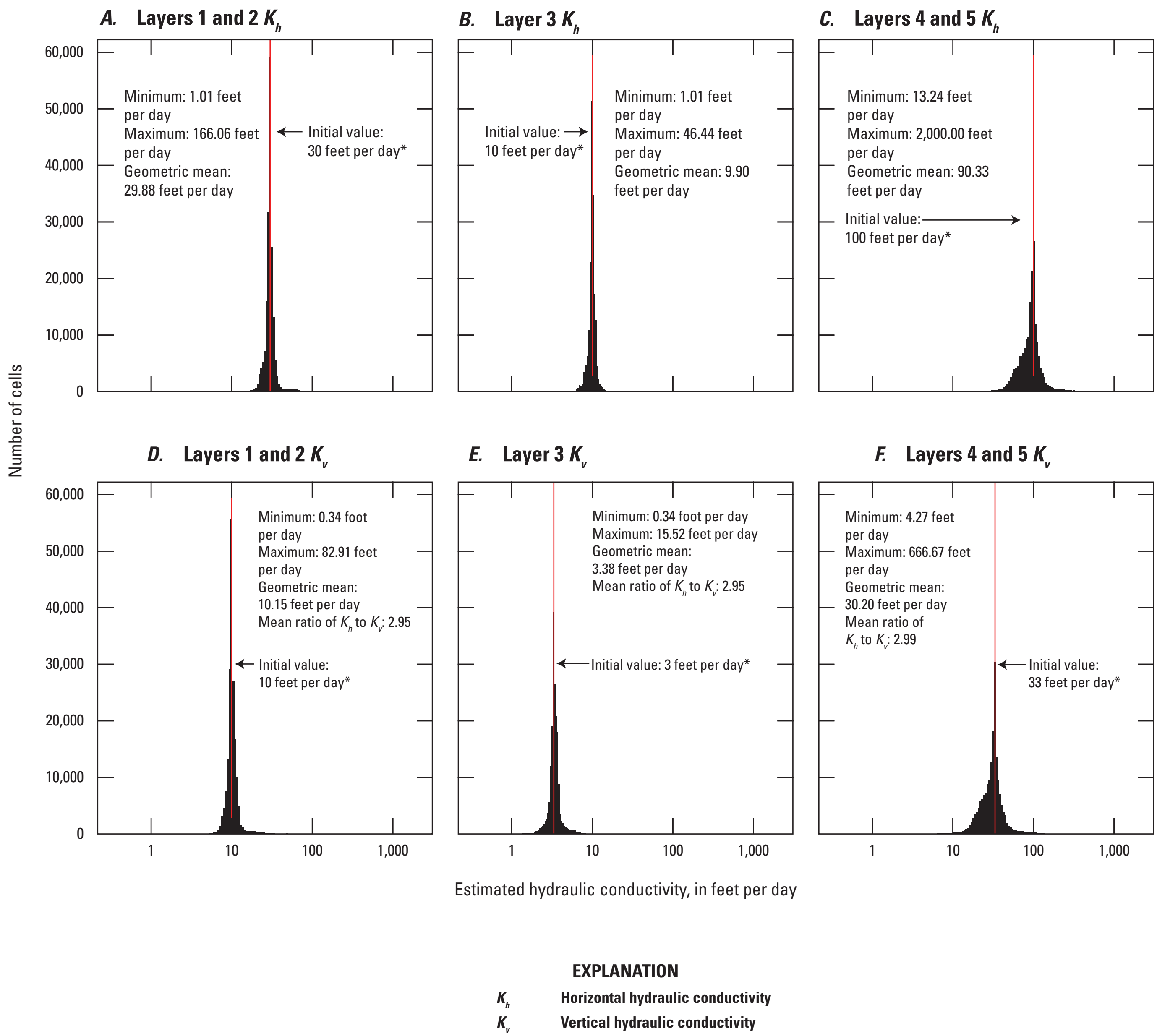

Figure 10.5. Histograms of estimated hydraulic conductivity values with statistics and initial values.

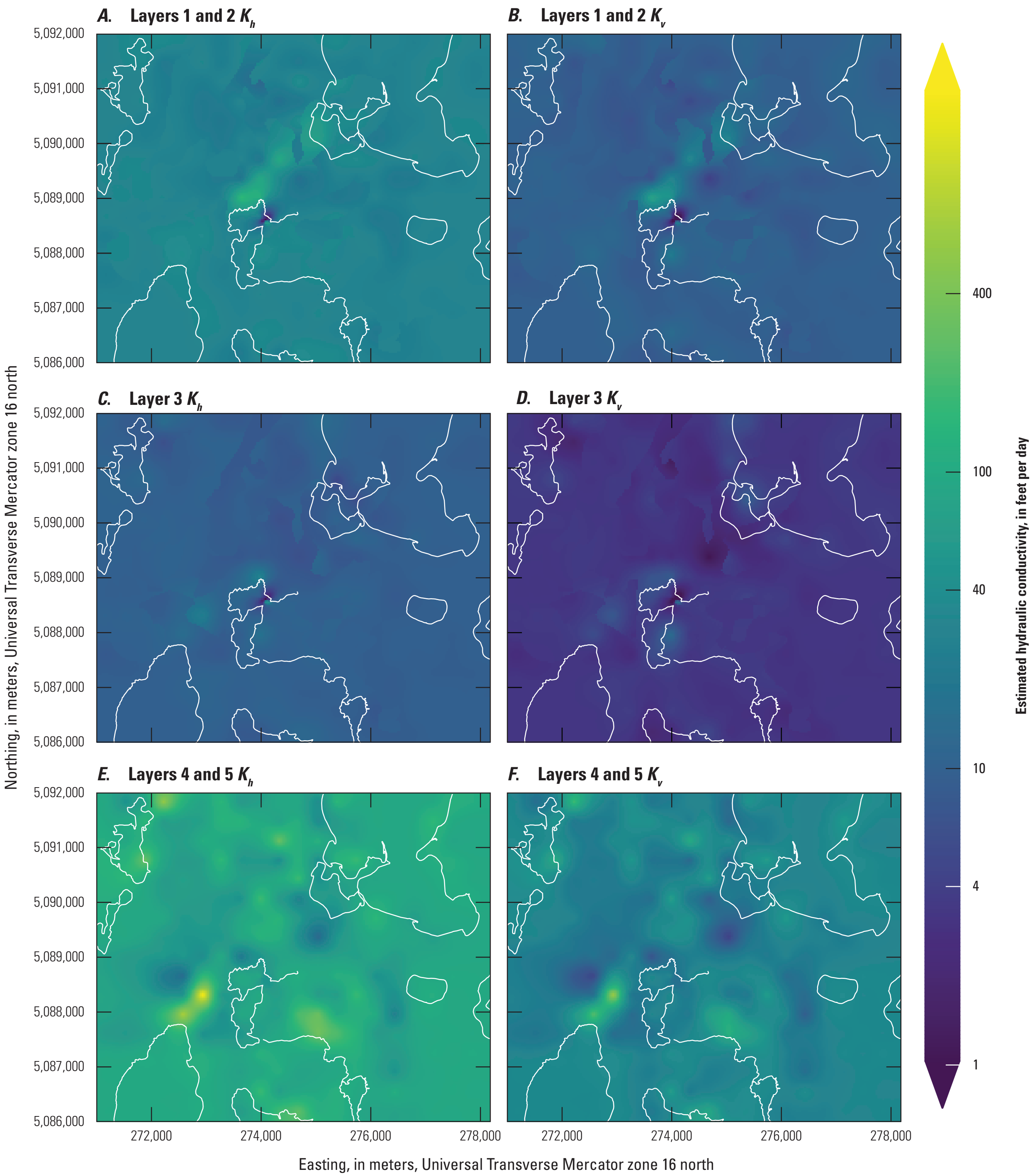

EXPLANATION

[K_h, horizontal hydraulic conductivity; K_v, vertical hydraulic conductivity]

Figure 10.6. Spatial distribution of estimated horizontal and vertical hydraulic conductivity for model layers.

Parameter Estimates

Table 10.3 summarizes initial parameter values, parameter uncertainties used in the linear analysis calculations, and the final parameter values estimated from history matching.

Figure 10.5 shows the populations of hydraulic conductivity values estimated at the pilot points. In general, the resulting geometric means in each layer remained similar to the starting values. The overall distributions are similar to those reported by Hunt and others (2013; table 6.3) for the nearby Trout Lake area. Estimated hydraulic conductivity values are shown spatially in figure 10.6. The following tables are presented in Microsoft Excel files available at https://dx.doi.org/10.3133/sir20205024:

Table 10.1. Input data sources for Soil-Water-Balance simulation.

Table 10.2. Observation weighting and objective function contribution by group.

Table 10.3. Initial and estimated parameter values. To facilitate comparison between the General-Head Boundary and Lake Packages, leakance and their equivalent conductance values are provided. *Initial values for pilot points at the Haskell Lake contamination site were set according to the nearest slug test measurement (appendix 5).

References Cited

Batten, W.G., and Lidwin, R.A., 1996, Water resources of the Lac du Flambeau Indian Reservation, Wisconsin, 1981–86: U.S. Geological Survey Water-Resources Investigation Report 94–4025, 47 p.

Haitjema, H.M., 1995, Analytic element modeling of groundwater: San Diego, Calif., Academic Press, 394 p.

Homer, C.G., Dewitz, J.A., Yang, L., Jin, S., Danielson, P., Xian, G., Coulston, J., Herold, N.D., Wickham, J.D., and Megown, K., 2015, Completion of the 2011 National Land Cover Database for the conterminous United States—Representing a decade of land cover change information: American Society for Photogrammetric Engineering and Remote Sensing, v. 81, no. 5, p. 345–354, accessed October 7, 2019, at https://pubs.er.usgs.gov/publication/70146301.

Hunt, R.J., Anderson, M.P., and Kelson, V.A., 1998, Improving a complex finite-difference ground water flow model through the use of an analytic element screening model: Ground Water, v. 36, no. 6, p. 1011–1017, https://doi.org/10.1111/j.1745-6584.1998.tb02108.x.

Hunt, R.J., Walker, J.F., Selbig, W.R., Westenbroek, S.M., and Regan, R.S., 2013, Simulation of climate-change effects on streamflow, lake water budgets, and stream temperature using GSFLOW and SNTEMP, Trout Lake Watershed, Wisconsin: U.S. Geological Survey Scientific Investigations Report 2013–5159, 118 p., https://doi.org/10.3133/sir20135159.

Institute of Hydrology, 1980, Low flow studies report no. 3—Research report: Wallingford, Oxon, United Kingdom, Institute of Hydrology Report no. 3, p. 12–19.

Juckem, P.F., Fienen, M.N., and Hunt, R.J., 2014, Simulation of groundwater flow and interaction of groundwater and surface water on the Lac du Flambeau Reservation, Wisconsin: U.S. Geological Scientific Investigations Report 2014–5020, 34 p., https://dx.doi.org/10.3133/sir20145020.

Leaf, A.T., Fienen, M.N., Hunt, R.J., and Buchwald, C.A., 2015, Groundwater/surface-water interactions in the Bad River watershed, Wisconsin: U.S. Geological Survey Scientific Investigations Report 2015–5162, 110 p., https://doi.org/10.3133/sir20155162.

Leaf, A.T., and Haserodt, M.J., 2020, MODFLOW–NWT and MODPATH models, data from aquifer tests and temperature profilers, and groundwater flux estimates used to assess groundwater/surface-water interactions in Haskell Lake, Wisconsin: U.S. Geological Survey data release, https://doi.org/10.5066/P9ZQGGHY.

National Oceanic and Atmospheric Administration (NOAA), 2018a, Daily summaries station details for Minocqua, WI, station GHCND, USC00475516: accessed March 19, 2018, at https://www.ncdc.noaa.gov/cdo-web/datasets/GHCND/stations/GHCND:USC00475516/detail.

National Oceanic and Atmospheric Administration (NOAA), 2018b, Daily summaries station details for St. Germain, WI, station GHCND, USC00477480: accessed March 19, 2018, at https://www.ncdc.noaa.gov/cdo-web/datasets/GHCND/stations/GHCND:USC00477480/detail.

Sibson, R., 1981, A brief description of natural neighbor interpolation, *in* Barnett, V., ed., Interpolating multivariate data: John Wiley and Sons, New York, p. 21–36.

Soil Survey Staff, 2011, Gridded Soil Survey Geographic (gSSURGO) Database for Wisconsin: U.S. Department of Agriculture, Natural Resources Conservation Service, accessed January 10, 2107, at https://www.arcgis.com/home/item.html?id=a23eb436f6ec4ad6982000dbaddea5ea.

U.S. Geological Survey, 2018, USGS water data for the Nation: U.S. Geological Survey National Water Information System database, accessed November 15, 2018, at https://doi.org/10.5066/F7P55KJN.

Vilas County Land Information & Mapping Department, 2016, Bare earth lidar DEM tiles: provided to the USGS on December 6, 2016.

Wahl, K.L., and Wahl, T.L., 1988, Effects of regional ground-water level declines on streamflow in the Oklahoma Panhandle: Proceedings of Symposium on Water-Use Data for Water Resources Management, American Water Resources Association, August 1988, Tucson, Arizona, p. 239–249.

Wisconsin Department of Natural Resources (WDNR), 2017, Wisconsin DNR drinking water system well construction reports: accessed various dates in 2017 and 2018 at https://dnr.wi.gov/topic/groundwater/data.html.

For more information about this publication, contact:
Director, USGS Upper Midwest Water Science Center
8505 Research Way
Middleton, WI 53562
608–828–9901

For additional information, visit: https://www.usgs.gov/centers/umid-water

Publishing support provided by the
Madison and Rolla Publishing Service Centers

Leaf and Haserodt—**Hydrology of Haskell Lake and Investigation of a Groundwater Contamination Plume, Lac du Flambeau Reservation, Wisconsin**—SIR 2020–5024

ISSN 2328-0328 (online)
https://doi.org/10.3133/sir20205024